

**Total Maximum Daily Loads for Dioxins
in the Houston Ship Channel**

**Contract No. 582-6-70860
Work Order No. 582-6-70860-02**

Final Report

Prepared by
*University of Houston
Parsons Water & Infrastructure*

Principal Investigator
Hanadi Rifai

PREPARED IN COOPERATION WITH THE
TEXAS COMMISSION ON ENVIRONMENTAL QUALITY AND
U.S. ENVIRONMENTAL PROTECTION AGENCY

The preparation of this report was financed through grants from the U.S. Environmental Protection Agency through the Texas Commission on Environmental Quality

TCEQ Contact:
Larry Koenig
TMDL Team
P.O. Box 13087, MC - 203
Austin, Texas 78711-3087
lkoenig@tceq.state.tx.us

October, 2006

TABLE OF CONTENTS

TABLE OF CONTENTS.....	ii
LIST OF TABLES.....	v
LIST OF FIGURES.....	vii
UNIT SYMBOLS, ABBREVIATIONS, AND CONVERSIONS.....	ix
CHAPTER 1 - INTRODUCTION.....	1
1.1 OVERALL DESCRIPTION OF THE DIOXIN PROJECT.....	2
1.2 PROBLEM STATEMENT.....	2
1.3 DESCRIPTION OF HOUSTON SHIP CHANNEL SYSTEM.....	3
1.4 DESCRIPTION OF THE SEAFOOD CONSUMPTION ADVISORY AND MOTIVATION FOR THE TMDL STUDY.....	5
1.5 DESCRIPTION OF THE TEF/TEQ METHODOLOGY.....	5
1.6 DESCRIPTION OF THE REPORT.....	9
CHAPTER 2 - MONITORING AND DATA COLLECTION.....	10
CHAPTER 3 - MODEL DEVELOPMENT.....	11
3.1 GENERAL WATERSHED CHARACTERISTICS.....	12
3.2 HYDRODYNAMIC MODEL OF THE HSC AND UPPER GALVESTON BAY.....	14
3.2.1 Hydrodynamic Model Issues.....	15
3.2.2 RMA2 Model Segmentation and Time Step.....	17

3.2.3	Data for Model Input.....	17
3.2.4	Model Calibration	31
3.3	HSCREAD INTERFACE.....	59
3.4	IN-STREAM WATER QUALITY MODEL OF THE HSC AND UPPER GALVESTON BAY	62
3.4.1	WASP Segmentation and Time Step	66
3.4.2	Model Input.....	66
3.4.3	Salinity Model.....	81
3.4.4	Dioxin Model Calibration	85
3.4.5	Sensitivity Analysis.....	89
3.4.6	Preliminary Load Scenarios	89
3.4.7	Next Steps in WASP Model Development	93
CHAPTER 4	- LOAD CALCULATION SPREADSHEET.....	94
4.1	SOURCE LOADS BY SEGMENT	94
4.1.1	Point Source Loads	94
4.1.2	Runoff Loads.....	98
4.1.3	Direct Deposition Loads	98
4.2	IN-STREAM LOADS	101
4.3	LOADS FROM SEDIMENT.....	105
4.4	PRELIMINARY LOAD REDUCTION SCENARIOS	107
CHAPTER 5	- STAKEHOLDER/PUBLIC EDUCATION AND INVOLVEMENT.....	110
5.1	SUMMARY OF SUPPORT ACTIVITIES	110

5.2 TECHNICAL PRESENTATIONS AT STAKEHOLDER MEETINGS	110
CHAPTER 6 - SUMMARY AND CONCLUSIONS.....	111
REFERENCES	1113
APPENDIX A – SUMMARY OF DIOXIN DATA COLLECTED IN THIS PROJECT	
APPENDIX B - CROSS-SECTIONS FROM BEAMS USED TO SET UP THE 1-D PORTION OF THE MAIN CHANNEL	
APPENDIX C - TIME SERIES FOR BOUNDARY CONDITIONS	
APPENDIX D - MODEL INPUT AND OUTPUT FILES	
APPENDIX E – POINT SOURCE DATABASE	
APPENDIX F – SLIDES PRESENTED AT STAKEHOLDER MEETINGS	

LIST OF TABLES

<u>TABLE #</u>	<u>TITLE</u>	<u>PAGE #</u>
Table 1.1	Toxicity Equivalent Factors (TEF) for Different TEQ Schemes	7
Table 3.1	Major Tributaries and USGS Gages	14
Table 3.2	Dimensions of Cross-Sectional Areas for Tributaries in the Model	26
Table 3.3	Tide Gages in the Modeled Area	27
Table 3.4	Upstream Boundary Conditions for the RMA2 Model	29
Table 3.5	Flow from Point Sources in the RMA2 Model	30
Table 3.6	Model Summary Statistics for Water Elevations	36
Table 3.7	Difference between Measured and Predicted Cross-Sectional Areas	38
Table 3.8	Model Summary Statistics for Water Flows	58
Table 3.9	Data Requirements for the Dioxin WASP Model for the HSC	64
Table 3.10	Physical Characteristics of WASP Segments	68
Table 3.11	Point Sources in the WASP Model	72
Table 3.12	Direct Deposition in the WASP Model	76
Table 3.13	Model Summary Statistics for Salinity	85
Table 3.14	Model Summary Statistics for 2378-TCDD	87
Table 4.1	Estimated 2378-TCDD Loads from Point Sources	97
Table 4.2	Estimated TEQ Loads from Point Sources	97
Table 4.3	Estimated Dioxin Runoff Loads by Subwatershed	99
Table 4.4	Dioxin Loads from Direct Deposition	100
Table 4.5	In-stream Loads of Dioxins by Segment	102

Table 4.6	Mass Balance Calculations for 2378-TCDD	103
Table 4.7	Mass Balance Calculations for TEQ	104
Table 4.8	Estimated Dioxin Loads from Bottom Sediment	106
Table 4.9	Dioxin Load Spreadsheet – Overall Reductions	107
Table 4.10	Dioxin Load Spreadsheet – Load Reduction Scenario 1	108
Table 4.11	Dioxin Load Spreadsheet – Load Reduction Scenario 2	109

LIST OF FIGURES

<u>FIGURE #</u>	<u>TITLE</u>	<u>PAGE #</u>
Figure 1.1	The Houston Ship Channel System	4
Figure 3.1	RMA2-WASP7 Modeling Process	12
Figure 3.2	RMA2 Model Segmentation	18
Figure 3.3	Bottom Elevations for the Houston Ship Channel	20
Figure 3.4	Bottom Elevations for the Tidal Portions of Major Tributaries to the HSC	21
Figure 3.5	Locations for Water Sampling in WO No. 582-0-80121-07	28
Figure 3.6	Observed and Simulated Water Surface Elevations in the HSC	32
Figure 3.7	Scatterplots of Observed and Modeled Water Surface Elevations in the HSC	34
Figure 3.8	Velocity and Flow Calibration Locations	37
Figure 3.9	Modeled and Measured Water Velocities	39
Figure 3.10	Modeled and Measured Water Flows	41
Figure 3.11	Scatterplots of Observed and Modeled Water Velocities using Discrete Values ..	42
Figure 3.12	Scatterplots of Observed and Modeled Water Flows using Discrete Values	43
Figure 3.13a	Goodness of Fit for HSC @ Morgan’s Point using Flow Regression	45
Figure 3.13b	Goodness of Fit for HSC @ Lynchburg using Flow Regression	46
Figure 3.13c	Goodness of Fit for HSC @ Battleship using Flow Regression	47
Figure 3.13d	Goodness of Fit for HSC @ Greens using Flow Regression	48
Figure 3.13e	Goodness of Fit for HSC @ I-610 using Flow Regression	49
Figure 3.13f	Goodness of Fit for Buffalo Bayou	50
Figure 3.13g	Goodness of Fit for Brays Bayou	51

Figure 3.13h	Goodness of Fit for Sims Bayou.....	52
Figure 3.13i	Goodness of Fit for Vince Bayou.....	53
Figure 3.13j	Goodness of Fit for Hunting Bayou	54
Figure 3.13k	Goodness of Fit for Greens Bayou	55
Figure 3.13l	Goodness of Fit for Carpenters Bayou	56
Figure 3.13m	Goodness of Fit fir San Jacinto River @ I-10	57
Figure 3.14	WASP Model Segmentation	67
Figure 3.15	Point Sources in the WASP Model	71
Figure 3.16	Salinity Calibration Locations.....	83
Figure 3.17	Modeled and Measured Salinity Concentrations	84
Figure 3.18	Longitudinal Profiles of Average Dioxin Concentrations.....	86
Figure 3.19	Observed versus Modeled Average Dioxin Concentrations	88
Figure 3.20	Sensitivity Analysis Results – Main Channel	90
Figure 3.21	Sensitivity Analysis Results – San Jacinto River.....	91
Figure 3.22	Summary of Load Scenarios	92
Figure 4.1	Relationship between Measured Dioxin Levels in Sludge and Effluent.....	96

UNIT SYMBOLS, ABBREVIATIONS, AND CONVERSIONS

Symbol or abbreviation	Text	Unit Equivalence	Unit Type
°C	degrees celcius		temperature
kg	kilograms	10 ³ grams	mass
g	grams	454 grams ~ 1 pound	mass
mg	milligrams	10 ⁻³ grams	mass
µg	micrograms	10 ⁻⁶ grams	mass
ng	nanograms	10 ⁻⁹ grams	mass
pg	picograms	10 ⁻¹² grams	mass
fg	femtograms	10 ⁻¹⁵ grams	mass
L	liter	3.78 liters ~ 1 gallon	volume
mL	milliliter	10 ⁻³ liters	volume
mBq	millibecquerel	27 microcuries (mCi)	radioactivity
µg/L	micrograms per liter	~10 ⁻⁹ , or 1 ppb	mass/volume concentration
ng/L	nanograms per liter	~10 ⁻¹² , or 1 ppt	mass/volume concentration
pg/L	picograms per liter	~10 ⁻¹⁵ , or 1 ppq	mass/volume concentration
ng/kg	nanograms per kilogram	=10 ⁻¹² , or 1 ppt	mass/mass concentration
mg/g	milligrams per gram	10 ⁻³	mass/mass concentrations
g/cm ²	gram per square centimeter		cumulative mass
mBq/g	millibecquerel per gram		radioactivity
ppm	parts per million	10 ⁻⁶	unitless concentration
ppb	parts per billion	10 ⁻⁹	unitless concentration
ppt	parts per trillion	10 ⁻¹²	unitless concentration
ppq	parts per quadrillion	10 ⁻¹⁵	unitless concentration

CHAPTER 1

INTRODUCTION

Polychlorinated dibenzo-*p*-dioxins (PCDDs) and dibenzofurans (PCDF) and polychlorinated biphenyls (PCBs) are halogenated aromatic compounds that have been widely found in the environment. The PCDDs include 75 congeners and PCDFs include 135 different congeners. Only 7 out of the 75 PCDD congeners and 10 of the 135 PCDF congeners have been identified as having dioxin-like toxicity. There are 209 PCB congeners, of which 13 are identified as having dioxin-like toxicity. These dioxin-like compounds are highly toxic and persistent environmental contaminants and, consequently, have received a great deal of attention by environmental regulators and researchers.

Dioxin (the term used to refer to dioxin-like compounds) presents a likely cancer hazard to humans¹ (U. S. Environmental Protection Agency, 2000a) and can cause health problems even at extremely low doses. Reproductive problems, behavioral abnormalities, and alterations in immune functions are among the health effects caused by exposure to dioxin. Because dioxin-like compounds have been proven to bioaccumulate in biological tissues, particularly in animals, the major route of human exposure is through the food chain. Thus, several food advisories have been issued across the United States to prevent people from consuming unhealthful doses of these compounds.

¹ U.S. Environmental Protection Agency (2000a). “Dioxin: Scientific Highlights from Draft Reassessment.” *Information Sheet 2*, National Center for Environmental Assessment, Office of Research and Development, Washington, DC.

1.1 OVERALL DESCRIPTION OF THE DIOXIN PROJECT

The overall purpose of this project is to develop a Total Maximum Daily Load (TMDL) allocation for dioxin in the Houston Ship Channel System, including upper Galveston Bay, and a plan for managing dioxins to correct existing water quality impairments and to maintain good water quality in the future.

The dioxin TMDL study has been divided into various phases. Phase I of the TMDL was focused on assessing current conditions and knowledge about dioxins. Phase II was focused on gathering data in all media to quantify dioxin levels in the channel and their sources. Phase III is focused on model development and load allocation.

This Work Order (582-6-70860-02) is part of Phase III and includes the following tasks:

1. Project administration,
2. Amending current Quality Assurance Project Plan (QAPP) to incorporate additional data collection,
3. Conducting dioxin monitoring and data collection in the Houston Ship Channel area.
4. Incorporating collected data into dioxin TMDL models,
5. Participating in stakeholder involvement with the dioxin TMDL project, and
6. Estimating TMDL allocations.

1.2 PROBLEM STATEMENT

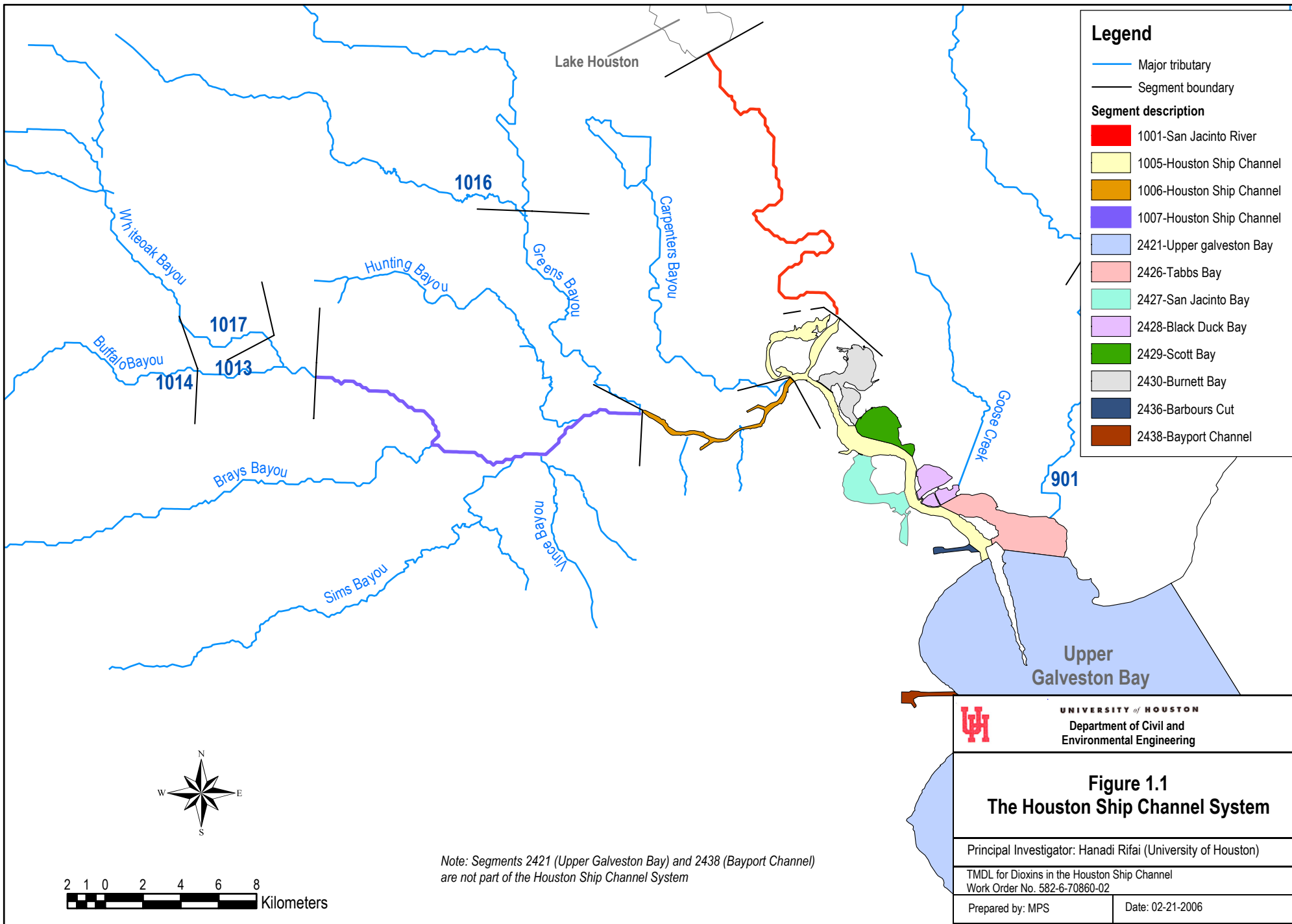
Section 303(d) of the Clean Water Act requires all states to identify waters that do not meet, or are not expected to meet, applicable water quality standards. For each listed water body that does not meet a standard, states must develop a total maximum daily load (TMDL) for each pollutant that has been identified as contributing to the impairment of water quality in that water

body. The Texas Commission on Environmental Quality (TCEQ) is responsible for ensuring that TMDLs are developed for impaired surface waters in Texas. The ultimate goal of these TMDLs is to restore the quality of the impaired water bodies.

1.3 DESCRIPTION OF HOUSTON SHIP CHANNEL SYSTEM

The Houston Ship Channel (HSC) system is a network of bodies of water in the vicinity of Houston, Texas (see Figure 1.1). This system is located in the San Jacinto River Basin. The designated water quality segments that comprise the “enclosed” portion of the HSC include the Cedar Bayou Tidal (Segment 0901), San Jacinto River Tidal (Segment 1001), HSC (Segments 1005, 1006, and 1007), Buffalo Bayou (Segments 1013 and 1014), Greens Bayou Above Tidal (Segment 1016), Whiteoak Bayou Above Tidal (Segment 1017), Tabbs Bay (Segment 2426), San Jacinto Bay (Segment 2427), Black Duck Bay (Segment 2428), Scott Bay (Segment 2429), Burnett Bay (Segment 2430), and Barbours Cut (Segment 2436). The HSC dioxin-impaired segments listed on the 303(d) list include 1001, 1005, 1006, 1007, 2426, 2427, 2428, 2429, 2430, and 2436. The system does not include portions of the Ship Channel located in Galveston Bay (segment 2421) or Bayport Channel (segment 2438). However, for the purpose of this TMDL study, those segments are included.

The designated uses assigned to the segments that comprise the HSC system and Upper Galveston Bay, according to the Texas Surface Water Quality Standards, are found in Texas Water Code §26.023.



1.4 DESCRIPTION OF THE SEAFOOD CONSUMPTION ADVISORY AND MOTIVATION FOR THE TMDL STUDY

Because dioxin-like compounds have been proven to bioaccumulate in biological tissue, particularly in animals, the major route of human exposure is through the food chain. Thus, several food advisories have been issued across the United States to prevent people from consuming high doses of these compounds. Section 307.6 of the Texas Surface Water Quality Standards establishes numerical criteria for specific toxic substances. For human health protection, the numerical criteria for dioxins are 1.34×10^{-7} , 1.40×10^{-7} , and 9.33×10^{-8} μg Texas-TEQ/L for water and fish, freshwater fish only, and saltwater fish only, respectively.

A seafood consumption advisory for catfish and blue crabs in the upper portion of Galveston Bay and the Houston Ship Channel (HSC) was issued by the Texas Department of Health in September 1990 as a result of dioxin found in organism tissue. As a result, the HSC system was placed on the 303(d) list and a TMDL study was initiated. The overall purpose of this project is to develop a total maximum daily load (TMDL) allocation for dioxin in the Houston Ship Channel System, including upper Galveston Bay, and a plan for managing dioxins to correct existing water quality impairments and maintain good water quality in the future.

1.5 DESCRIPTION OF THE TEF/TEQ METHODOLOGY

The 31 dioxin-like compounds are often found in complex mixtures. For risk assessment purposes, a toxicity equivalency procedure was developed to describe the cumulative toxicity of

these mixtures². This procedure involves assigning individual toxicity equivalency factors (TEFs) to the CDD, CDF, and PCB congeners. Considered most toxic of the dioxin-like congeners is 2,3,7,8-TCDD, assigned a TEF of 1.0. All other congeners have lower TEF values ranging from 0.00001 to 0.5 (Table 1.1), with the exception of 1,2,3,7,8-PeCDF that is assigned a TEF of 1 in the WHO₉₈ methodology. To calculate the toxic equivalency (TEQ) of a mixture, the concentration of individual congeners is multiplied by their respective TEF, and the sum of the individual TEQs is the TEQ concentration for the mixture. This is described mathematically as follows:

$$TEQ = \sum_{i=1}^n (Congener_i \cdot TEF_i) \quad (1.1)$$

Since 1989, three different TEF schemes have been used for evaluating the TEQ of CDDs, CDFs, and dioxin-like PCBs. To differentiate the scheme used to quantify a TEQ, the EPA in its Dioxin Exposure Assessment adopted the following nomenclature:

² U.S. Environmental Protection Agency (2000b). “Exposure and Human Health Reassessment of 2,3,7,8-Tetrachlorodibenzo-p-Dioxin (TCDD) and Related Compounds. Part I: Estimating Exposure to Dioxin-Like Compounds. Volume: Sources of Dioxin-Like Compounds in the United States.” *EPA600/P-00/001Ab*.

Table 1.1 Toxicity Equivalent Factors (TEF) for Different TEQ Schemes

Compound	I-TEQ _{DF}	TEQ _{DFP} -WHO ₉₄	TEQ _{DFP} -WHO ₉₈	Texas TEQ
2,3,7,8-TCDD	1	1	1	1
1,2,3,7,8-PeCDD	0.5	0.5	1	0.5
1,2,3,4,7,8-HxCDD	0.1	0.1	0.1	0.1
1,2,3,6,7,8-HxCDD	0.1	0.1	0.1	0.1
1,2,3,7,8,9-HxCDD	0.1	0.1	0.1	0.1
1,2,3,4,6,7,8-HpCDD	0.01	0.01	0.01	
OCDD	0.001	0.001	0.0001	
2,3,7,8-TCDF	0.1	0.1	0.1	0.1
1,2,3,7,8-PeCDF	0.05	0.05	0.05	0.05
2,3,4,7,8-PeCDF	0.5	0.5	0.5	0.5
1,2,3,4,7,8-HxCDF	0.1	0.1	0.1	0.1
1,2,3,6,7,8-HxCDF	0.1	0.1	0.1	0.1
1,2,3,7,8,9-HxCDF	0.1	0.1	0.1	0.1
2,3,4,6,7,8-HxCDF	0.1	0.1	0.1	0.1
1,2,3,4,6,7,8-HpCDF	0.01	0.01	0.01	
1,2,3,4,7,8,9-HpCDF	0.01	0.01	0.01	
OCDF			0.0001	
PCB-77		0.0005	0.0001	
PCB-81		-	0.0001	
PCB-105		0.0001	0.0001	
PCB-114		0.0005	0.0005	
PCB-118		0.0001	0.0001	
PCB-123		0.0001	0.0001	
PCB-126		0.1	0.1	
PCB-156		0.0005	0.0005	
PCB-157		0.0005	0.0005	
PCB-167		0.00001	0.00001	
PCB-169		0.01	0.01	
PCB-170		0.0001	-	
PCB-180		0.00001	-	
PCB-189		0.0001	0.0001	

I-TEQ_{DF}

This abbreviation refers to the International TEF scheme described by the EPA in 1989³. This scheme assigns TEF values for the 7 dioxins (CDDs) and 10 furans (CDFs). In the abbreviation, “I” represents “International,” TEQ refers to the 2,3,7,8-TCDD Toxic Equivalence of the mixture, and the subscript DF indicates that only dioxins and furans are included in the

³ Environmental Protection Agency (1989).

TEF scheme. This abbreviation is often shortened to I-TEQ, where it is understood that the mixture refers to both dioxins and furans.

I-TEQ_{DFP-WHO94}

This abbreviation refers to the 1994 World Health Organization (WHO) extension of the TEF scheme to include 13 dioxin-like PCBs⁴. It is noted that the TEFs for dioxins and furans remain as established by EPA in 1989. In this abbreviation, the subscript DFP indicates that dioxins, furans, and PCBs are included in the TEF scheme. If only one or two kinds of compounds are included in a mixture, the subscript should change to reflect the ones that are being considered for evaluating the TEQ. The subscript 94 indicates the year in which the changes to the TEF scheme were made.

TEQ_{DFP-WHO98}

This abbreviation refers to the 1998 re-evaluation of the previously established TEFs by the World Health Organization⁵. Again, the subscript DFP indicates the presence of the three dioxin-like groups in the mixture; the absence of one of the groups would be reflected by the omission of the respective subscript. The TEFs for 1,2,3,7,8-PeCDD, OCDD, and PCB-77 were changed, a TEF for PCB-81 was added, and TEFs for PCB-170 and PCB-180 were set to zero. The Texas TEQ excludes 1,2,3,4,6,7,8-HpCDD; OCDD; 1,2,3,4,6,7,8-HpCDF; 1,2,3,4,7,8,9-HpCDF; OCDF; and PCBs. For the remaining congeners, this TEF scheme assumes the same values given in the WHO₉₄ scheme.

⁴ Ahlborg et al, 1994

1.6 DESCRIPTION OF THE REPORT

This document constitutes the final report for Work Order No. 582-6-70860-02 (Contract No. 582-6-70860) of the Dioxin TMDL Project and summarizes the activities undertaken by the University of Houston, in conjunction with Parsons during the period September 28, 2005 to August 31, 2006.

Chapter 2 presents a summary of all the data collected under this project as well as some trend analyses. A detailed description of modeling activities and results to date is presented in Chapter 3. Chapter 4 presents preliminary load estimation calculations. Chapter 5 summarizes the activities conducted by the project team in support of the stakeholder and public outreach process. Finally, a summary of the activities conducted in this work order as well as the conclusions derived from the work are included in Chapter 6.

⁵ Van der Berg, 1998

CHAPTER 2

MONITORING AND DATA COLLECTION

Monitoring and data collection in this project encompassed two main subtasks: (i) monitoring and data collection to assess current levels of dioxins in the HSC, and (ii) sampling to evaluate sources of dioxins to the HSC system. A comprehensive summary of data collected by the project team between 2002 and 2005 was provided in Quarterly Report 3 for this Work Order and is attached in electronic form in Appendix A.

CHAPTER 3

MODEL DEVELOPMENT

The goal of this task is to use models to elucidate the sources and major processes controlling observed levels of dioxins in the Houston Ship Channel and to identify the maximum permissible loading that would not impair water quality. Development of a preliminary mass-balance of dioxins in the HSC was completed during WO7 using the MEGA-TX model (a modification of the QUAL-TX model completed for this project) to ensure that all the sources and process had been identified. In addition, a steady-state WASP model of the HSC was developed as well as a 1-month transient WASP simulation.

The modeling approach for this Work Order consisted of a hydrodynamic model coupled to an in-stream water quality model for the HSC and its major tributaries, for use in developing total maximum daily loads (TMDLs) for dioxin. The models are being used for several purposes:

- to aid in understanding the processes affecting the fate of dioxins in the HSC system,
- to quantify pollutant loadings to the various water quality segments and allocate them among sources, and
- to quantify the loading reductions required to achieve water quality standards.

Because the output from the hydrodynamic model (RMA2) can not directly be read by the in-stream water quality model (WASP7) and because segmentation for WASP7 is much coarser than that for RMA2, an interface (HSCREAD) was written as part of this project. Figure 3.1 shows a schematic of the modeling approach for this project.

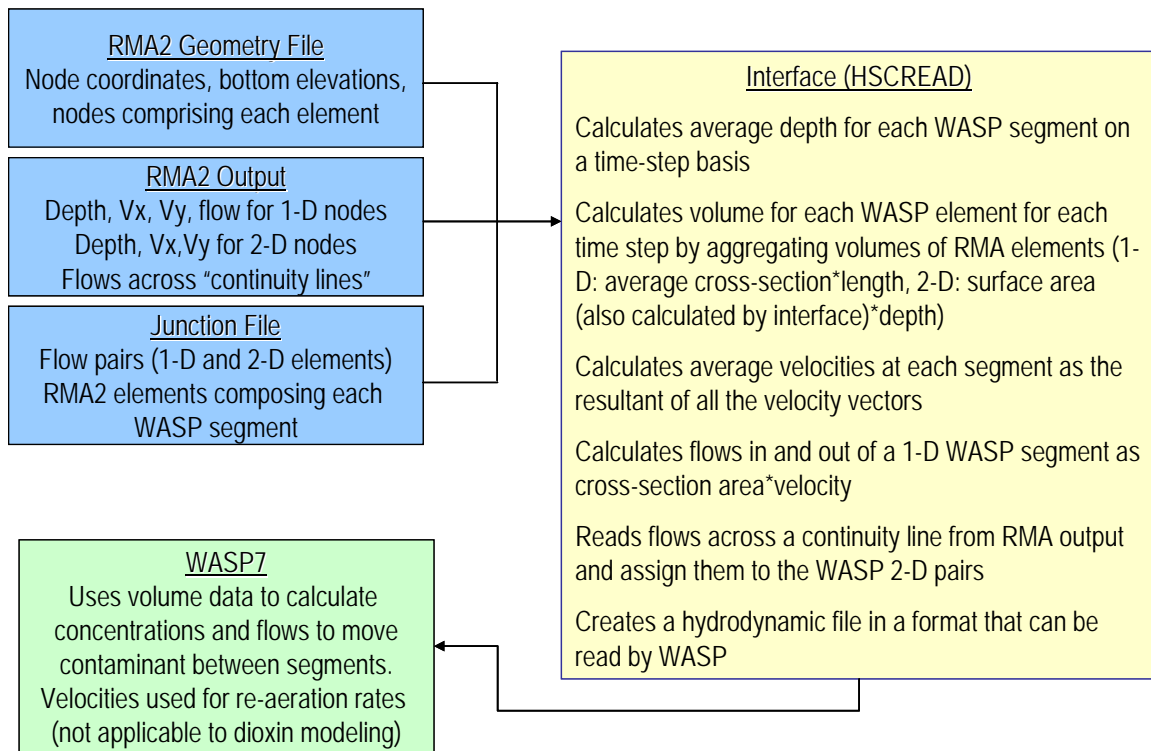


Figure 3.1 RMA2-WASP7 Modeling Process

3.1 GENERAL WATERSHED CHARACTERISTICS

Climatology

The climate throughout the Houston area is predominantly marine due to its proximity to the Gulf of Mexico and Galveston Bay. Prevailing winds are from the south and southeast, except during winter months when periodic passages of high-pressure cells bring polar air and prevailing northerly winds.

Temperatures are moderated by the influence of the warm Gulf waters, which results in mild winters. Average monthly temperatures range from 29.9°C (85.9°F) in July to 10.9°C (51.7°F) in December.

Another effect of the nearness of the Gulf is abundant rainfall. The peak rainfall period is

during the fall months with a secondary peak in the spring. Annual average precipitation is about 137 centimeters (54 inches). Significant snowfall is rare, but traces of snow are recorded during many winters. The relative humidity in the area is high, with the annual average ranging from 60 percent at 12:00 noon to 87 percent at 6:00 p.m.

Hydrology

The Houston Ship Channel system is an estuarine system that is composed of the tidally-influenced Houston Ship Channel and San Jacinto River and free-flowing tributaries which become tidal as they approach the Houston Ship Channel. The San Jacinto River is tidal from the Lake Houston Dam to the Houston Ship Channel.

The Houston Ship Channel has been dredged at mid-channel to a project depth of 15 meters to allow for the passage of ocean-going vessels. In the upper channel from the Turning Basin to the confluence with the San Jacinto River, widths range from 100 to 670 meters and average depths range from 4.8 to 14.4 meters. In the lower channel from the San Jacinto River to Morgan's Point, widths range from 450 to 790 meters and average depths range from 3.6 to 15.5 meters. During low-flow conditions on the San Jacinto River, widths range from 70 to 1,020 meters and the average depths range from 5.5 to 13 meters.

The tributaries of the Houston Ship Channel are characterized by moderately low flows dominated by domestic wastewater effluents except during periods of intense rainfall when the flows can rise dramatically. The United States Geological Survey maintains continuous flow recording gages on most of the tributaries as indicated in Table 3.1.

Table 3.1 Major Tributaries and USGS Gages

Tributary	Station Description	USGS gage	Watershed Area (km²)	Long-term median flow (m³/s)
San Jacinto River	San Jacinto River at Sheldon	08072050 ^a	7,370	NA
Lake Houston	Lake Houston near Sheldon	08072000 ^a	7,240	NA
Buffalo Bayou	Buffalo Bayou at Shepherd	08074000	916	3.3
Whiteoak Bayou	Whiteoak Bayou at Heights	08074500	221	1.1
Greens Bayou	Greens Bayou at Ley Rd	08076700 ^b	466	38.7 ^b
Greens Bayou	Greens Bayou at Houston	08076000	176	0.7
Halls Bayou	Halls Bayou at Houston	08076500	73	0.3
Garners Bayou	Garners Bayou near Humble	08076180	79	0.4
Brays Bayou	Brays Bayou at Houston	08075000	243	2.9
Sims Bayou	Sims Bayou at Houston	08075500	161	1.2
Vince Bayou	Vince Bayou at Pasadena	08075730	21	0.1
Patrick Bayou	None	None	11	NA
Carpenters Bayou	None	None	66	NA
Hunting Bayou	Hunting Bayou at IH-610	08075770	41	0.3
Goose Creek	Goose Creek at Baytown	08067525 ^a	40	NA
Cedar Bayou	Cedar Bayou near Baytown	08067510	433	NA
Clear Creek	Clear Creek at Friendswood	08077540 ^c	255	NA

^a Only water elevation data are available for the simulation period

^b Flow data for this gage appear too high so data from upstream gage is to be used in the model

^c Recent data for this gage are not available

NA – not available

3.2 HYDRODYNAMIC MODEL OF THE HSC AND UPPER GALVESTON BAY

This section summarizes the development of a hydrodynamic model of the Houston Ship Channel System (including Upper Galveston Bay and Bayport Channel) using the RMA2 WES 4.5 Program (ERDC, 2005). An initial RMA2 model was developed during the second quarter of this Work Order. However, due to a number of issues encountered with the initial model, the RMA2 model segmentation was significantly changed during Summer 2006. The model details and results presented in this report correspond to the current model segmentation and are preceded by a summary of the issues that motivated the changes to the model.

RMA2 is a two-dimensional depth averaged finite element hydrodynamic numerical

model. It computes water surface elevations and horizontal velocity components for subcritical, free-surface two-dimensional flow fields (ERDC, 2005). The RMA2 model is comprised of elements and nodes. Elements represent a finite stretch of the channel or tributary, and hold water. Each 1-D element is composed of three nodes, while each 2-D element is composed of either 6 or 8 nodes. Nodes are the points where water surface elevation and velocity calculations are performed, and all linkages between elements occur at nodes.

3.2.1 Hydrodynamic Model Issues

The initial version of the Houston Ship Channel RMA2 model presented a number of problems listed below:

- The net flow out of the side bays was high, even though most of the bays do not have any freshwater inflow. Flow in and out of side bays is the result of tidal elevation and, thus, net flow should be near zero,
- Mass-balance was not preserved for individual RMA2 elements. The RMA2 model globally maintains mass-conservation in a weighted residual manner, however, checks on an element-basis should be done separately by using continuity lines or by calculating volumes as a function of flows in and out of elements. Large mass conservation discrepancies indicate possible oscillations and a need to improve model resolution and/or correct large boundary break angles (ERDC, 2005),
- The model output flows for continuity lines with only one element at the interface (2 nodes) were found to be inaccurate,
- There were flow losses between some of the 1-D elements, and
- Wetting/drying of the upstream reaches (Buffalo and Whiteoak Bayou) caused the long-term

run to crash.

To address the above mentioned issues the following changes were made to the model:

- The geometry of 1-D elements at some junctions was modified to eliminate water leaks,
- Upstream reaches with bottom elevations above -0.5 m mean sea level (msl) were eliminated and the associated volume replaced using off-channel storage,
- The RMA2 model segmentation was refined (from 1032 to 3356 elements) to minimize mass-balance problems. The goal of the refinement was that for each of the WASP segments, the difference in volumes calculated using the following two methods would not be greater than 3% of the volume at any time step:

$$V_t = V_{t-1} + (Q_{in_t} - Q_{out_t}) \cdot dt \quad (3.1)$$

and

$$V_t = \overline{A_{xs_t}} \cdot L \quad (\text{for 1-D elements}) \quad (3.2a)$$

$$V_t = A_s \cdot \overline{D_t} \quad (\text{for 2-D elements}) \quad (3.2b)$$

where: V_t is volume at time t , Q_{in} is flow into a WASP segment, Q_{out} is flow out of a WASP segment, dt is time step, $\overline{A_{xs_t}}$ is the average cross-section area of a 1-D WASP segment, L is the length of a 1-D WASP segment, A_s is the surface area of a 2-D WASP segment, and $\overline{D_t}$ is the average depth of a 2-D WASP segment, and

- Continuity lines were specified so that at least two RMA2 elements were on each side of the continuity line.

3.2.2 RMA2 Model Segmentation and Time Step

The segmented model includes a 1-D section from the Turning Basin until the confluence with the San Jacinto River and a 2-D section from the San Jacinto River confluence until Eagle Point (boundary of segment 2421). The channel was discretized into 108 linear elements (including the tidal portions of the major tributaries), 3228 2-D elements, 16 junction elements, and 4 transition elements. The grid was defined using the SMS 9.0 software (Brigham Young University, 2005). The model grid is shown in Figure 3.2.

The model was set up for the period March 20 to April 21, 2005, using a 6-minute time step. This time period was selected because it corresponded to the period when flow measurements were made in this project. The time step in the initial model (30 minutes) proved problematic because it caused numerical dispersion in the WASP model. The time step was, consequently, reduced to 6 minutes, which is the resolution at which gage data are available from NOAA. The first 480 time steps (48 hours) are used to allow the model to stabilize, and minimize the effects of errors in assumed initial conditions (spin-up time). It is noted that the model can be run for any period for which freshwater inflows, winds, and boundary tide conditions are provided.

3.2.3 Data for Model Input

Geometry and Bottom Elevation Data

For the 1-D section of the model, two sources of data were relied upon: (i) HSC cross-sections from the deep draft channel survey, available on-line at <http://beams.swg.usace.army.mil/surveys.html>, and (ii) cross sections for major tributaries from

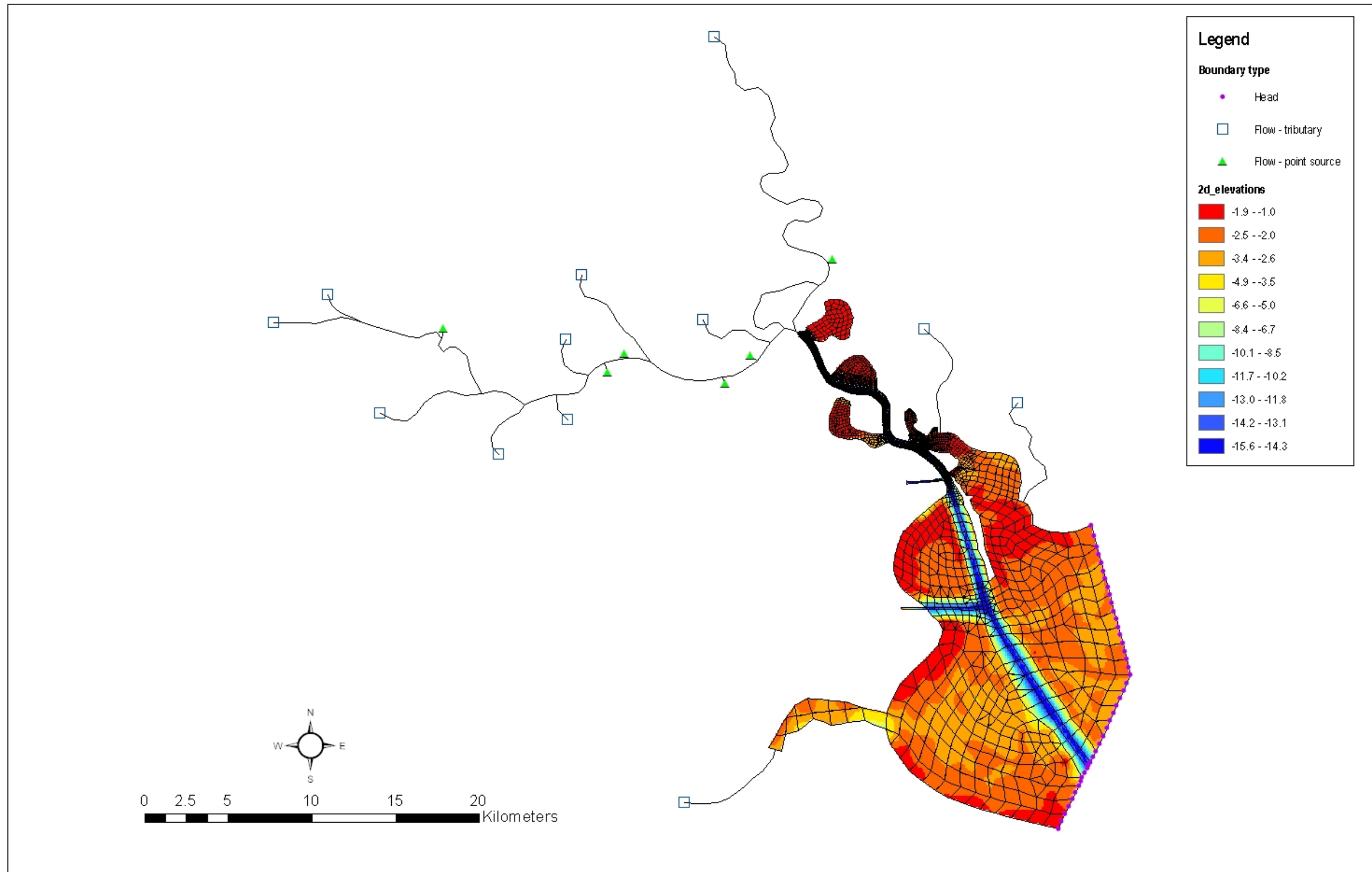


Figure 3.2 RMA2 Model Segmentation

the Tropical Storm Allison Recovery Project (TSARP). For the 2-D section of the model, bathymetry data were obtained from the Texas General Land Office website <http://www.glo.state.tx.us/> and interpolated for the selected mesh (Figure 3.2) to assign bottom elevations.

Data from the TSARP were used to assign bottom elevations to the nodes in the main channel and the major tributaries, as shown in Figures 3.3 and 3.4, respectively. The RMA2 model accepts only trapezoidal cross-sections, so the dimensions for the various 1-D elements were determined as follows: (i) for the main channel, the cross-sections for the dredged portions were obtained from the deep channel survey (see Appendix B); (ii) the shallow portions of the main channel were simulated using off-channel storage⁶; to determine the width of the off-channel storage, the total width of the channel at the various nodes was measured using aerial photographs for the project area, the depth of the off-channel storage was assumed to be 2 m for most locations; (iii) for the tributaries, constant channel dimensions were assumed so that the average cross-sectional areas (water surface elevation at about 0 m above mean sea level-msl) were within 10% of the areas measured during flow sampling in Spring 2005 as summarized in Table 3.2⁷; and (iv) off-channel storages were assigned to the first node of most of the major tributaries to account for the volume of water between the boundary of the tidal sections and the beginning of the modeled segments as illustrated in Figure 3.4. The slope of the off-channel storage was used as a calibration parameter.

⁶ “The off-channel assignment should be thought of as the average combined left and right over bank volumetric contributions. The volume of the off-channel storage interacts with the continuity equation, but makes no contribution to the momentum equation.” (ERDC, 2005).

⁷ An attempt was made to simulate the tributaries using the cross-sections obtained from TSARP, but the steep side slopes caused the model to crash.

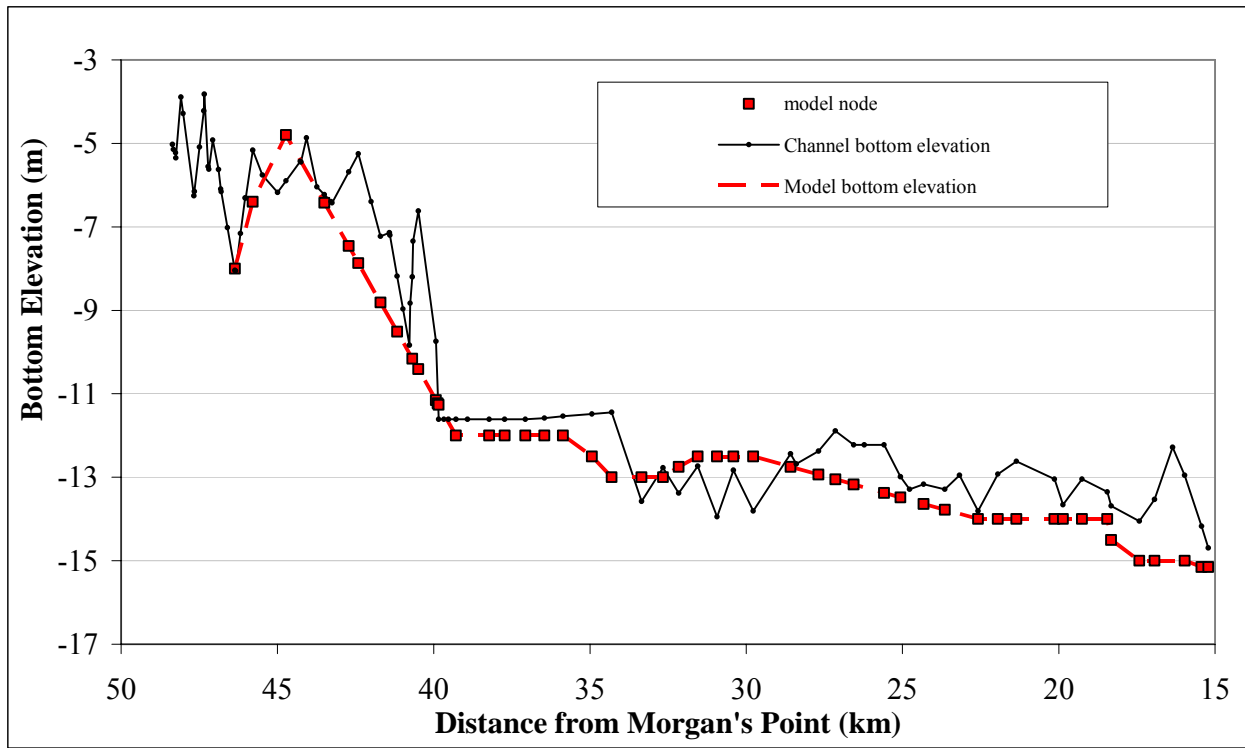
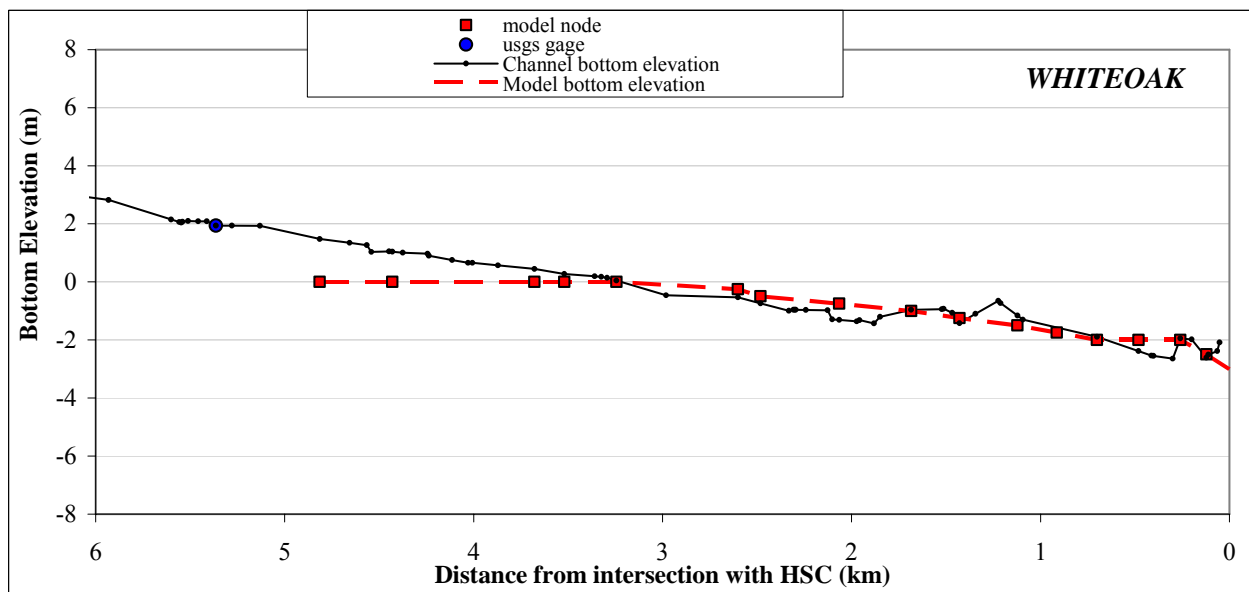
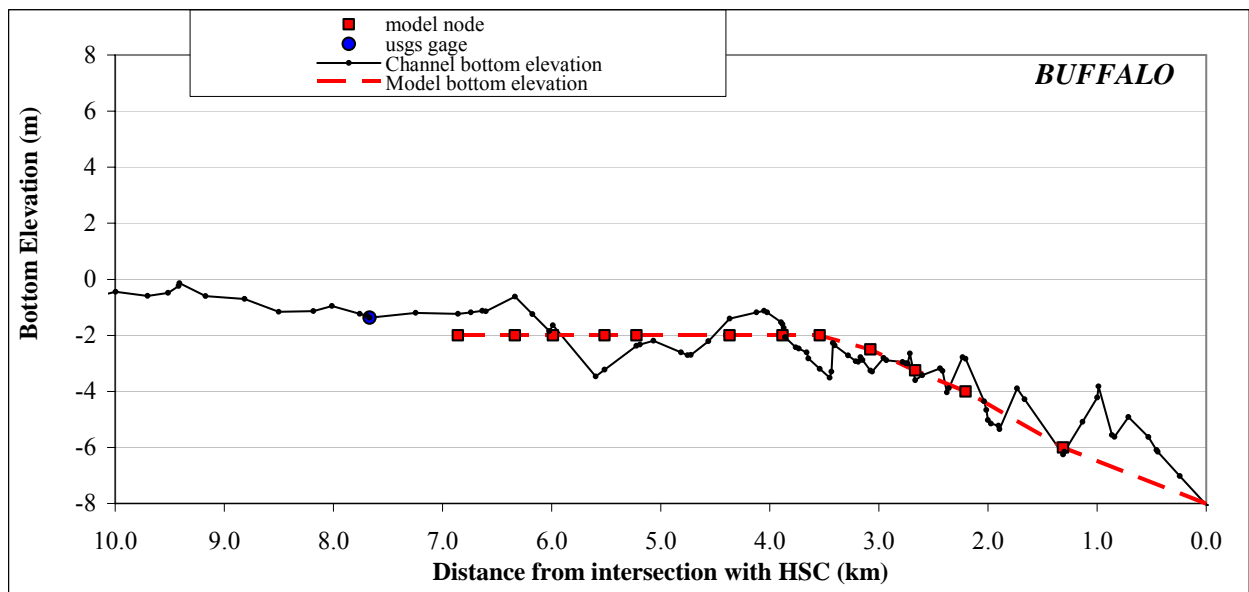
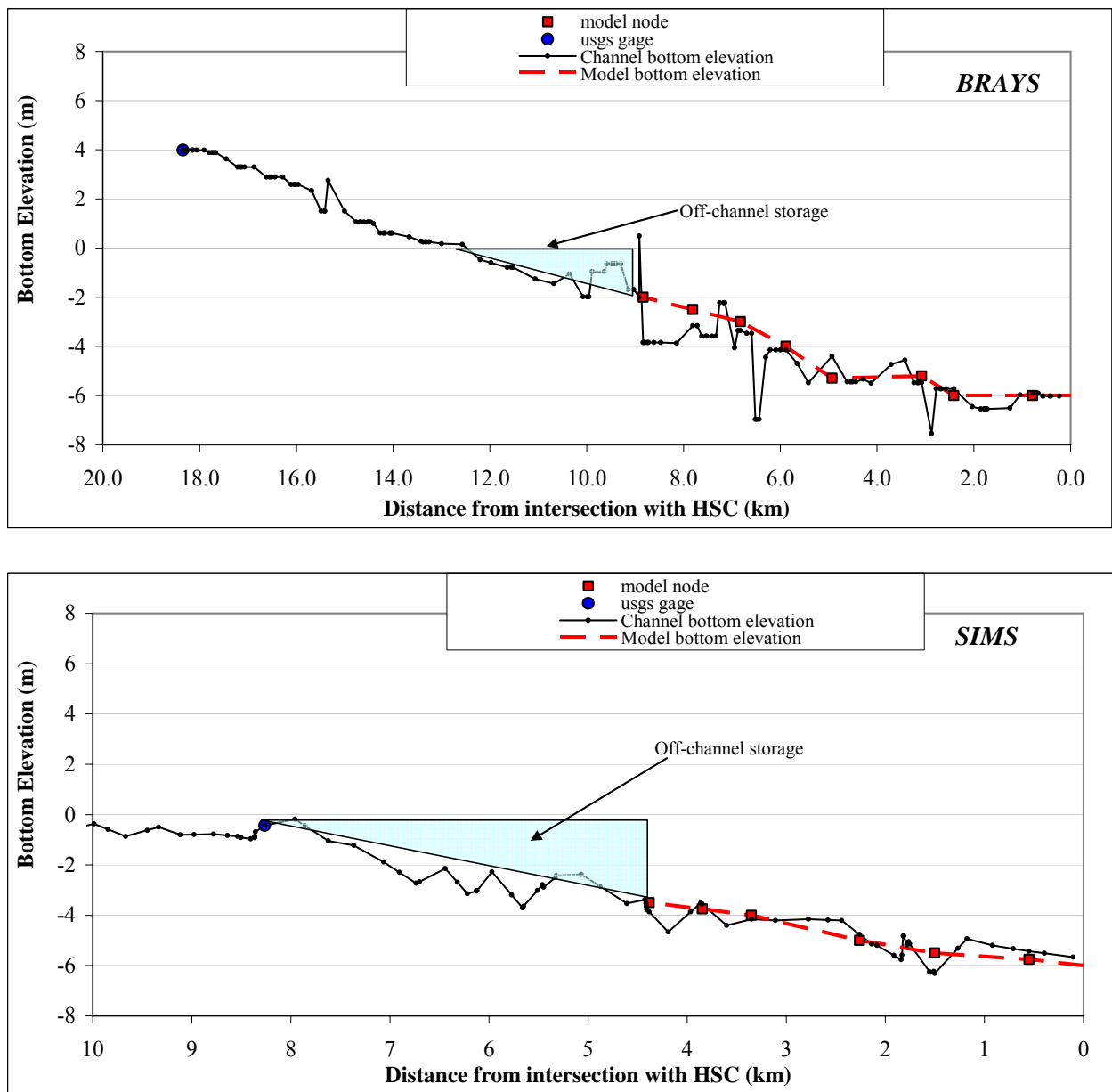


Figure 3.3 Bottom Elevations for the Houston Ship Channel



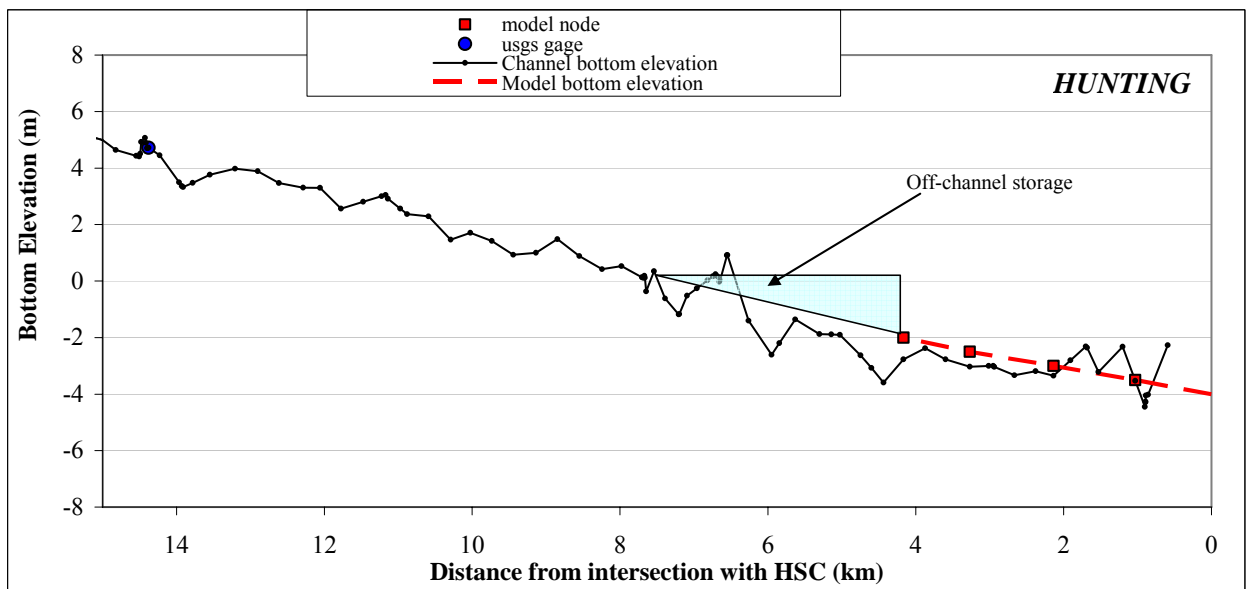
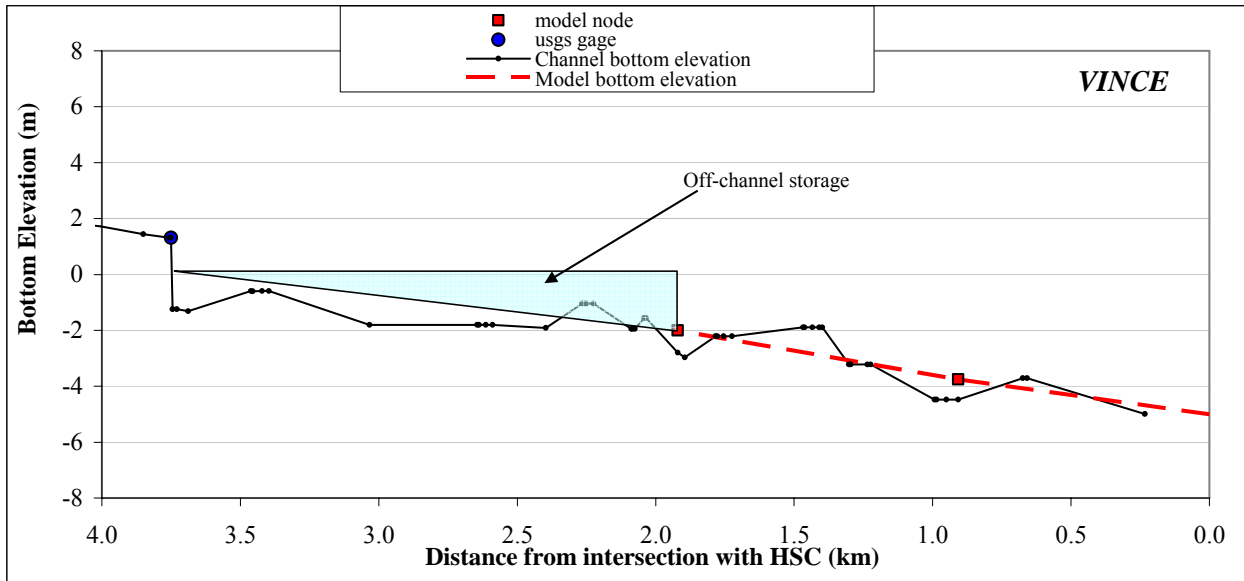
Bottom elevations were obtained from the TSARP cross-sections for the relevant portions of the various tributaries

Figure 3.4 Bottom Elevations for the Tidal Portions of Major Tributaries to the HSC



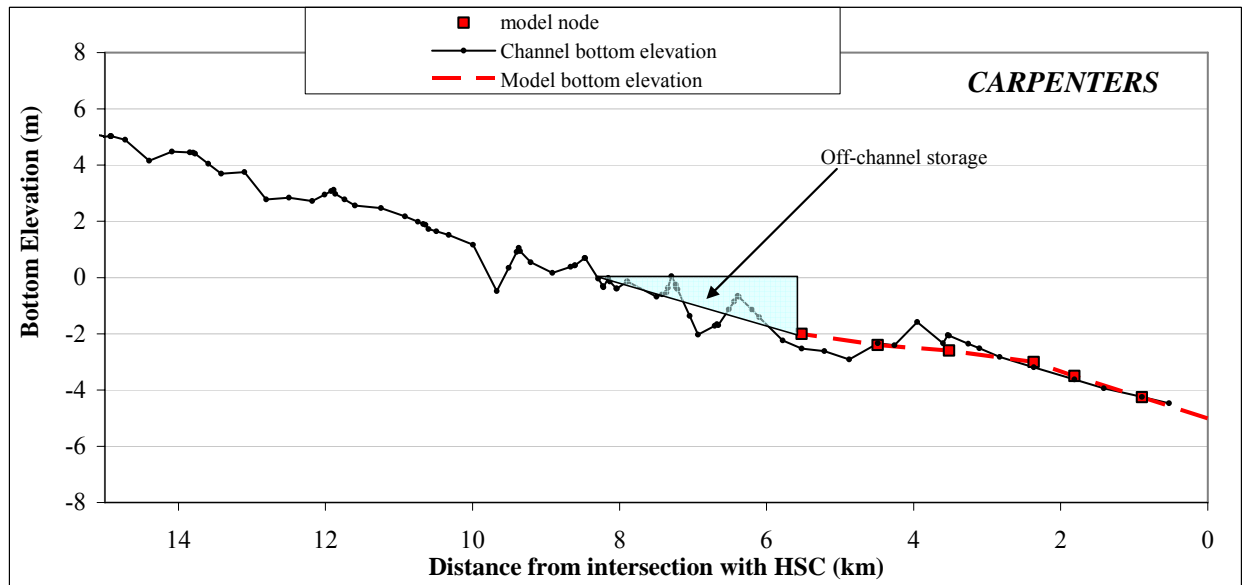
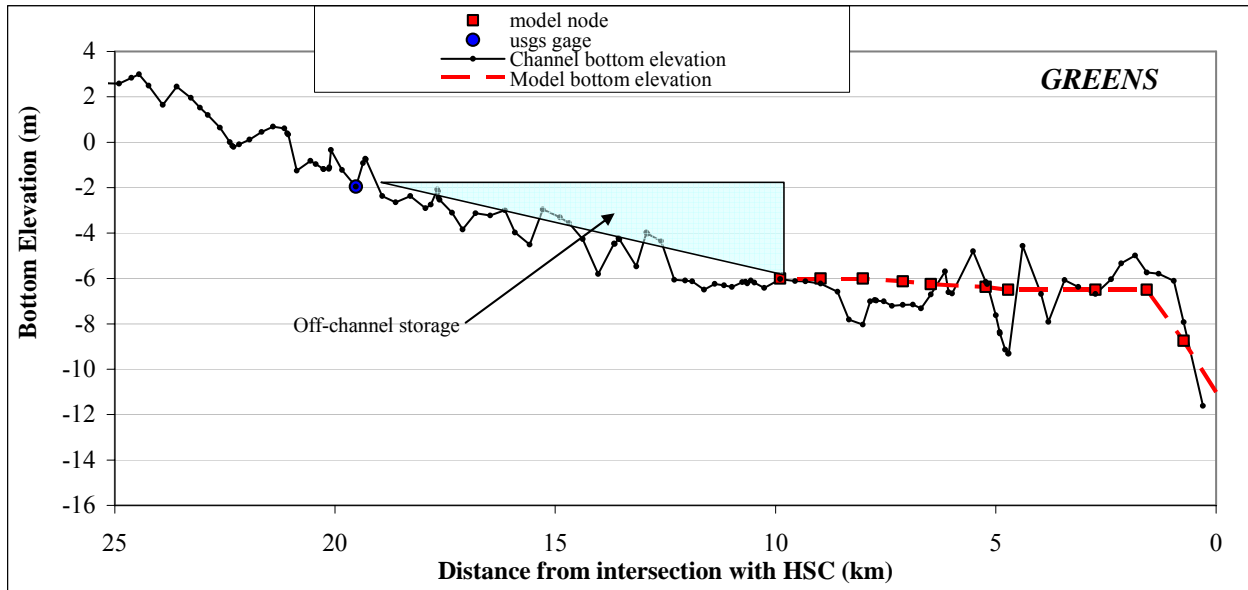
Bottom elevations were obtained from the TSARP cross-sections for the relevant portions of the various tributaries

Figure 3.4 Bottom Elevations for the Tidal Portions of Major Tributaries to the HSC – Cont’d



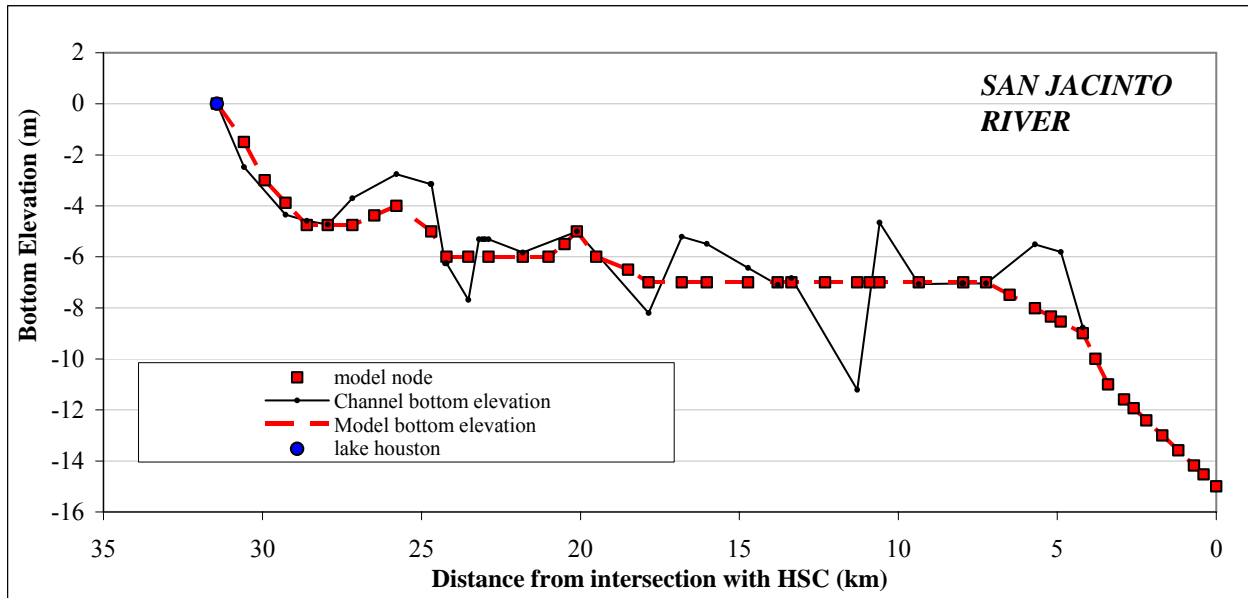
Bottom elevations were obtained from the TSARP cross-sections for the relevant portions of the various tributaries

Figure 3.4 Bottom Elevations for the Tidal Portions of Major Tributaries to the HSC – Cont'd



Bottom elevations were obtained from the TSARP cross-sections for the relevant portions of the various tributaries

Figure 3.4 Bottom Elevations for the Tidal Portions of Major Tributaries to the HSC – Cont'd



Bottom elevations were obtained from the TSARP cross-sections for the relevant portions of the various tributaries

Figure 3.4 Bottom Elevations for the Tidal Portions of Major Tributaries to the HSC – Cont'd

For the entire model grid, the bottom roughness coefficient was assumed to change with depth using an RMA2 model feature that provides for real-time adjustment of the Manning’s n-value of an element depending upon the water depth. Generally, the deeper the water, the lower the roughness value. The corresponding n-value is calculated in the model using the following equation:

$$n = \frac{n_{nv}}{D_{avg}^{RC}} + 0.036 \cdot e^{\frac{-D_{avg}}{2}} \quad (3.3)$$

where n = Manning’s n-value,

n_{nv} = maximum n-value for non-vegetated water (final calibration value 0.03),

RC = roughness by depth coefficient (final calibration value 0.08), and

D_{avg} = average depth.

Table 3.2 Dimensions of Cross-Sectional Areas for Tributaries in the Model

Tributary	Average Measured Area (m ²)	Bottom Width (m)	Side Slopes	Average Depth (m) ^a	Average Modeled Area (m ²)
Buffalo Bayou at McKee St.	137	12	3.5	4.7	134
Whiteoak Bayou	121 ^b	12	3.5	4.3	116
Brays Bayou at Broadway Blvd.	300	35	3.5	5.4	332
Sims Bayou at Lawndale Ave.	169	10	3.5	5.4	158
Vince Bayou at North Richey St.	132	25	3	3.4	122
Hunting Bayou at Federal Rd.	103	16	3.5	3.4	97
Greens Bayou at I-10 bridge	247	20	3	6.3	246
Carpenters Bayou at South Sheldon Rd.	69	20	3.5	2.5	74
Goose Creek	115 ^b	12	3.5	4.1	108

^a From preliminary model runs

^b Flow was not measured at those tributaries. The cross-sectional area was determined using TSARP cross-sections

Tide Data

There are four NOAA stations and one USGS station in the modeled area (Table 3.3 and Figure 3.5). Six-minute gage data for the simulation period were downloaded from TCOON⁸ <http://lighthouse.tamucc.edu/TCOON/HomePage>. Hourly gage data for the San Jacinto River station were obtained from the USGS. Tide data for Eagle Point was input to the model as the downstream boundary condition. Water surface elevations for the other stations were used for calibration purposes. It is noted that because the boundary data had spikes that might cause numerical problems in RMA2 (divergence), the data series was smoothed using a Daniell smoothing technique⁹ available in the Statistica package.

Table 3.3 Tide Gages in the Modeled Area

Station Description	Gage ID	Gage Maintained By
Eagle Point	87710131	NOAA
Morgan’s Point	87706131	NOAA
Battleship Texas	87707431	NOAA
Manchester	87707771	NOAA
San Jacinto River at Sheldon	08072050	USGS

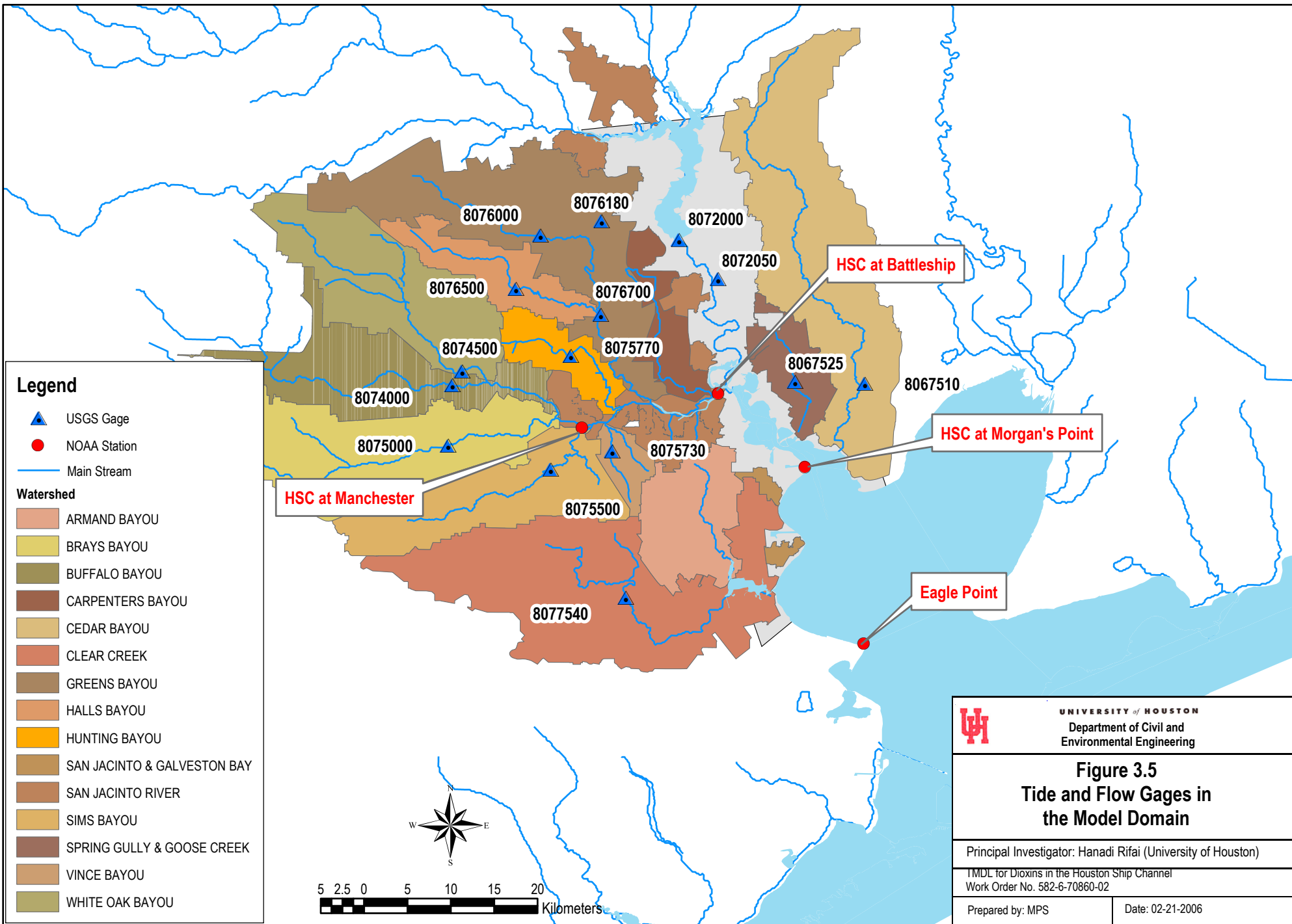
A database containing the tide data is included in Appendix C.

Freshwater Inflow Data

Hourly flow data for the USGS gages in the modeled area (Figure 3.5) were obtained for the period January 2002 to May 2005. These flow data were used as the upstream boundary

⁸ Texas Coastal Ocean Observation Network

⁹ This is a simple equal weight smooth where the weight of neighboring observations is divided by two for each time step away from the time step of interest. So for a time series with $t = -3, -2, -1, 0, 1, 2, 3$ the weights of the observations would be $1/8, 1/4, 1/2, 1, 1/2, 1/4, 1/8$.



Legend

- USGS Gage
- NOAA Station
- Main Stream

Watershed

- ARMAND BAYOU
- BRAYS BAYOU
- BUFFALO BAYOU
- CARPENTERS BAYOU
- CEDAR BAYOU
- CLEAR CREEK
- GREENS BAYOU
- HALLS BAYOU
- HUNTING BAYOU
- SAN JACINTO & GALVESTON BAY
- SAN JACINTO RIVER
- SIMS BAYOU
- SPRING GULLY & GOOSE CREEK
- VINCE BAYOU
- WHITE OAK BAYOU

UNIVERSITY of HOUSTON Department of Civil and Environmental Engineering	
Figure 3.5 Tide and Flow Gages in the Model Domain	
Principal Investigator: Hanadi Rifai (University of Houston)	
TMDL for Dioxins in the Houston Ship Channel Work Order No. 582-6-70860-02	
Prepared by: MPS	Date: 02-21-2006

condition for the main tributaries in the model. For the tributaries with no available flow data, either a constant flow rate or a flow series from a tributary with a similar drainage area was assumed. Table 3.4 presents a summary of the assumed flow boundary conditions for the various tributaries.

Table 3.4 Upstream Boundary Conditions for the RMA Model

Tributary	Boundary Type	Source of data
Buffalo Bayou	Transient unit flow rate	Hourly data for gage 08074000
Whiteoak Bayou	Transient unit flow rate	Hourly data for gage 08074500
Brays Bayou	Transient unit flow rate	Hourly data for gage 08075000
Sims Bayou	Transient unit flow rate	Hourly data for gage 0807550 for the model period are not available. Assumed hourly data for Brays Bayou
Vince Bayou	Transient unit flow rate	Hourly data for gage 08075730
Hunting Bayou	Transient unit flow rate	Hourly data for gage 08075770
Greens Bayou	Transient unit flow rate	Hourly dataset for gage 08076700 for the simulation period is incomplete and flows appear too high. Summation of hourly data for gages 08076000, 08076180, and 08076500
Carpenters Bayou	Transient unit flow rate	No USGS gages are located in this watershed. Assumed hourly data for Hunting Bayou (similar drainage area)
San Jacinto River	Transient unit flow rate	Rating curve for gage 08072000
Goose Creek	Constant unit flow rate (0.5 m ³ /s)	Average flow rate for Hunting Bayou (similar drainage area) for simulation period
Cedar Bayou	Constant unit flow rate (1 m ³ /s)	Assumed
Clear Creek	Constant unit flow rate (2 m ³ /s)	Average flow for period of record for gage 08077540

For the San Jacinto River, hourly gage height data were obtained for Lake Houston (gage 08072000) and hourly discharges from the Lake were calculated using a rating curve developed by the USGS (see Appendix C).

Flows from point sources discharging to the tributaries downstream of the USGS gages (Table 3.5) were added to those reported from the USGS. For point sources discharging directly

to the main channel, flows were input at five locations as summarized in Table 3.5. To include these inflows into the system, model elements (or reaches) were created at the points of discharge and a constant flow rate equal to the summation of the average self-reported flows for years 1997-2002 was used. The only exception was the flow from the City of Houston-69th Street Plant. Self-reported monthly average flows for 2005 for this plant were downloaded from the EPA Permit Compliance System (PCS) database at www.epa.gov/enviro. The monthly flow rates were then converted to hourly values using conversion factors developed for the Buffalo Bayou and Whiteoak Bacteria TMDL Project (University of Houston, 2005a). The hourly flow dataset for the 69th Street Plant is included in Appendix C.

Table 3.5 Flow from Point Sources in the RMA2 Model

Stream	Model node	Total Flow (m³/s)
Brays Bayou	Boundary	0.5
Sims Bayou	Boundary	1.5
Vince Bayou	Boundary	0.7
Greens Bayou	Boundary	0.9
Goose Creek	Boundary	0.2
Main Channel – 69th St	3106	3.5 ^a
Main Channel	3035	1.4
Main Channel	3021	0.5
Main Channel	2993	1.2
Main Channel	2962	1.7
San Jacinto River	2980	0.5

^a Average self-reported flow. A 1-hr time series was input to the model.

Meteorology

Hourly wind speed and direction data for the NOAA station at Eagle Point was input to the model (Appendix C). Wind data are used in the model to calculate wind friction to obtain proper setup and system circulation of shallow areas with strong wind influences. Wind data were

globally applied throughout the model domain.

Rainfall and evaporation can be input to the model by element or as a global condition. However, as of this writing such data have not been included in the model. These two parameters are not expected to have a significant impact on the model, especially in the main channel. Furthermore, not including precipitation data is justified by the fact that there were no significant rainfall events during the simulation period.

Appendix D contains the ASCII input decks (geometry and boundary conditions) for the RMA2 model of the HSC.

3.2.4 Model Calibration

Water Surface Elevation

The RMA2 model of the HSC system was first calibrated to NOAA and USGS water elevation data for the model period. The main calibration parameter was the Manning's n-value. Figure 3.6 compares the simulated and observed water surface elevation time series for the various gages. It can be seen that the model accurately reproduces the tide heights observed at Morgan's Point, Battleship, and Manchester (IH-610), with a slight decrease in accuracy as one moves upstream in the system. However, the water surface elevations for the USGS gage in the San Jacinto River could not be matched; the model simulates the general patterns of the data, but the modeled levels are consistently below the observed values. There appears to be a datum problem with the data for this location that results in measured water levels in the San Jacinto River that are about 30 cm higher than those measured in the HSC and Galveston Bay. The USGS

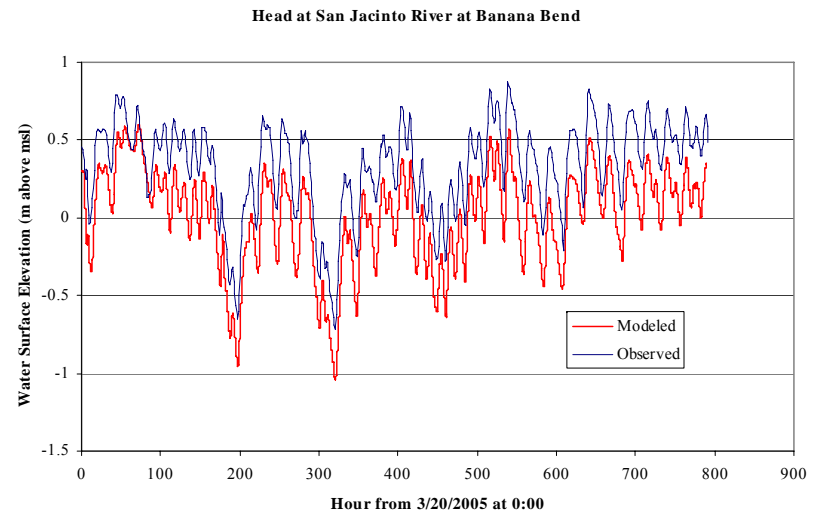
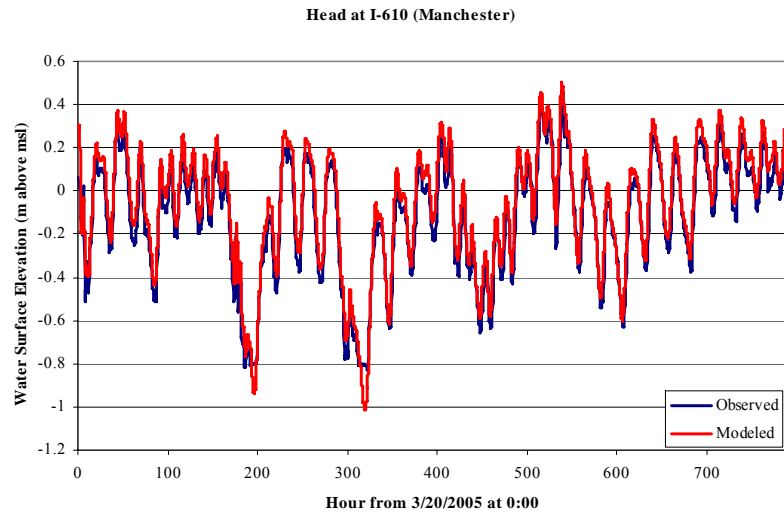
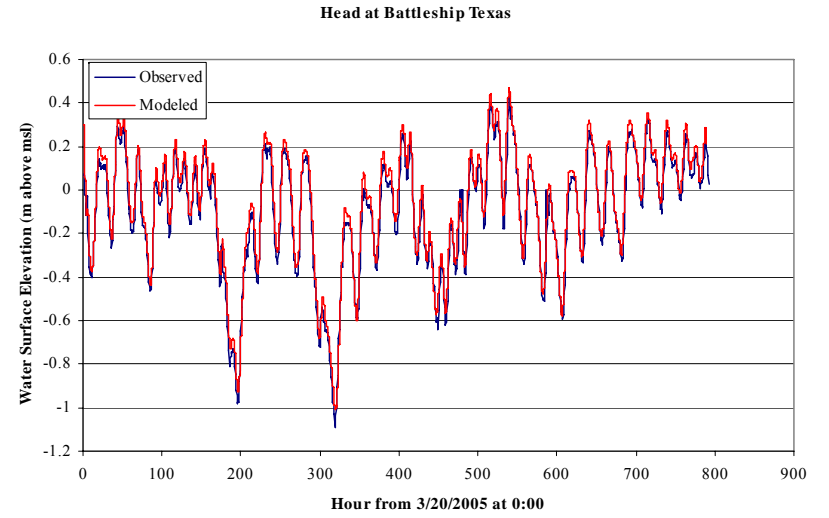
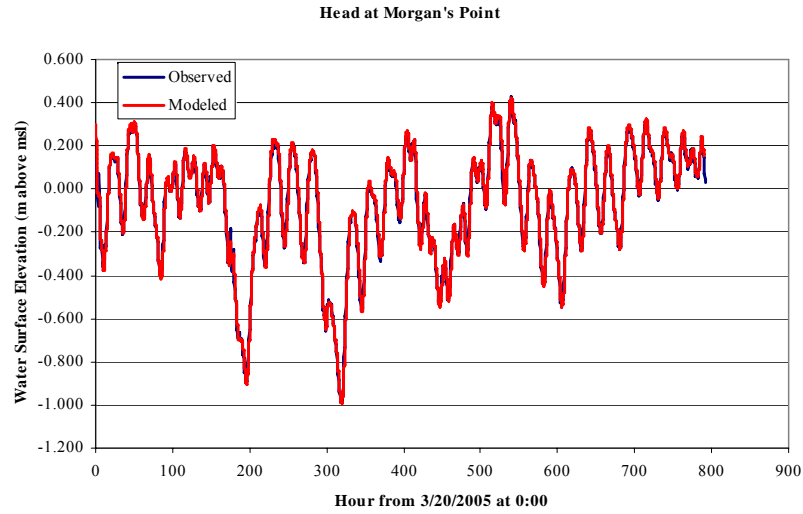


Figure 3.6 Observed and Simulated Water Surface Elevations in the HSC

was contacted to resolve this issue but no response has been received as of this writing.

Plots of modeled versus observed tide data are presented for the three NOAA stations in Figure 3.7. The best-fit line and the 1:1 line are also presented in the plots to aid in determining the goodness-of-fit. It can be seen that the regression lines are very close to the 1:1 line, with slopes around 1 and relatively small intercepts (between 0.7 and 6.6 cm). This observation confirms that the model is simulating the tide data well.

In addition to the plots previously presented, a variety of model statistics were calculated to measure model performance. These are discussed in Stow *et al.*, (2003) and Legates and McCabe (1999) and include:

1. the correlation coefficient of model predictions and observations, r :

$$r = \frac{\sum_{i=1}^n (O_i - \bar{O})(P_i - \bar{P})}{\sqrt{\sum_{i=1}^n (O_i - \bar{O})^2 \sum_{i=1}^n (P_i - \bar{P})^2}} \quad (3.4)$$

2. the model efficiency, MEF :

$$MEF = \frac{\sum_{i=1}^n (O_i - \bar{O})^2 - \sum_{i=1}^n (P_i - O_i)^2}{\sum_{i=1}^n (O_i - \bar{O})^2} \quad (3.5)$$

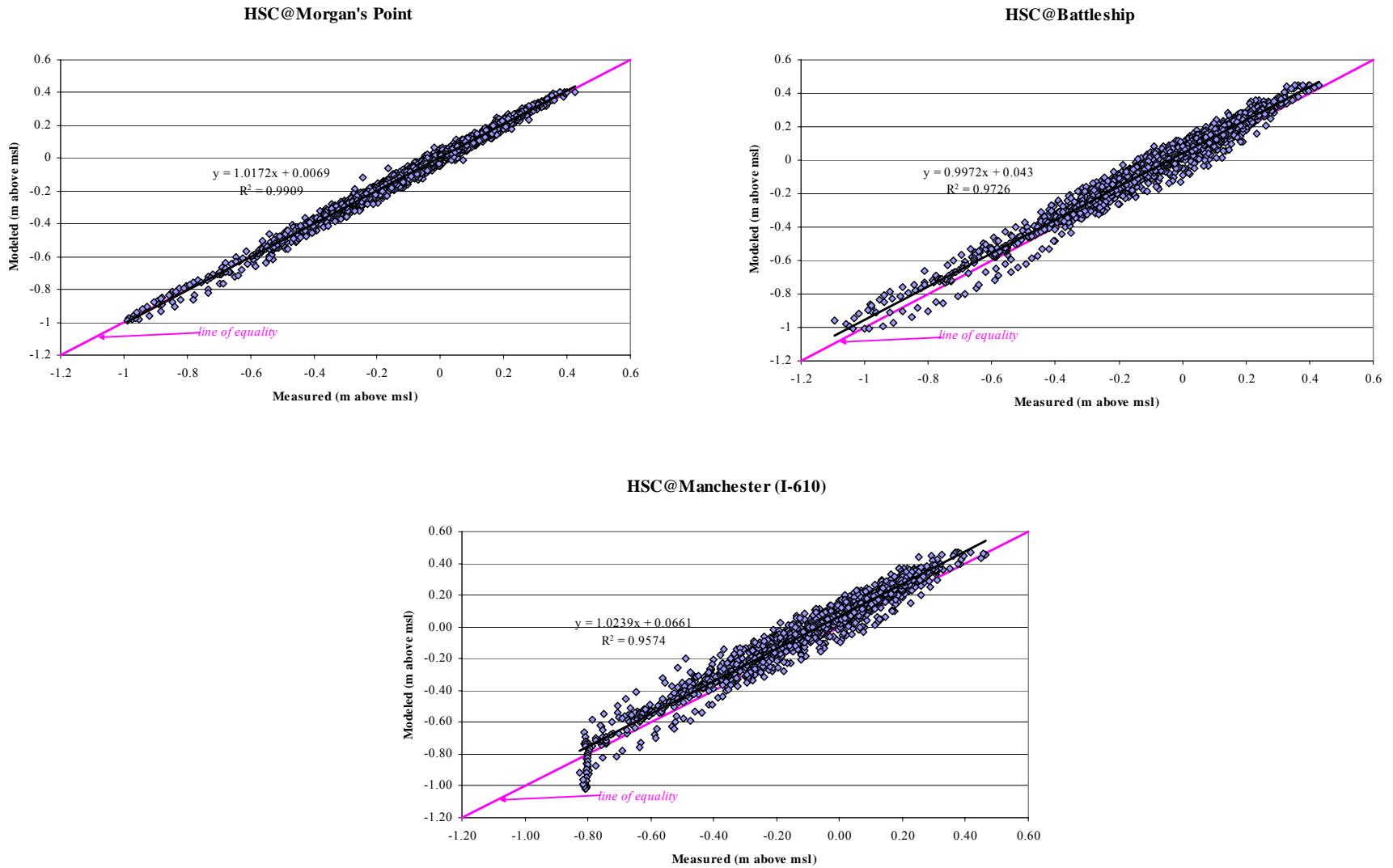


Figure 3.7 Scatterplots of Observed and Modeled Water Surface Elevations in the HSC

3. the index of agreement, d :

$$d = 1.0 - \frac{\sum_{i=1}^n (P_i - O_i)^2}{\sum_{i=1}^n (|P_i - \bar{O}| + |O_i - \bar{O}|)^2} \quad (3.6)$$

4. the root mean squared error, $RMSE$:

$$RMSE = \frac{\sqrt{\sum_{i=1}^n (P_i - O_i)^2}}{n} \quad (3.7)$$

where n =number of observations, O_i = i th of n observations, P_i = i th of n predictions, and \bar{O} and \bar{P} =observation and prediction averages, respectively.

The correlation coefficient, r , ranges from -1 to 1 and measures the tendency of the predicted and observed values to vary together linearly¹⁰. The model efficiency, MEF , measures how well a model predicts relative to the average of observations; a value close to 1 indicates a good match between observations and model predictions. The index of agreement, d , varies from 0 to 1 , with higher values indicating better agreement between the model and observations. Finally, the root mean squared error, $RMSE$, measures the magnitude of the discrepancies between predicted and observed values, with values close to zero indicating a good match. A summary of the different statistics calculated for water surface elevations at the various gages is presented in Table 3.6. Results presented in Table 3.6 indicate an excellent level of agreement between predicted and observed values.

¹⁰ This parameter is equivalent to the square root of the coefficient of determination (r^2) of the best-fit line presented in Figure 3.7.

Table 3.6 Model Summary Statistics for Water Elevations

Statistic	HSC@Morgan’s	HSC@Battleship	HSC@I-610
<i>r</i>	0.996	0.992	0.986
MEF	0.991	0.960	0.915
<i>d</i>	0.998	0.990	0.987
<i>RMSE(m)</i>	0.001	0.001	0.002

Velocity and Flow

The model was calibrated to the velocities and flows measured in the channel during Spring 2005. The locations of the observation points are shown in Figure 3.8. The calibration procedure was as follows: first, the average cross-section areas for the entire simulation period were calculated for each location to verify that they were within acceptable criteria ($\pm 10\%$ of the measured areas); second, the velocity time-series were compared to the measured data, model parameters (Manning’s *n* and off-channel storage slope) were adjusted until the velocity series matched the ranges of measured values; and, finally, once cross-sectional areas and velocities were calibrated, output flow time-series were compared to measured flows to verify the model results. Table 3.7 summarizes the percent error in average cross-sectional areas predicted by the model.

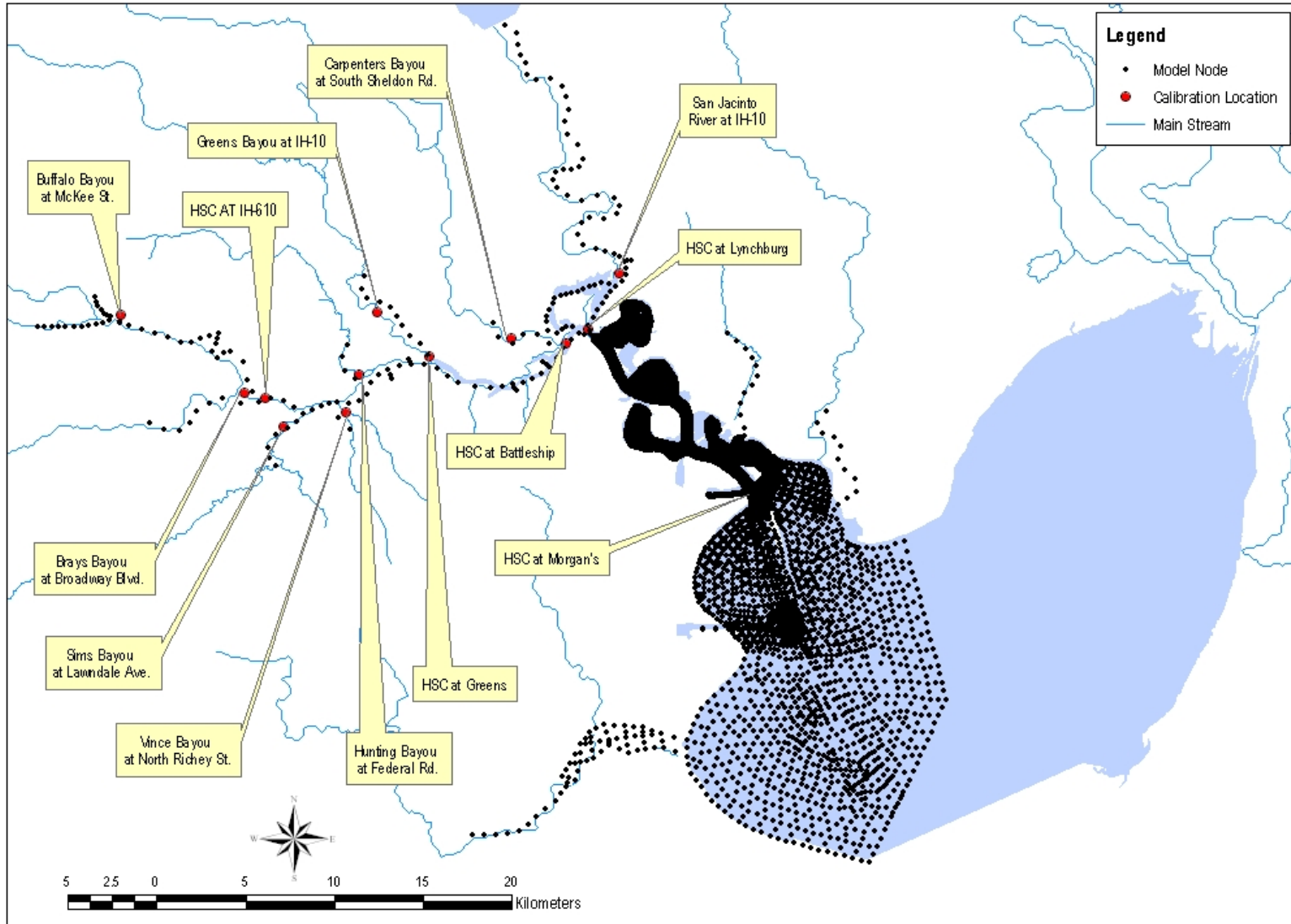


Figure 3.8 Velocity and Flow Calibration Locations

Table 3.7 Difference between Measured and Predicted Cross-sectional Areas

Location	Model node	Average Measured Area (m ²)	Average Modeled Area (m ²)	Error ^b
HSC@Morgan's Point	NA ^a	3853	4023	4%
HSC@Lynchburg Ferry	2753	4330	3955	-9%
HSC@Battleship	2951	3824	3835	0%
Carpenters Bayou@Sheldon Rd	2963	69	74	7%
San Jacinto River@I-10	2957	1438	1312	-9%
HSC@Greens Bayou	3015	2250	2101	-7%
Greens Bayou&I-10	3031	247	246	0%
Hunting Bayou@Federal Rd	3055	103	97	-6%
Vince Bayou@North Richey St	3071	132	122	-8%
Sims Bayou@Lawndale Ave	3085	169	158	-7%
HSC@I-610	3087	1542	1492	-3%
Brays Bayou@Broadway Blvd	3097	300	332	11%
Buffalo Bayou@McKee St	3118	137	150	9%

^a This observation location is in the 2-D section of the model, so parameters were calculated for a continuity line rather than at a single node

^b Error was calculated as $\frac{(A_{\text{mod}} - A_{\text{obs}})}{A_{\text{obs}}} \cdot 100\%$

Figure 3.9 displays the time series of observed and predicted water velocities for the thirteen sampled locations. While there is some deviation between observed and modeled velocities (especially for some of the tributaries), the ranges of predicted values correspond to those measured in the field. It should be recognized that there is substantial error or uncertainty in the flow measurement data, and in regression-based flow predictions based on those measurements. This error is due both to measurement problems, as well as temporal error and the fact that the flows are constantly changing with tide while flow measurements take several minutes. Thus, when looking at calibration results for an individual site, the measurement may be as much or more responsible than the model for the calibration error.

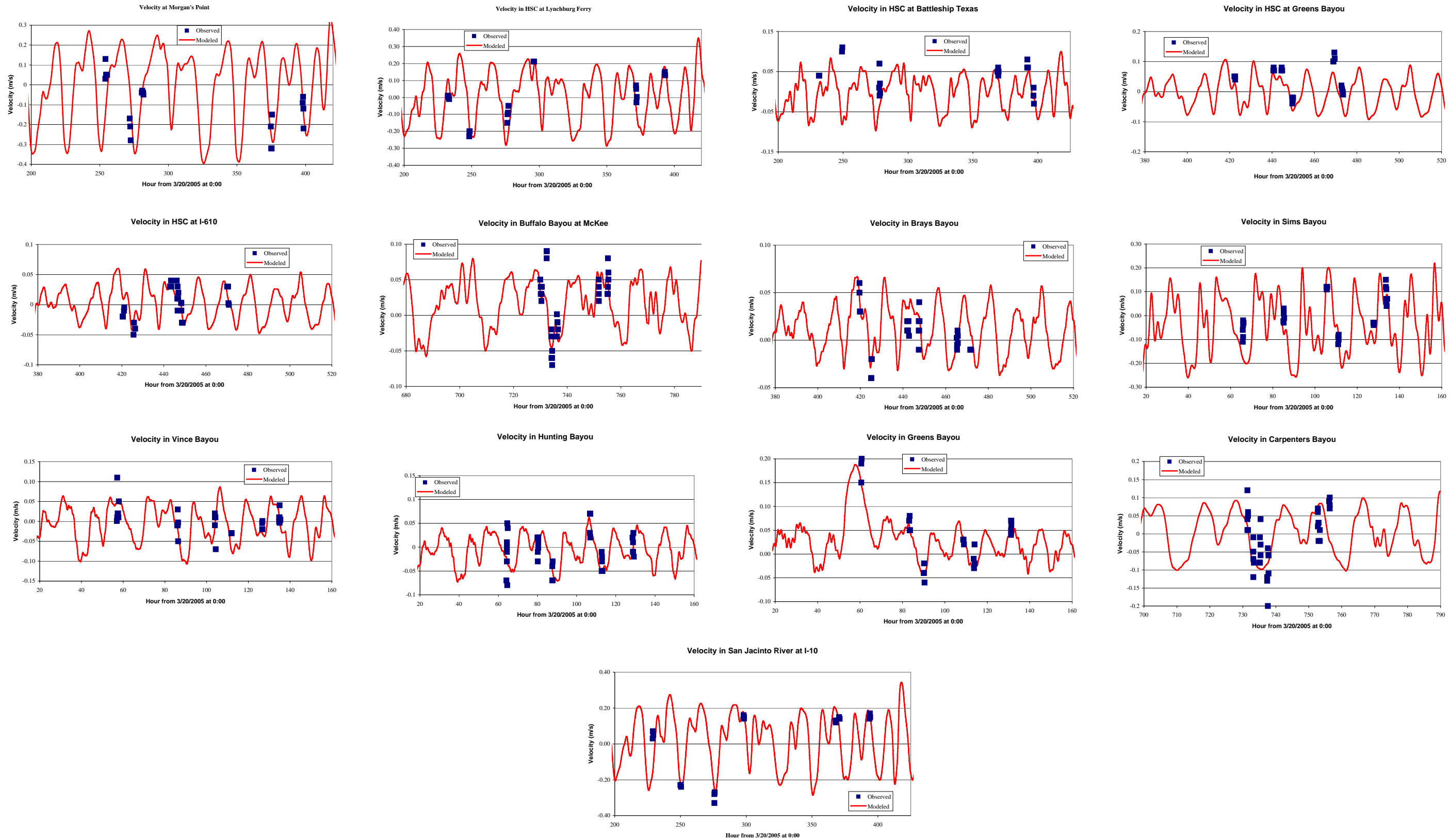


Figure 3.9 Modeled and Measured Water Velocities

Similarly, Figure 3.10 provides a graphic comparison of predicted to measured flows at the thirteen observation locations in the HSC system. As expected from the calibration of cross-sectional areas and water velocities, the model predicts reasonably well the magnitude and direction of the flows.

To measure model performance, scatterplots of modeled versus observed data were prepared and compared to 1:1 lines for all the observation locations (Figures 3.11 and 3.12). When one-to-one comparisons are made, the model performance is rather poor. The best results were obtained for HSC@Lynchburg, HSC@Greens, San Jacinto River, Greens Bayou, Sims Bayou, and Brays Bayou. One-to-one calibration at HSC@Battleship showed the worst results, with a best-fit-line slope near zero. It is noted, however, that a comparison between the time series produced by the model and a few observations available for each location is, by itself, not an indication of overall model performance. Furthermore, in most of the tributaries several measurements that varied within a relatively wide range were made within a period of an hour or shorter. The model is not expected to simulate these sudden changes in velocity and flow. This caused the slopes of the best-fit lines to be significantly different from 1.

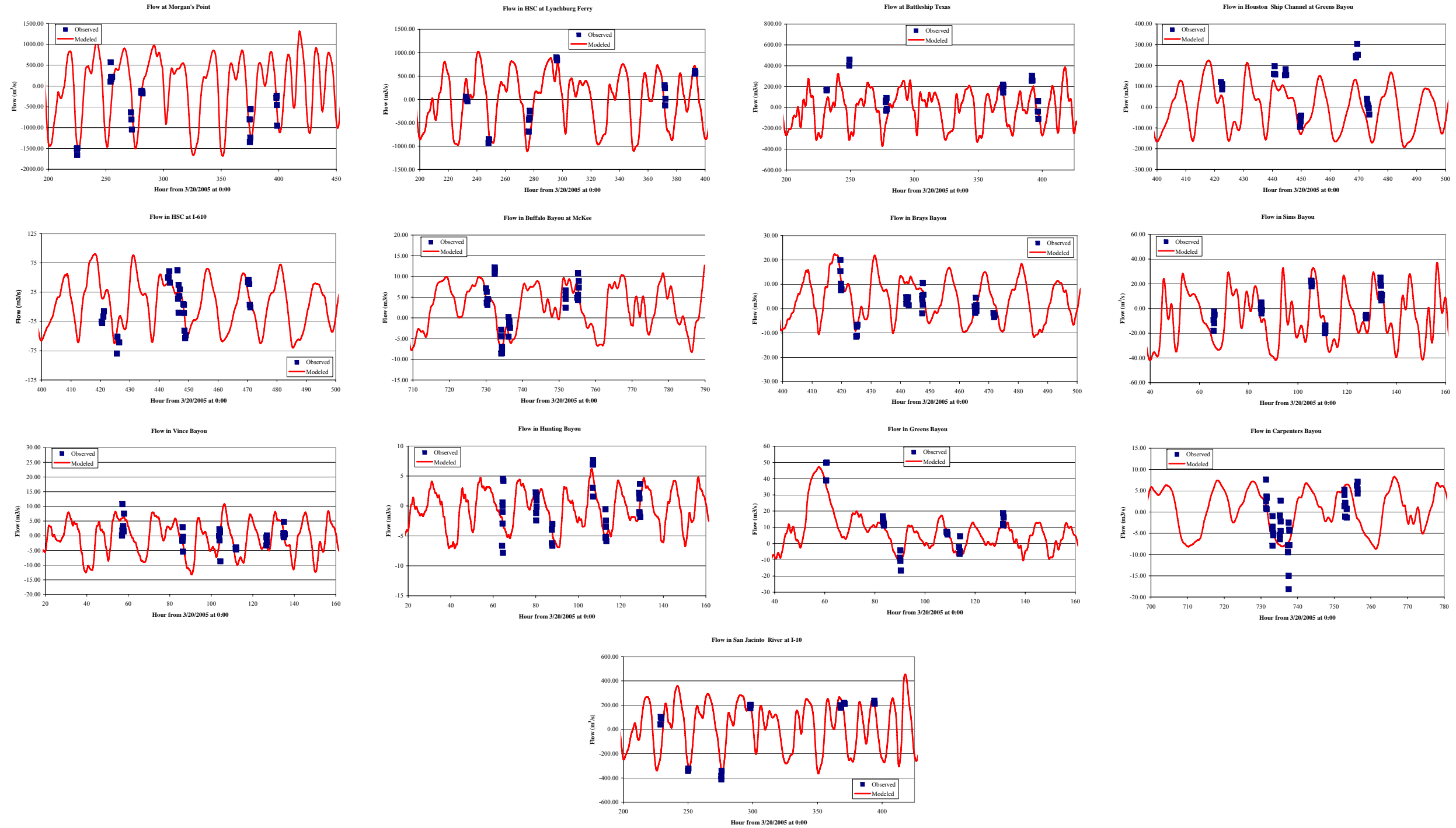


Figure 3.10 Modeled and Measured Water Flows

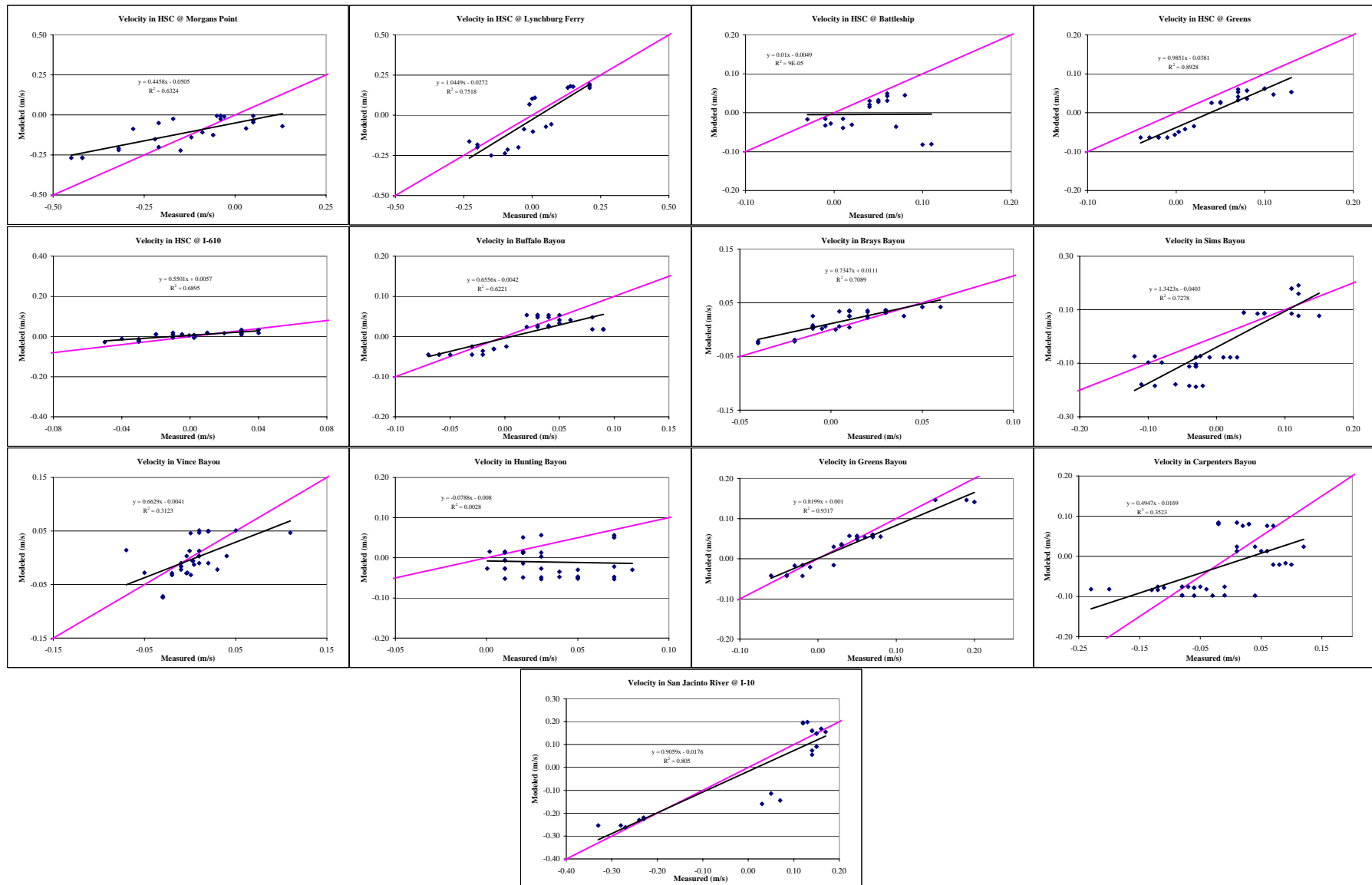


Figure 3.11 Observed and Modeled Water Velocities using Discrete Measured Values

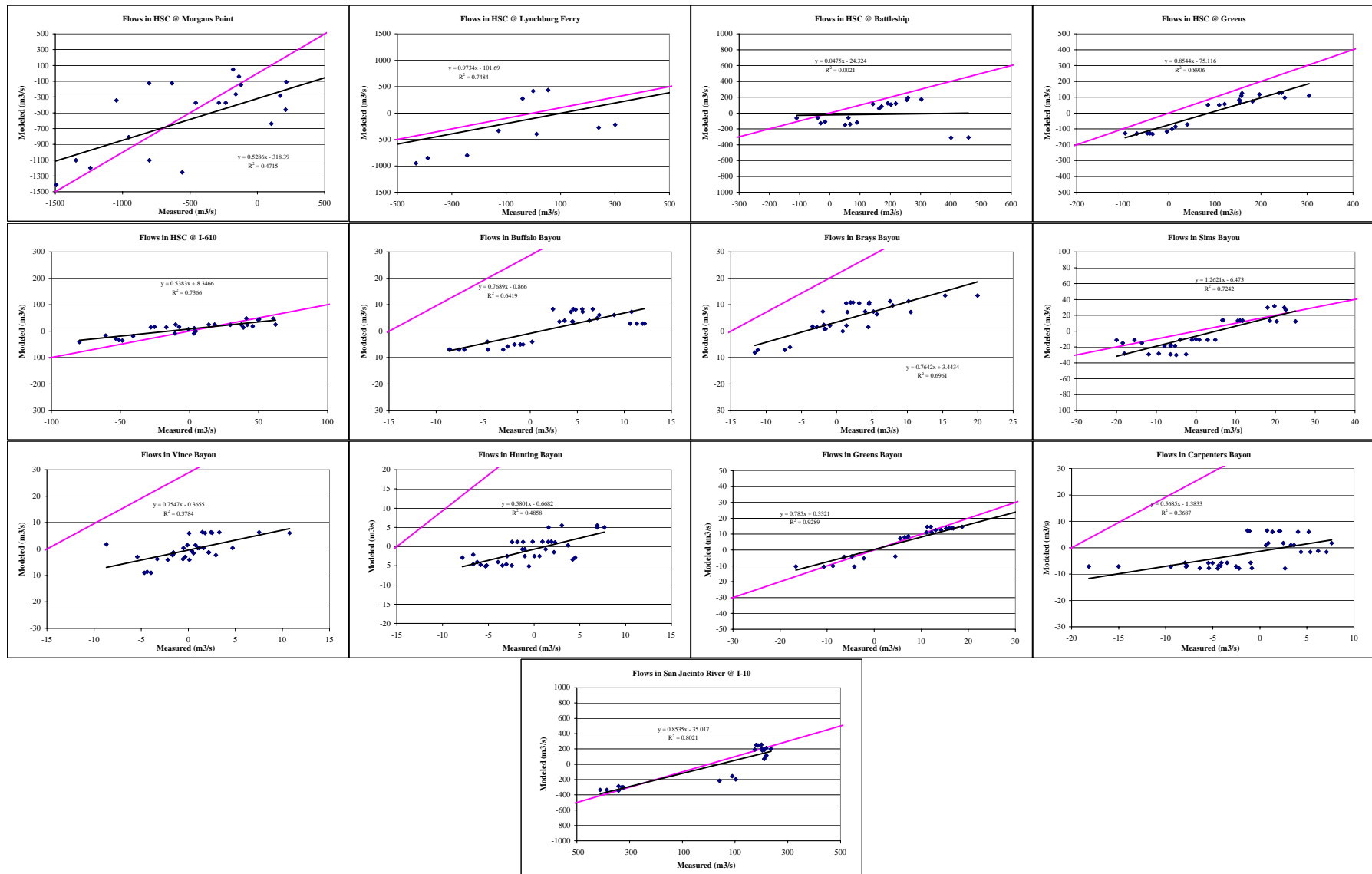


Figure 3.12 Observed and Modeled Water Flows using Discrete Measured Values

In order to get a reflection of how well the model reproduces the overall patterns, a second criterion was applied, as shown in Figures 3.13a through m. The criterion used in the figures consists of comparing the model flow output (blue line) to continuous time-series developed by the project team using linear regressions (green line) between the measured flows and the change in height for the various locations (University of Houston, 2005b)¹¹. For this criterion, the calibration targets included the coefficient of determination (r^2) and the flow duration curve. The top plots, comparisons of model results with the flows from regressions, clearly show that the model output reflects the magnitude and pattern of the observed data for most locations. For the main channel (Figures 3.13a to 3.13e), the model performance is good based on r^2 values varying between 0.61 and 0.92. In addition, the simulation agrees well with the observed flow duration curves across all flow conditions, with the exception of the location in Greens Bayou where positive flows are being underpredicted while negative flows are slightly overpredicted. For the tributaries, the best results were obtained for Carpenters Bayou and the San Jacinto River. While the model is overpredicting the negative flows for Buffalo, Vince, Sims, and Hunting Bayous, and is overpredicting most of the flows for Brays Bayou, results are within reasonable ranges and the model was considered calibrated.

¹¹ The green line shown corresponds to a smoothing of the regression presented in the Final Report for WO7. In addition, the regression for San Jacinto River presented in the Final Report for WO No. 582-0-80121-07 was modified to include the impact of freshwater inflows. The updated regression statistics are included in Appendix C.

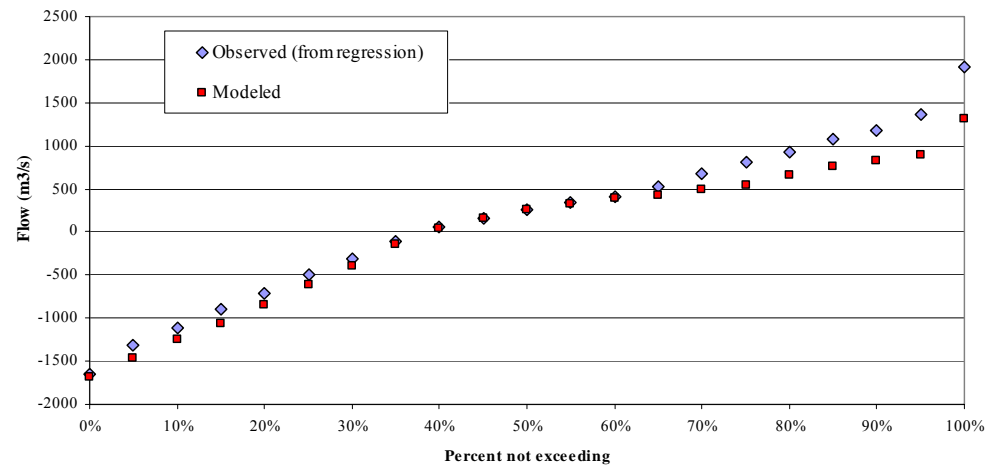
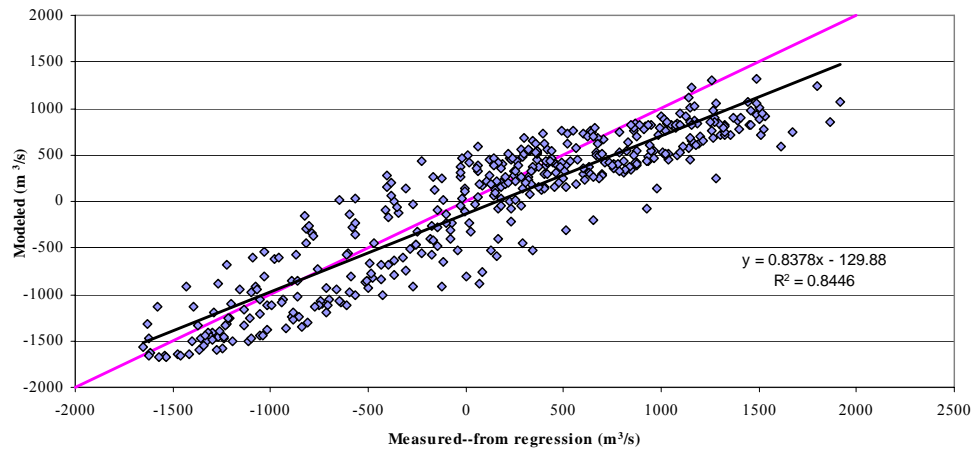
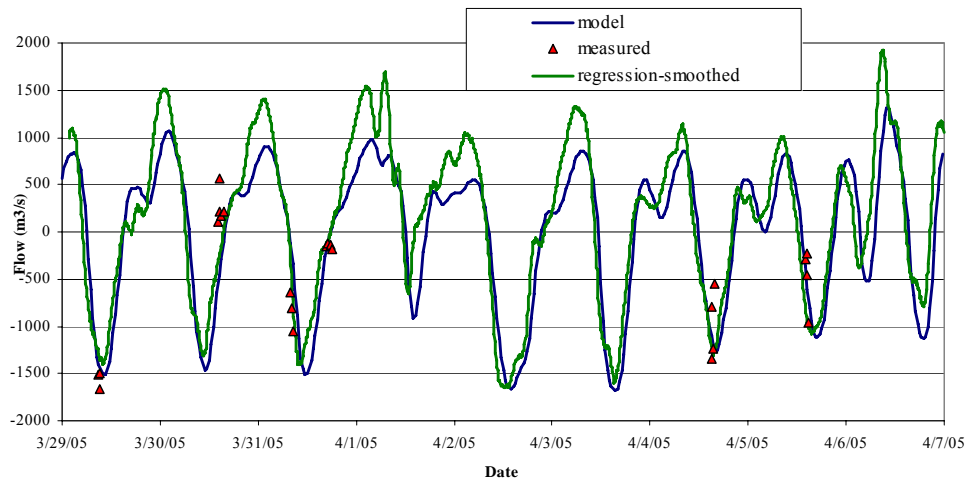


Figure 3.13a Goodness of Fit for HSC @ Morgans Point using Flow Regression

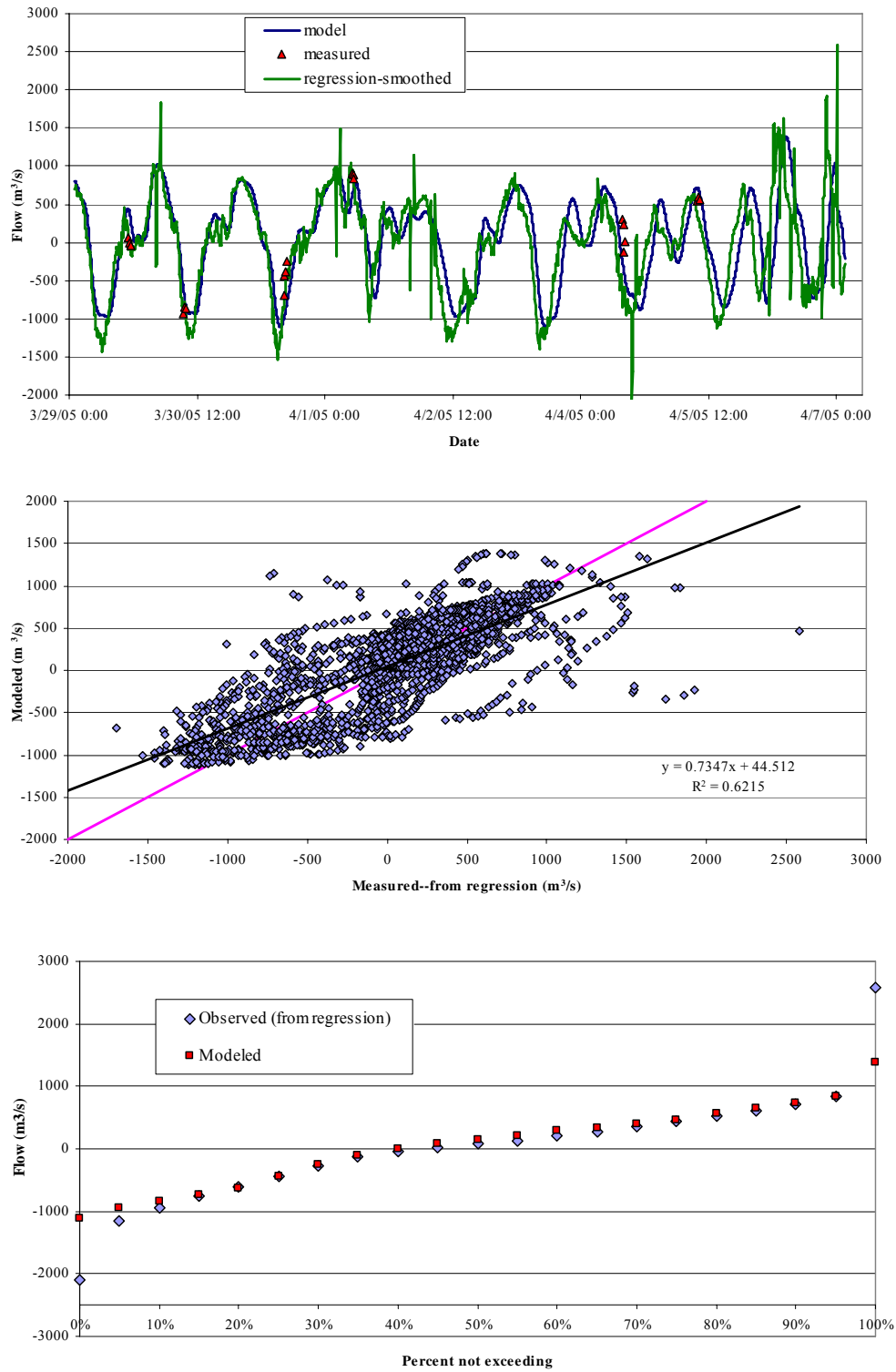


Figure 3.13b Goodness of Fit for HSC @ Lynchburg using Flow Regression

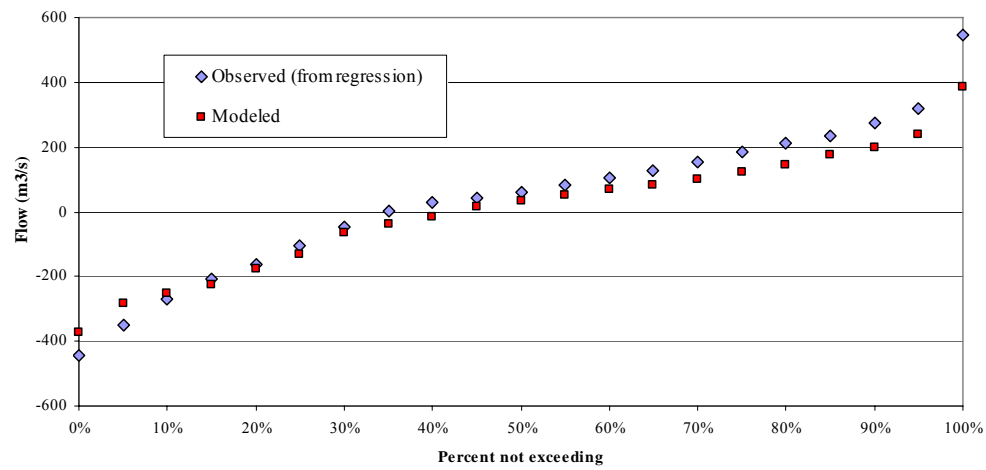
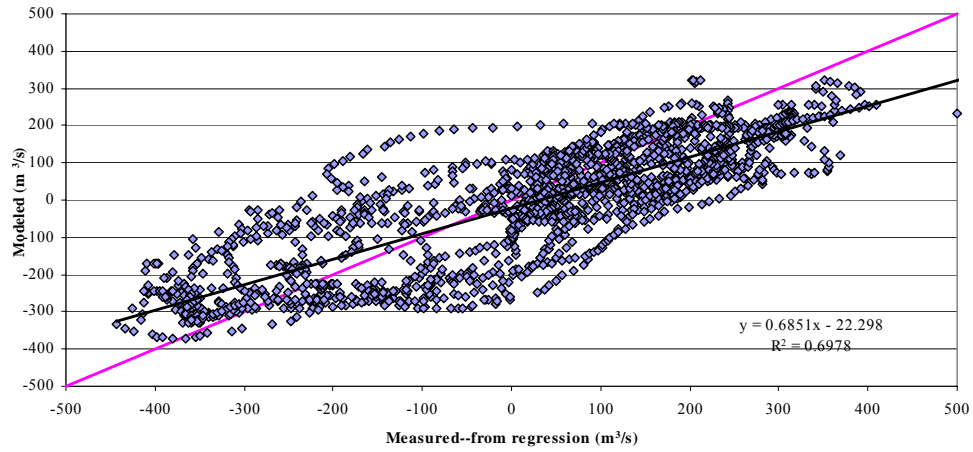
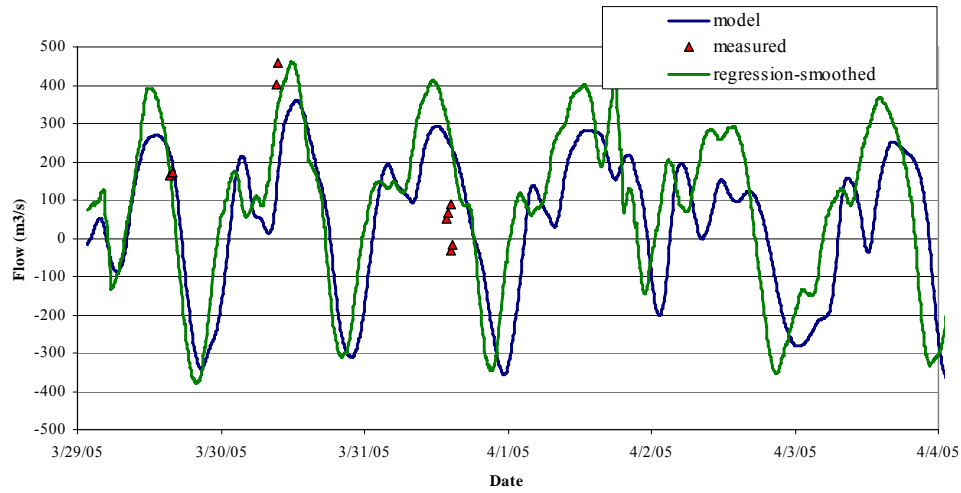


Figure 3.13c Goodness of Fit for HSC @ Battleship using Flow Regression

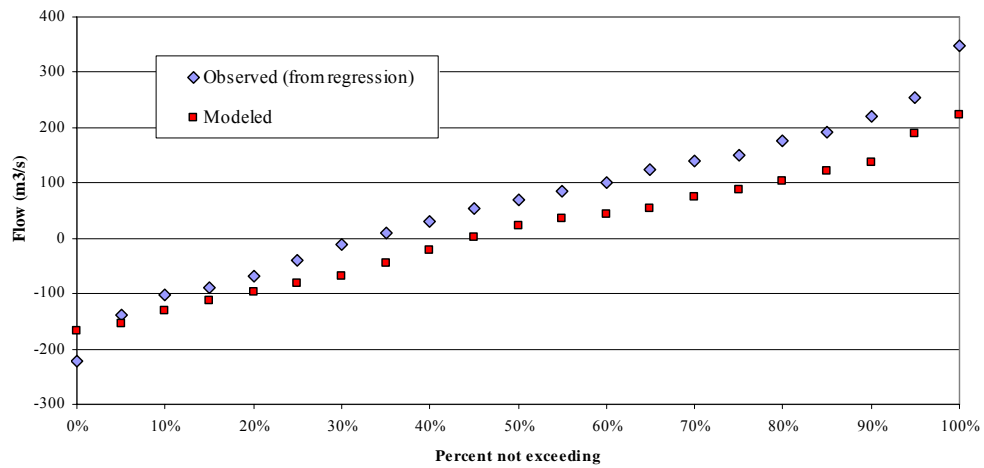
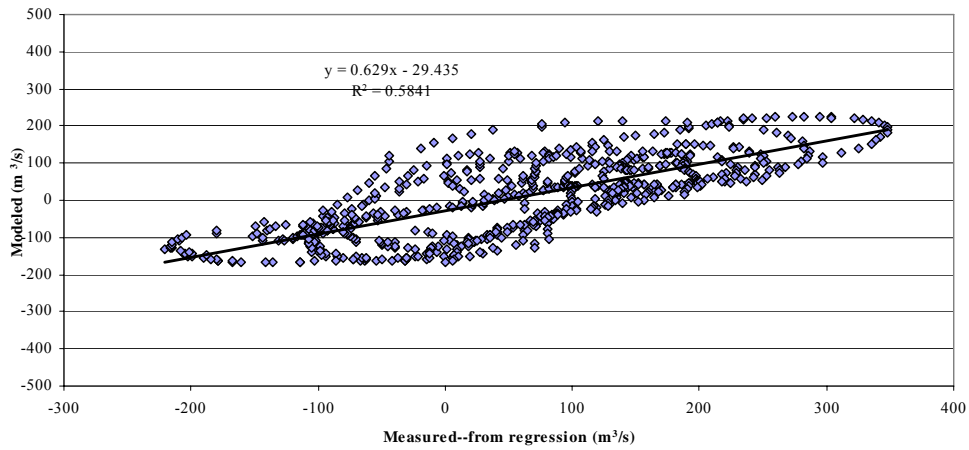
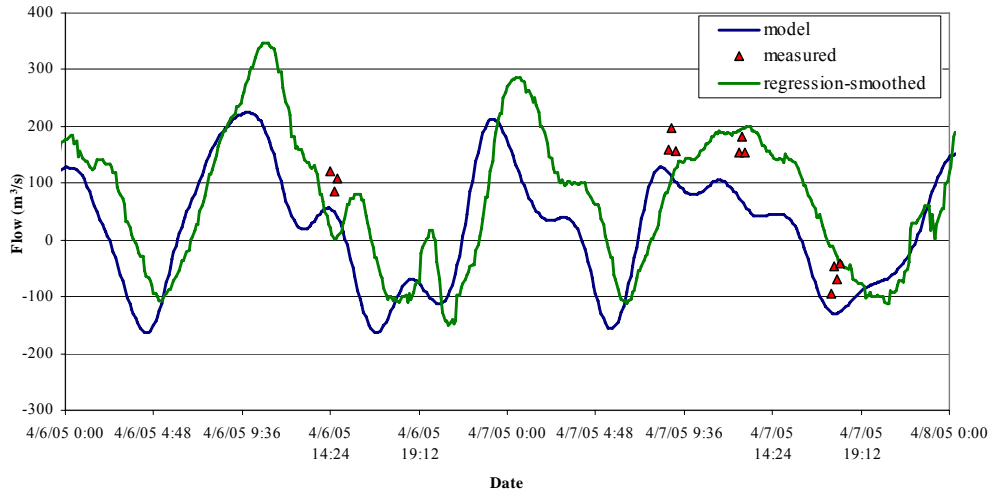


Figure 3.13d Goodness of Fit for HSC @ Greens using Flow Regression

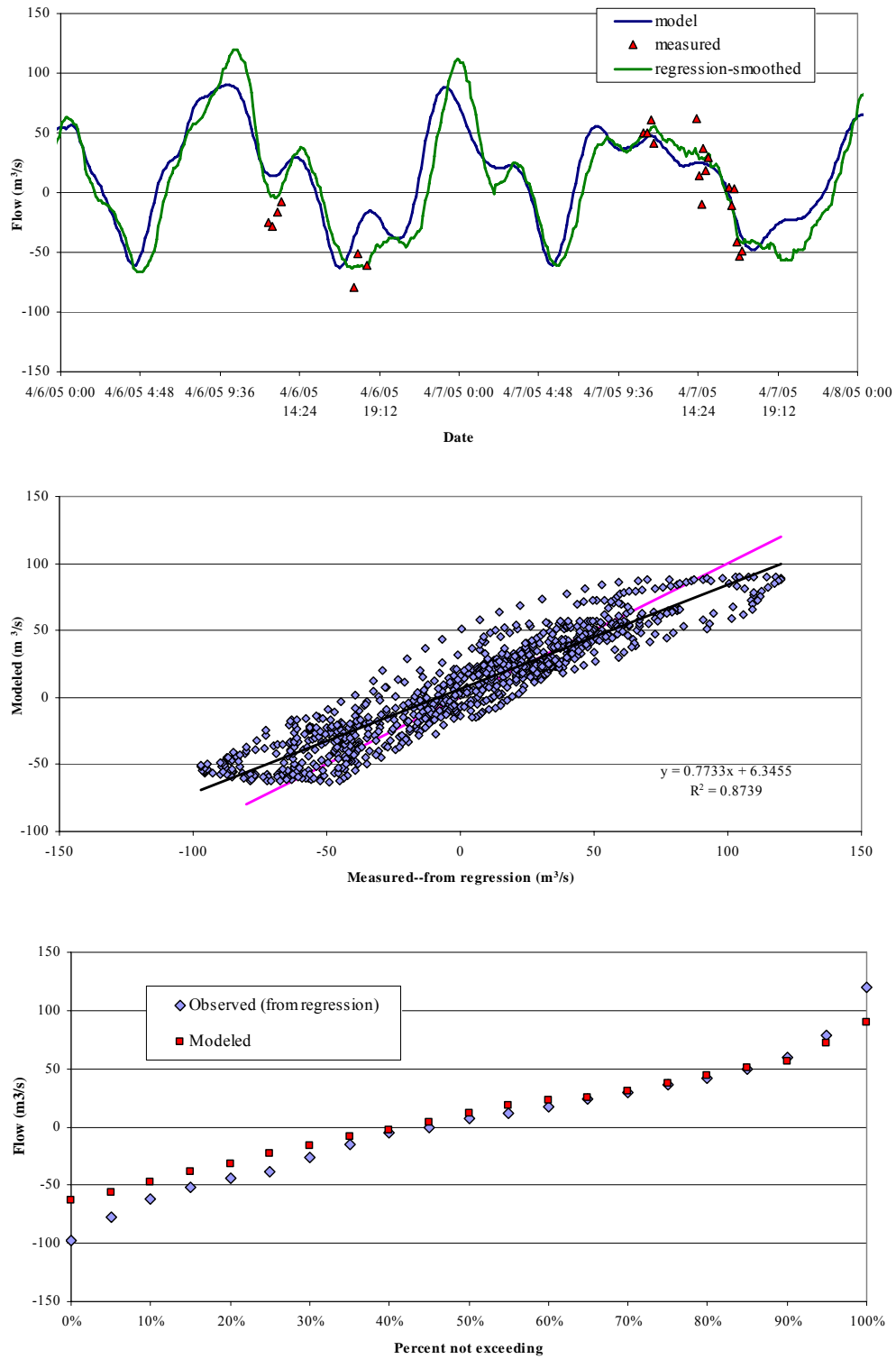


Figure 3.13e Goodness of Fit for HSC @ I-610 using Flow Regression

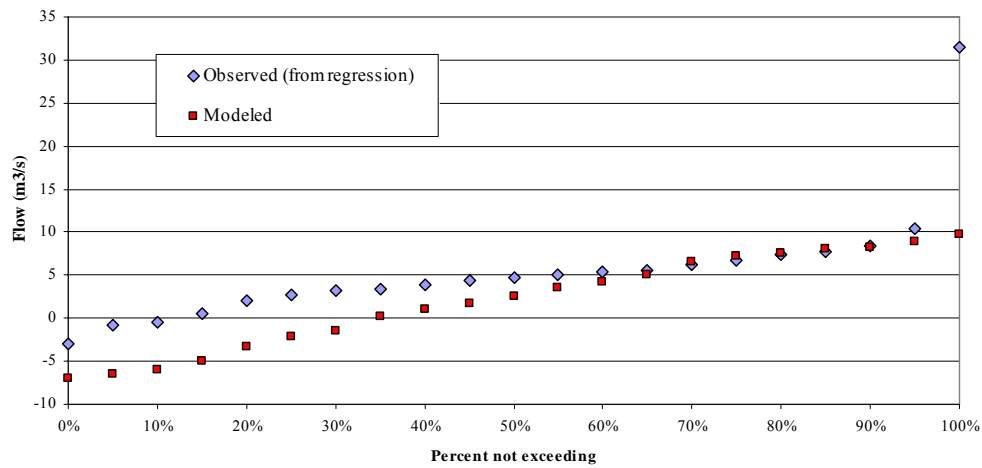
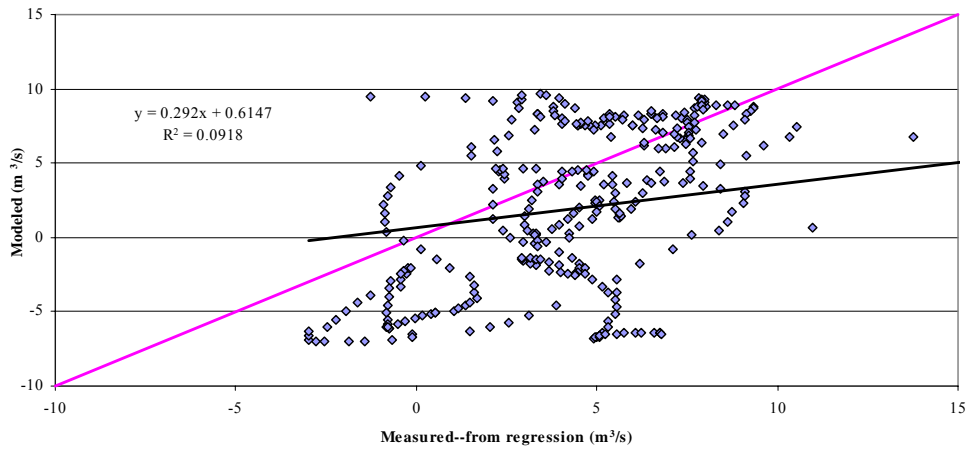
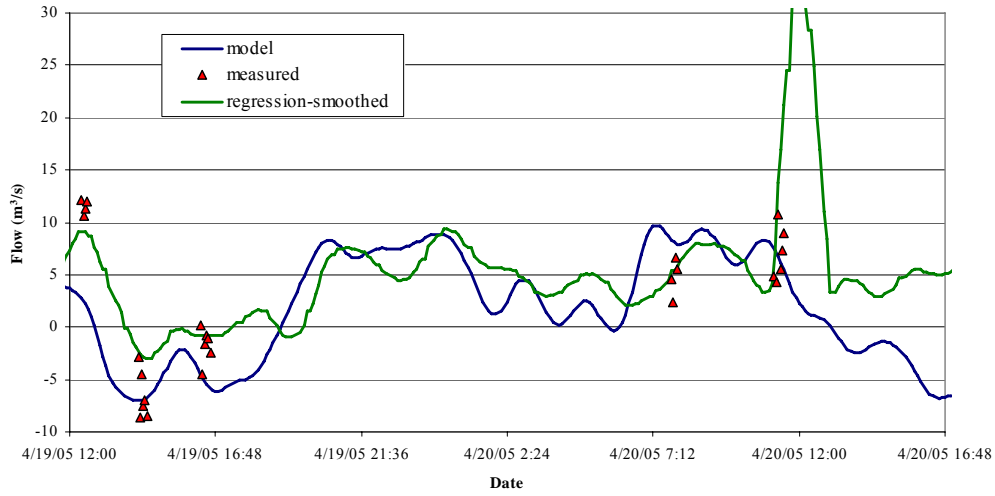


Figure 3.13f Goodness of Fit for Buffalo Bayou using Flow Regression

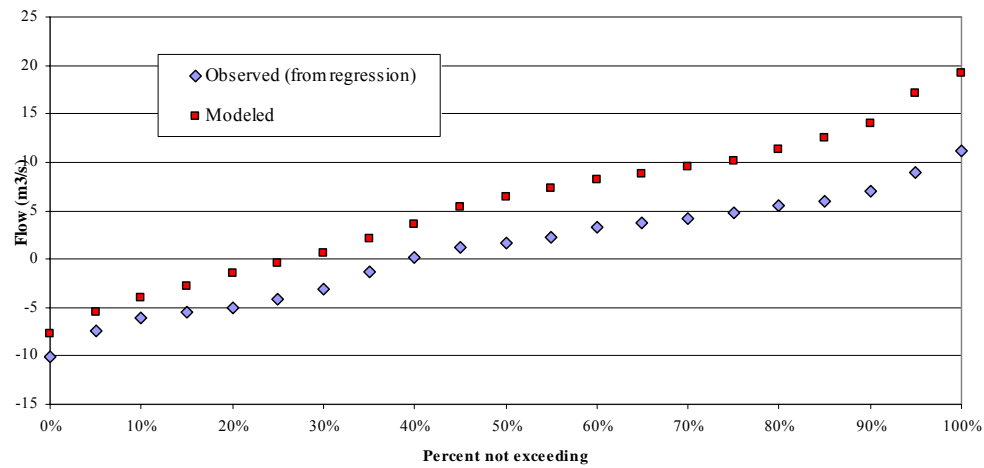
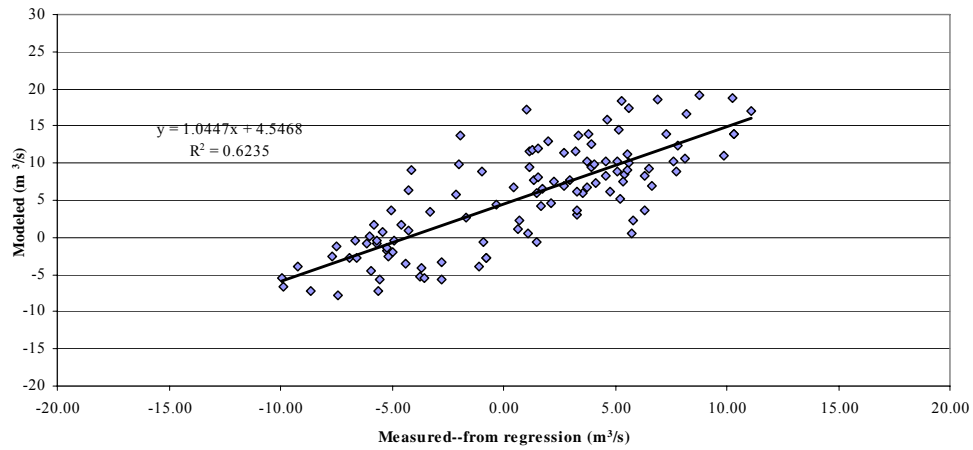
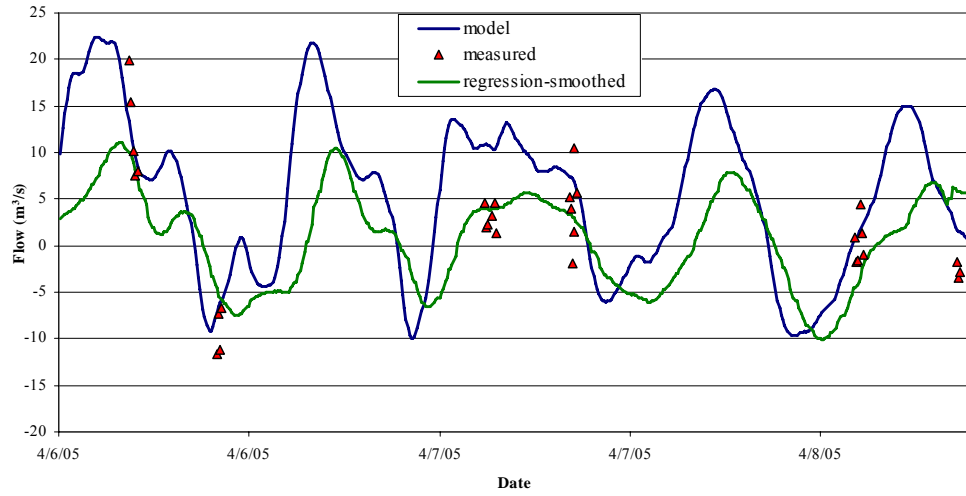


Figure 3.13g Goodness of Fit for Brays Bayou using Flow Regression

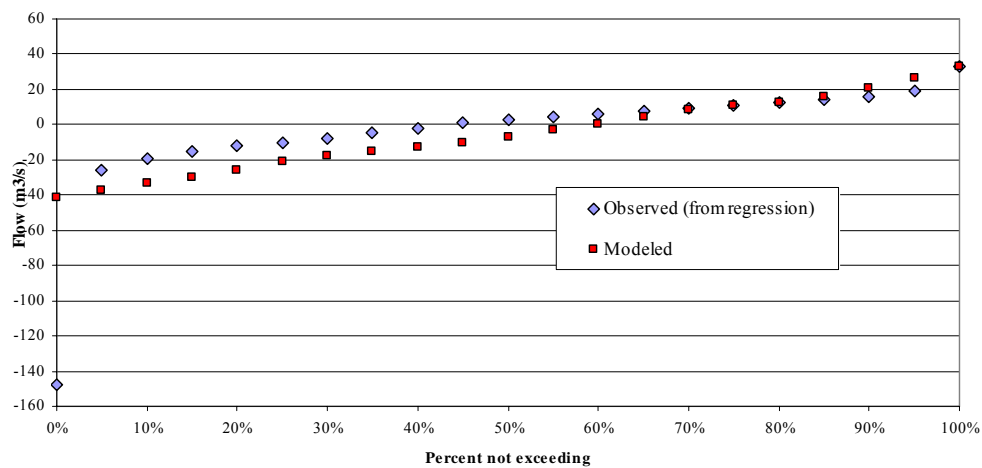
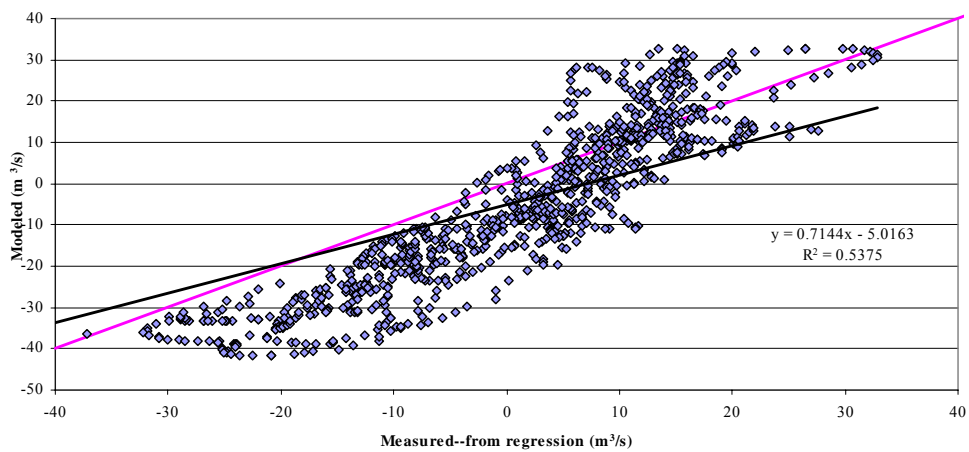
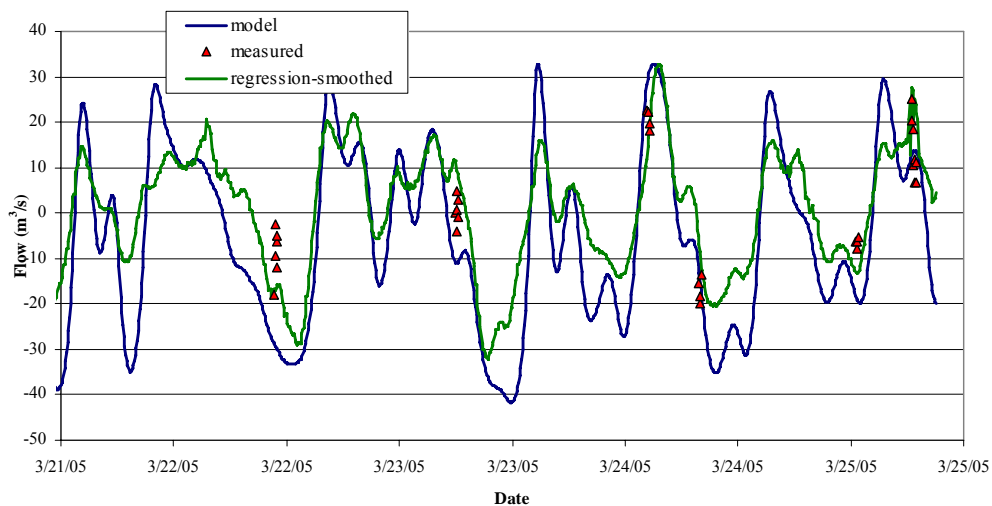


Figure 3.13h Goodness of Fit for Sims Bayou using Flow Regression

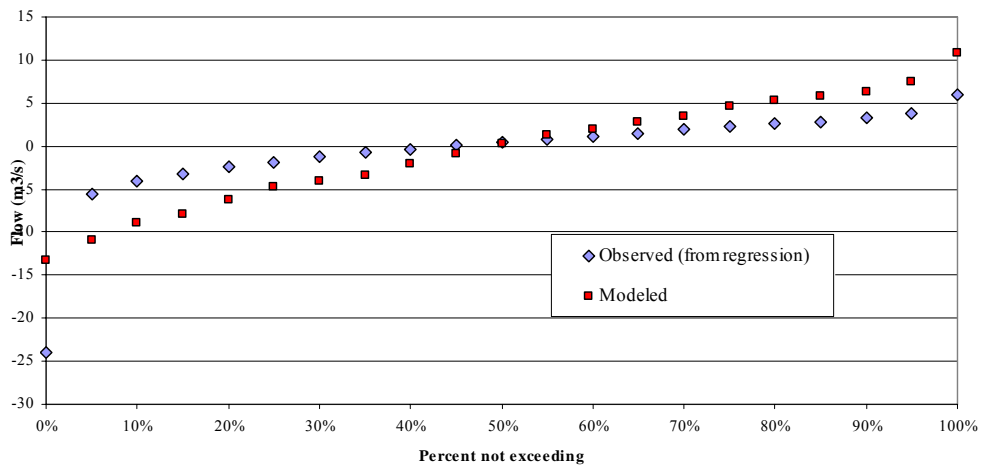
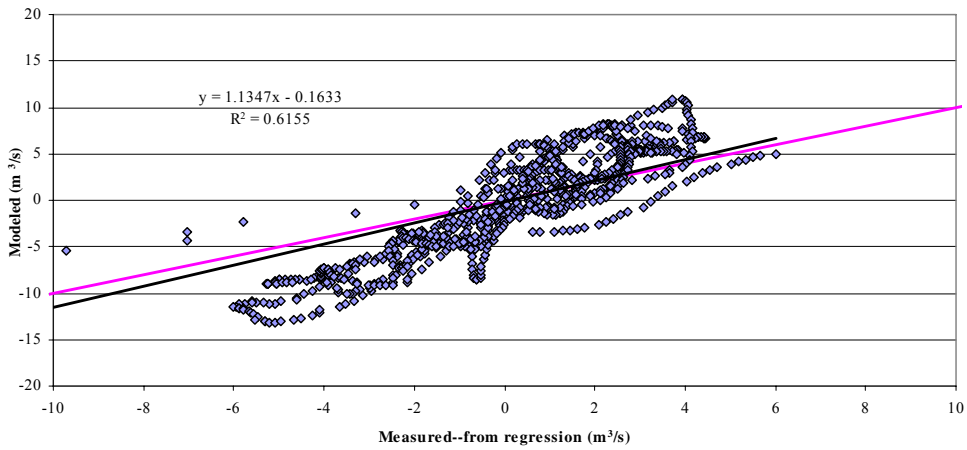
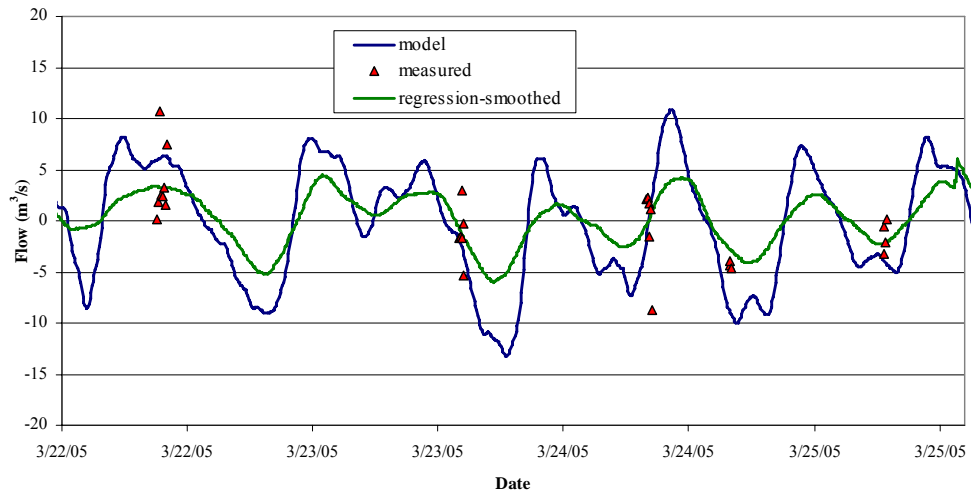


Figure 3.13i Goodness of Fit for Vince Bayou using Flow Regression

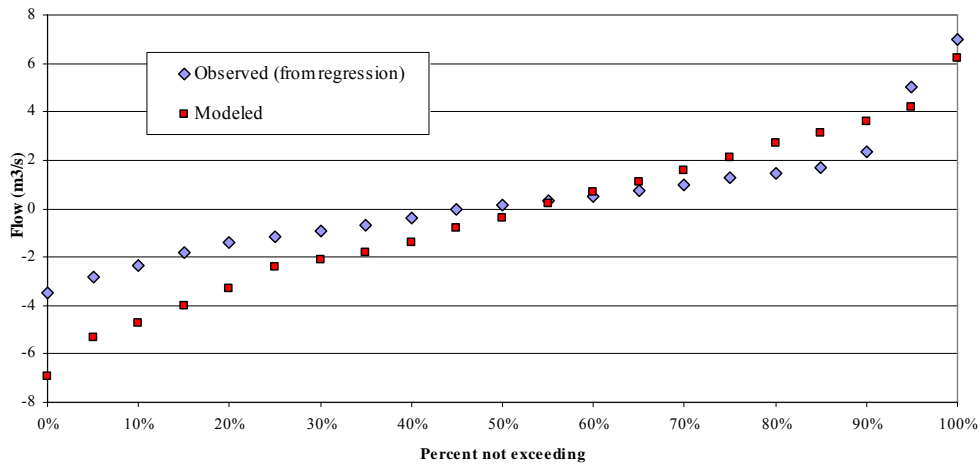
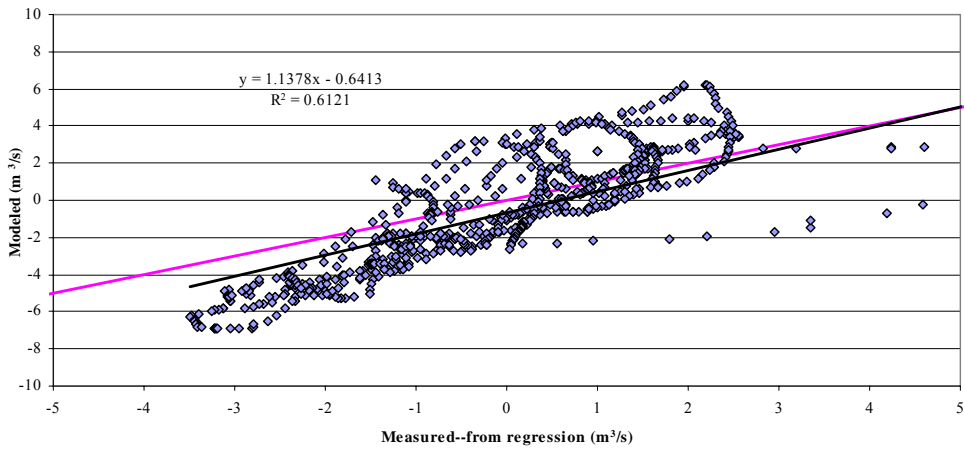
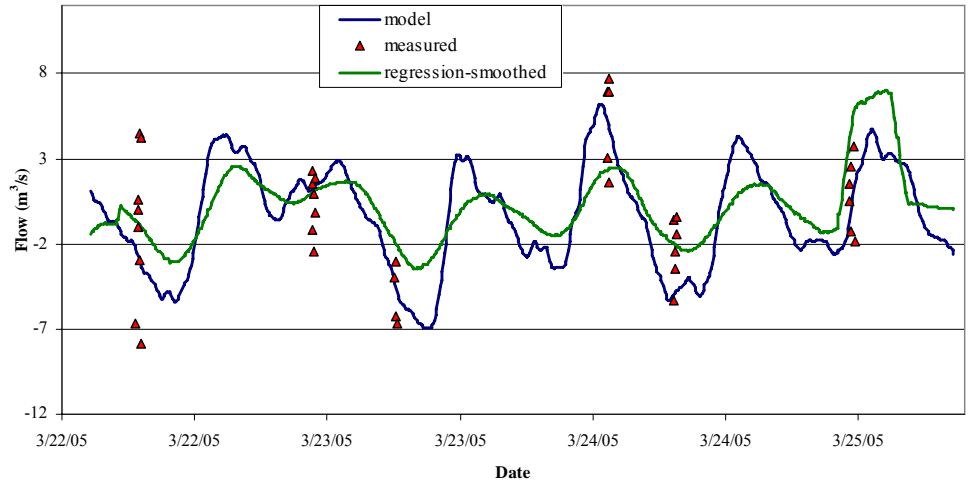


Figure 3.13j Goodness of Fit for Hunting Bayou using Flow Regression

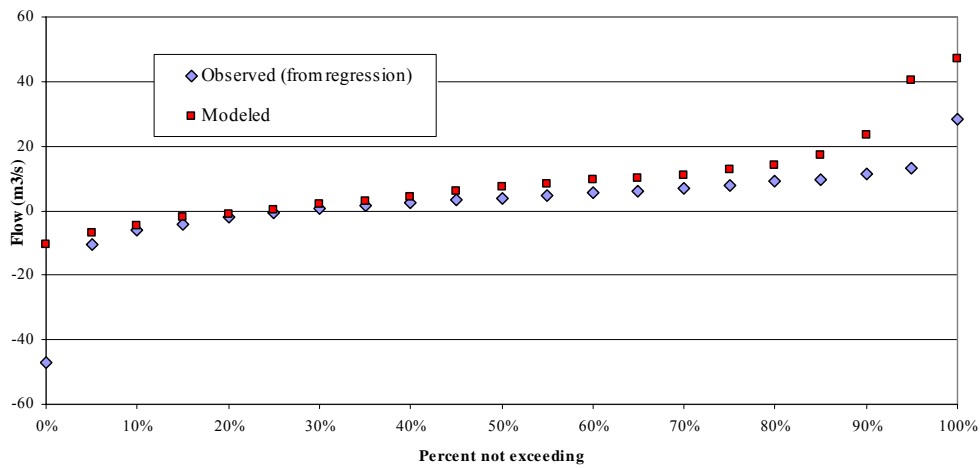
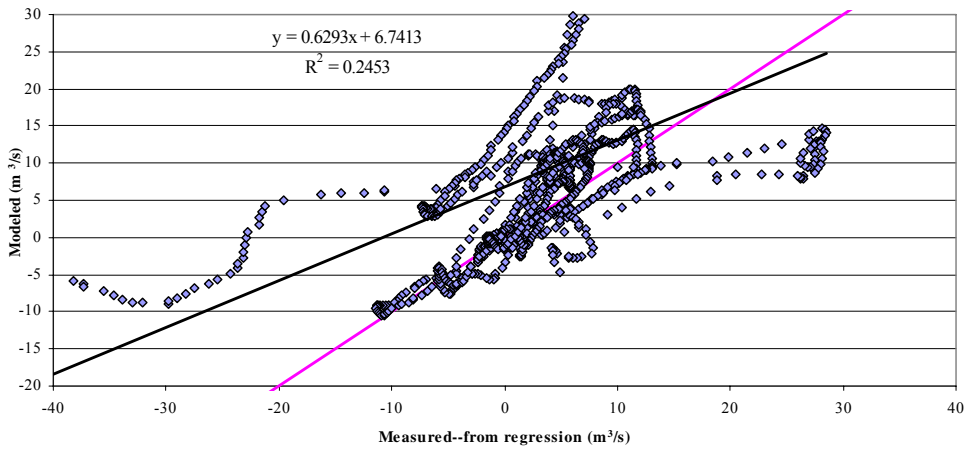
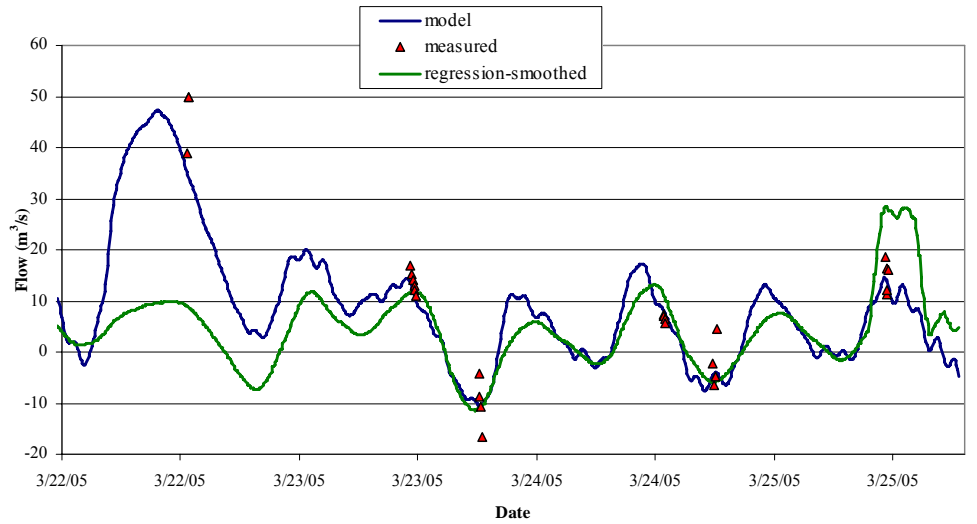


Figure 3.13k Goodness of Fit for Greens Bayou using Flow Regression

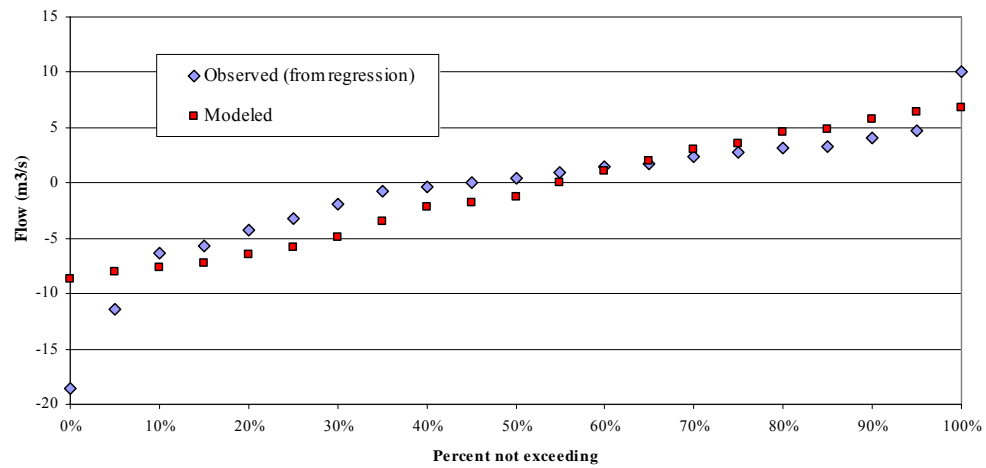
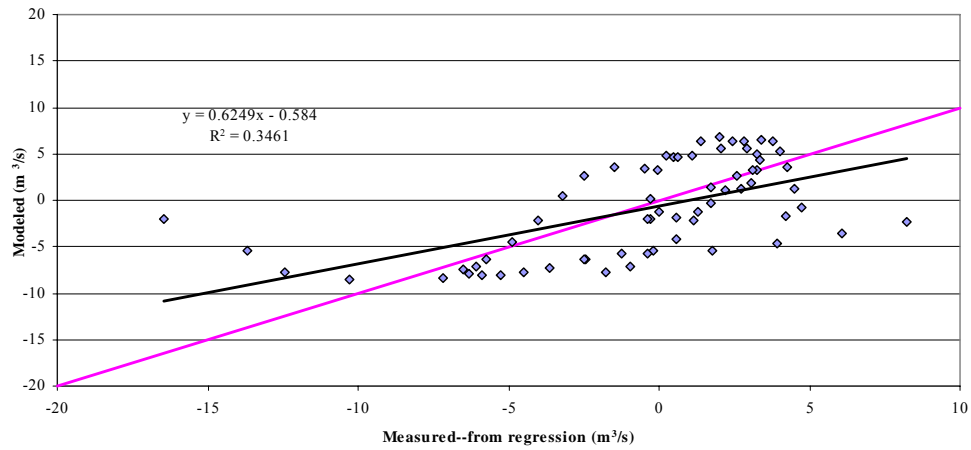
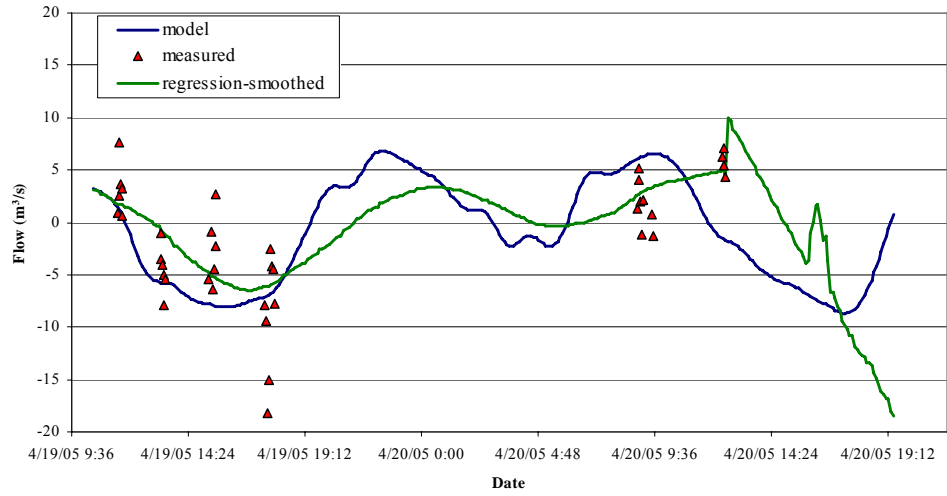


Figure 3.13l Goodness of Fit for Carpenter's Bayou using Flow Regression

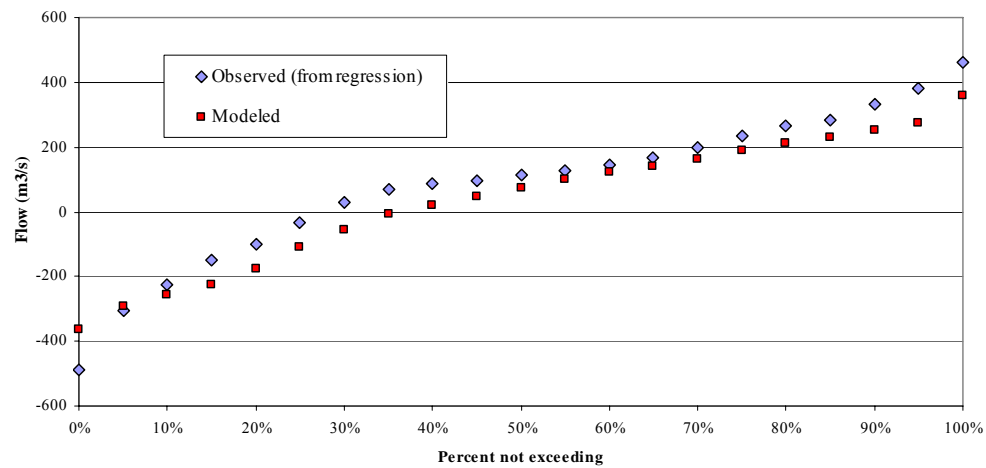
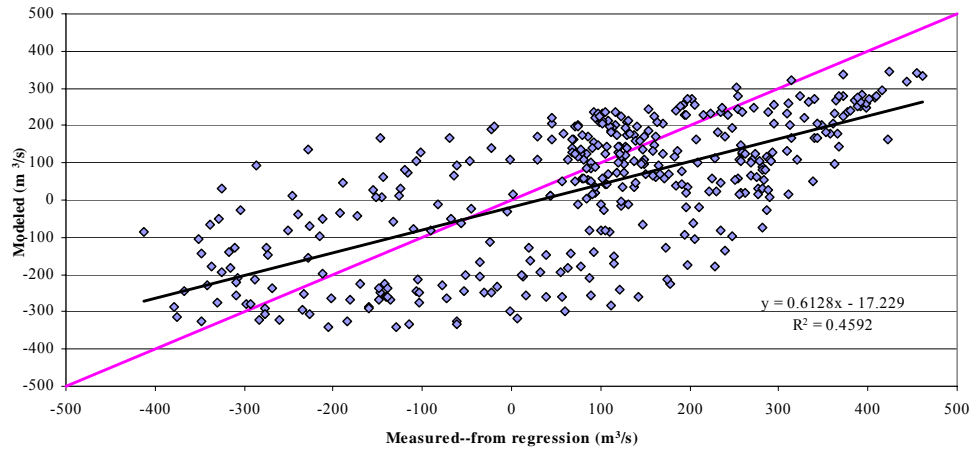
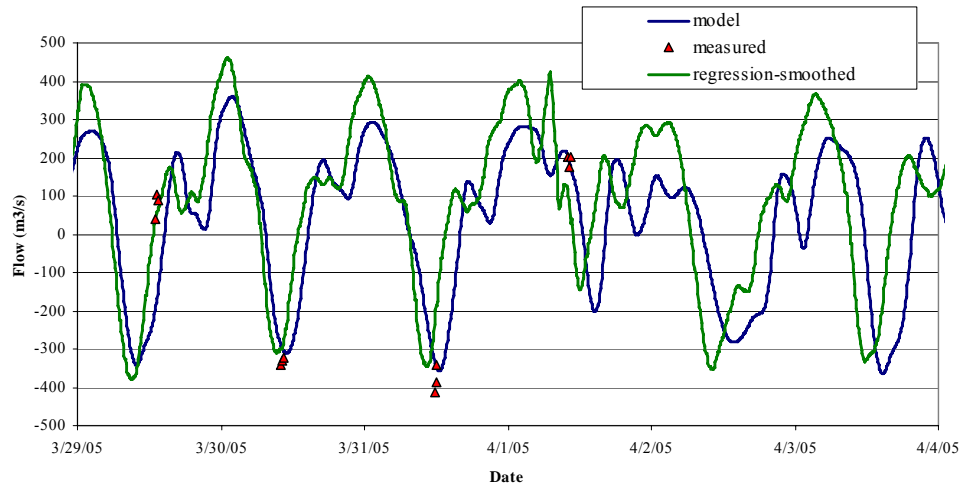


Figure 3.13m Goodness of Fit for San Jacinto River @ I-10 using Flow Regression

Finally, the statistics described in Equations 3.4 through 3.7 were computed to quantify model performance and compare the goodness-of-fit for the different locations. The summary statistics are presented in Table 3.8.

Table 3.8 Model Summary Statistics for Water Flows

Observation Point	r^a	MEF^b	d^c	$RMSE (m^3/s)$
HSC@Morgan's	0.919	0.811	0.947	17.660
HSC@Lynchburg	0.788	0.596	0.883	8.448
HSC@Battleship	0.782	0.581	0.865	2.795
HSC@Greens	0.764	0.408	0.819	3.589
HSC@I-610	0.935	0.847	0.953	0.595
Buffalo Bayou	0.303	-0.662	0.506	0.381
Brays Bayou	0.735	-1.116	0.709	0.317
Sims Bayou	0.733	0.426	0.835	0.495
Vince Bayou	0.785	0.175	0.847	0.118
Hunting Bayou	0.782	0.076	0.834	0.072
Greens Bayou	0.495	-0.685	0.608	0.405
Carpenters Bayou	0.543	0.082	0.728	0.260
San Jacinto River	0.683	0.335	0.807	3.674

^a A negative value indicates that the observed and predicted values are inversely correlated

^b A value near 1 indicates a close match, a value near zero indicates that the model predicts individual observations no better than the average of observations, a negative value indicates that the observation average would be a better predictor than the model results (Stow *et al.*, 2003)

^c Higher values indicate higher agreement between the model and observations

The RMA2 output file for the calibrated model is included in Appendix D.

3.3 HSCREAD INTERFACE

Once the hydrodynamic model was completed, it was necessary to organize the RMA2 output in a format that could be read by WASP7. In addition, because the model segmentation for WASP7 differed from that of RMA2 (the WASP segments are coarser than the RMA2 elements), it was necessary to “aggregate” the RMA2 results for all the elements that composed a WASP segment. These two operations were accomplished using an interface (HSCREAD) written for this project using Fortran 90. Briefly, HSCREAD reads the output and geometry files from RMA2 and processes 1-D and 2-D segments as follows:

- Reads a “junction file” that includes the segment continuity, pair of segments at each flow interface, and the RMA2 nodes that are part of each WASP segment.
- For 1-D segments (tributaries and main channel up to the confluence with the San Jacinto River):
 - Reads from a user supplied file how many 1-D RMA2 elements are part of a given 1-D WASP segment;
 - Calculates the average depth of the WASP segment (the depths are weighted by the length of the individual RMA2 elements to obtain a representative average depth);
 - Calculates the volume of the WASP segment by aggregating the volumes of the individual RMA2 elements composing the segment, the volume of each RMA2 element is calculated as the average of the cross-sectional areas upstream and downstream times the length of the element;

- Calculates the flow into the WASP segment (velocity of the upstream node times the cross-sectional area at the upstream node), and in a similar way the flow out of the segment (using data for the downstream node); and
- Calculates the average velocity of the WASP segment
- For 2-D segments (main channel downstream of Lynchburg Ferry and Galveston Bay):
 - Reads from a user supplied file how many 2-D RMA2 elements are part of a given 2-D WASP segment;
 - Computes the surface area of each RMA2 element (on the horizontal plane) using the coordinates for the nodes composing the element;
 - Calculates the average depth of the WASP segment (the depths are weighted by the surface area of the individual RMA2 elements to obtain a representative average depth);
 - Calculates the volume of the WASP segment by aggregating the volumes of the individual RMA2 elements composing the segment. Volume of each RMA2 2-D element is calculated as the average depth times the surface area;
 - Reads from the RMA2 output, the flow crossing all the interfaces of the 2-D segments (continuity lines should be defined at the model interfaces and the segments related to each continuity line are supplied in the “junction file”); and
 - Computes the average velocity for a WASP element by adding the velocity components of the different nodes comprising the segment.
- Because there was a small difference in the volume of WASP elements calculated using the two methods described in equations 3.1 and 3.2, flows were corrected to eliminate any potential errors with the water quality model.

- For the 1-D elements, HSCREAD adjusts the flows as follows: flows from upstream boundaries are kept unchanged since they correspond to flows measured at USGS gages; for the most upstream segment of each tributary, flow out of the segment is corrected using:

$$Q_{out_t} = Q_{in_t} - \frac{V_t - V_{t-1}}{dt} \quad (3.8)$$

For subsequent segments, the corrected flow out of the previous segment is assumed as the incoming flow and the outgoing flow is calculated using equation 3.8. If a WASP element is downstream of a junction (i.e. after a tributary discharges into the channel), the flow in is the sum of the two corrected outflows.

- For 2-D segments, the flow adjustment was performed using an Excel spreadsheet. In this case, flows out of segments with no inflows (e.g. side bays) are adjusted first and used to correct the flows in the neighboring segments. In both cases, flows are adjusted using equation 3.8. HSCREAD reads the corrected flows from a CSV file supplied by the user.
- When all the calculations are completed, HSCREAD formats a “HYD” file, which is the hydrodynamic file that can be read by WASP. Five records comprise the external hydrodynamic file:

Record 1 - Data Options : includes number of segments connected by flows, number of interfacial flow pairs from the hydrodynamic file, WASP time step (an even multiple of the hydrodynamic time step), beginning time for the hydrodynamic file, ending time for the hydrodynamic file.

Record 2 - Segment Interface Pairs

Record 3 - Initial Segment Properties: volume, average depth, and average velocity of segment "i" at beginning of time step (this record is only input once for each segment). It is noted that WASP uses velocities only to calculate re-aeration rates and, thus, this parameter is not relevant in dioxin simulations.

Record 4 -- Segment Interfacial Flows (repeated for each time step): positive numbers indicate flows from the “upstream” to the “downstream” segment in the interface (as specified in record 2), while negative numbers indicate flows in the opposite direction.

Record 5 -- Segment Properties: volume, average depth, and average velocity of segment "i" for each time step. This record is repeated for each time step.

3.4 IN-STREAM WATER QUALITY MODEL OF THE HSC AND UPPER GALVESTON BAY

This section summarizes the progress to date in the development of a 2378-TCDD model for the Houston Ship Channel using the Water Quality Analysis Simulation Program (WASP). WASP is a dynamic compartment model that can be used to simulate contaminant fate and transport in surface water and the underlying benthic sediment layer. WASP simulates the time-varying processes of advection, dispersion, point and non-point mass loading, deposition/resuspension, and boundary exchange. For this study WASP version 7.1 (Wool et al, 2004) is being used. The model consists of four modules: EUTRO, TOXI, HEAT, and Mercury. EUTRO is used to model BOD/DO, nutrients, and eutrophication; TOXI is used to simulate toxic chemicals (tracers, organics, metals), and HEAT is used to simulate temperature. The Mercury module simulates various mercury species and sediment balances.

To model dioxin in the HSC, the TOXI model is used. TOXI can simulate up to six

systems and 13 levels of complexity as summarized in Table 3.8. For the dioxin model, level 3 solids (simulated TSS), equilibrium level 3 (hydrophobic sorption), and kinetics 1 or 2 are needed. For this level of complexity, the equations used in the constituent mass balance are (for a 1-D system):

$$\frac{\partial C}{\partial t} = \frac{\partial}{\partial x} \left(-U_x A C + E_x A \frac{\partial C}{\partial x} \right) + A(S_L + S_B + S_K) \quad (3.9a)$$

where C = concentration of the water quality constituent (mg/L)

t = time (days)

A = cross-sectional area (m²)

U_x = longitudinal advective velocity (m/s)

E_x = longitudinal dispersion coefficient (m²/s)

S_L = direct and diffuse loading rate (g/m³-d)

S_B = boundary loading rate (g/m³-d)

S_K = total kinetic transformation rate (g/m³-d)

or

$$\frac{\partial C}{\partial t} = -\frac{\partial}{\partial x} (UC) + \frac{\partial}{\partial x} \left(E_x \frac{\partial C}{\partial x} \right) - \frac{C_s}{S} W_d + \frac{C_{s,b}}{S_b} W_e + S_B + S_K \quad (3.9b)$$

where W_d = rate of sediment deposition (g/m³-s)

W_e = scour rate of sediment (g/m³-s)

C_s = constituent sorbed concentration in the water column (mg/L)

$C_{s,b}$ = constituent sorbed concentration in the bottom sediment (mg/kg)

S = concentration of suspended sediment (mg/L)

S_b = sediment concentration in bottom sediment (mg/kg)

and

$$C_s = K_p S C_w \quad (3.10a)$$

$$K_p = f_{oc} K_{oc} \quad (3.10b)$$

where C_w is the concentration of dissolved constituent (mg/L), K_p is the linear partitioning coefficient, f_{oc} is the organic carbon mass fraction of suspended sediment (g/g), and K_{oc} is the organic-carbon partitioning coefficient of the constituent (L/kg).

A list of WASP input requirements for the dioxin model is included in Table 3.9.

Table 3.9 Data Requirements for the Dioxin WASP Model for the HSC

Data Group	Description	Source
A	Model Identification and Simulation Control	Basic simulation information including variables to simulate obtained from the statement of the problem
B	Exchange Coefficients Dispersion coefficient-water column Dispersion coefficient-pore water Cross-sectional area Characteristic length	Calibration to salinity values Literature values Channel data Channel data
C	Volumes For water column: number of segments and volumes for each time step For benthic segments: number of segments and volumes	Hydrodynamic file Number of segments equal to water column segments, volumes calculated using site data
D	Flows - <i>Surface Water</i> Flow routing Flow time function - <i>Pore Water</i> Flow routing Flow time function - <i>Sediment Transport</i> Area for settling and resuspension Flow routing Velocity (settling or resuspension)	Hydrodynamic file Hydrodynamic file Conceptual model Literature values Channel data Conceptual model Sediment load study for the HSC, initial settling velocities

Data Group	Description	Source
		estimated using Stoke’s equation. Refine initial estimates with channel-specific calibration
E	Boundary Concentrations Concentrations for each system at segments that import, export, or exchange water with locations outside the network	Dioxin dataset collected for this project
F	Waste Loads Point source loadings Non-point source loadings	NPDES permit files, MEGA-TX model for the HSC, Spring 2003 effluent data, and regressions for non-measured outfalls Estimated using GIS and spreadsheets models
G	Parameters Spatially variable characteristics of the water body that affect the particular processes being modeled. Dissolved organic carbon concentration Fraction organic carbon of solids Total lumped first-order decay rate	Dataset collected for this project Dataset collected for this project Literature values
H	Constants Organic carbon partitioning coefficient First-order loss rate constant Volatilization rate constant Water column biodegradation rate Benthic biodegradation rate Photolysis rate	Measured effective coefficients using data collected in this project (not needed if DOC and f_{oc} are input in Data Group G) Literature values Literature values Literature values Literature values Literature values
I	Kinetic Time Functions Not used in the dioxin model	
J	Initial Conditions Concentration of each modeled system (dioxin and TSS) for each segment	Dioxin dataset collected for this project

3.4.1 WASP Segmentation and Time Step

While a large number of small model elements were used in the RMA2 hydrodynamic models to simulate the sinuosity of the main channel and bayous and the change in bottom elevations in the channel and Upper Galveston Bay, there was no need for high spatial resolution simulations in the WASP water quality model, both from a water quality management perspective and to match the resolution of the field measurements of water quality. The WASP model segmentation was developed by aggregating RMA2 elements to reaches maintaining the minimum segmentation required for water quality management purposes.

The WASP model for the HSC consists of 60 1-D water surface segments, 45 2-D water surface elements, and 105 benthic segments (one underlying each of the surface water segments) (Figure 3.14). Thirty-eight segments correspond to the main channel from Buffalo Bayou to the downstream boundary (as shown in Figure 3.14), nineteen to the major tributaries, twenty-one to San Jacinto River (including the Old River), and the remaining twenty-seven comprise the side bays, Barbours Cut, Bayport Channel, Clear Lake, and Upper Galveston Bay. Table 3.10 summarizes the physical characteristics of the WASP segments.

3.4.2 Model Input

Hydrodynamics

As mentioned in Sections 3.2 and 3.3, the WASP model is linked to an RMA2 hydrodynamic model to obtain data on flows, velocities, and depths. Volumes are calculated by the HSCREAD interface.

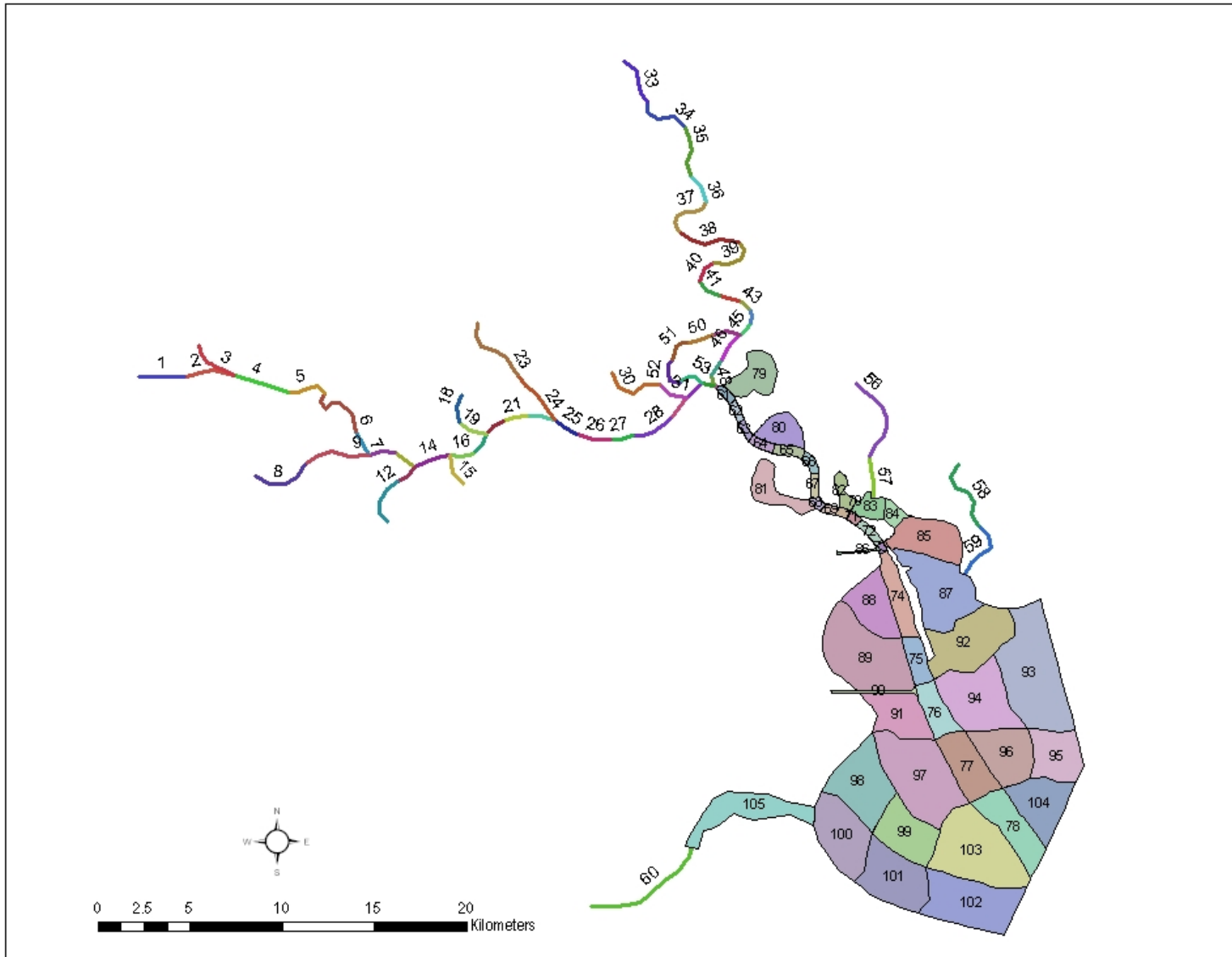


Figure 3.14 WASP Segmentation
Figure 3.14 WASP Model Segmentation

Table 3.10 Physical Characteristics of WASP Segments

Surface Water Segments					Underlying Benthic Segments		Surface Water Segments					Underlying Benthic Segments	
Segment ID	Location	Monitoring Station ^a	Average Depth ^b (m)	Average Volume ^b (m ³)	Segment ID	Volume ^c (m ³)	Segment ID	Location	Monitoring Station ^a	Average Depth ^b (m)	Average Volume ^b (m ³)	Segment ID	Volume ^c (m ³)
1	Buffalo Bayou		2.0	96,798	106	6487	54	Main Channel		14.9	2,632,324	159	20779
2	Buffalo Bayou	11347	4.3	266,451	107	13370	55	Main Channel@Lynchburg	11261	14.4	825,632	160	8384
3	Whiteoak Bayou	11382	2.3	101,969	108	8715	56	Goose Creek	11092	2.2	4,924,174	161	1842
4	Main Channel		4.9	608,267	109	14635	57	Goose Creek		2.1	810,158	162	1842
5	Main Channel		8.0	932,217	110	15121	58	Cedar Bayou	11111	2.5	3,664,753	163	2114
6	Main Channel	11292	11.5	4,244,499	111	32865	59	Cedar Bayou		2.8	2,545,674	164	2114
7	Main Channel		11.9	2,268,546	112	39806	60	Clear Creek		2.5	1,261,266	165	2000
8	Brays Bayou		4.0	556,381	113	19837	61	Main Channel		12.2	5,723,495	166	46979
9	Brays Bayou	11305	5.9	1,158,605	114	27919	62	Main Channel		11.4	5,170,410	167	45334
10	Main Channel@I-610		11.9	2,245,585	115	20858	63	Main Channel		11.7	4,694,034	168	40110
11	Main Channel		12.9	2,103,952	116	23076	64	Main Channel		11.1	7,470,443	169	67485
12	Sims Bayou		4.8	1,073,598	117	11547	65	Main Channel	16618	11.1	9,849,836	170	88793
13	Sims Bayou	11302	5.9	207,008	118	5882	66	Main Channel		12.0	7,211,333	171	60377
14	Main Channel	11287	12.7	3,842,081	119	35426	67	Main Channel		11.8	6,887,017	172	58658
15	Vince Bayou	11300	4.9	596,054	120	9049	68	Main Channel		12.4	4,458,985	173	36136
16	Main Channel		12.4	2,530,291	121	24335	69	Main Channel		11.9	4,174,445	174	35273
17	Main Channel		12.4	2,189,398	122	21487	70	Main Channel		12.7	4,066,406	175	32196
18	Hunting Bayou		2.9	140,516	123	5458	71	Main Channel		13.0	4,447,822	176	34316
19	Hunting Bayou	11298	3.9	155,614	124	7035	72	Main Channel		12.2	9,010,688	177	73787
20	Main Channel		12.9	2,436,429	125	23178	73	Main Channel@Morgan'sPoint	11252	13.8	2,760,060	178	20110
21	Main Channel	11280	12.9	2,798,920	126	26012	74	Main Channel	13309	10.3	43,888,568	179	428683
22	Main Channel@ Greens		12.9	3,072,696	127	28556	75	Main Channel		10.9	28,442,631	180	262365
23	Greens Bayou		6.2	1,403,951	128	22307	76	Main Channel	14560	10.7	40,978,241	181	384931
24	Greens Bayou	11274	8.9	1,068,982	129	23061	77	Main Channel		9.9	67,610,031	182	683579
25	Main Channel	11270	12.9	4,265,288	130	28740	78	Main Channel d/s boundary		10.4	75,383,547	183	724710
26	Main Channel		13.9	7,130,079	131	50704	79	Burnett Bay	13343/13344/16496	1.2	5,518,599	184	458138
27	Main Channel	15979	13.9	5,019,038	132	40100	80	Scott Bay	13342/17971	1.3	4,529,331	185	349504
28	Main Channel		13.9	8,730,199	133	69146	81	San Jacinto Bay	16499/13339	2.0	7,868,853	186	392706
29	Main Channel	11265	14.9	5,293,291	134	43447	82	Black Duck Bay	13340/13341	2.2	2,684,141	187	124263
30	Carpenters Bayou	11272	3.0	604,483	135	11566	83	Tabbs Bay	13337	1.9	3,615,722	188	188420
31	Carpenters Bayou		4.9	242,950	136	8267	84	Tabbs Bay		1.7	1,965,090	189	120217

Surface Water Segments					Underlying Benthic Segments	
Segment ID	Location	Monitoring Station ^a	Average Depth ^b (m)	Average Volume ^b (m ³)	Segment ID	Volume ^c (m ³)
32	Main Channel@Battleship	11264	14.9	4,779,565	137	37940
33	San Jacinto River		3.9	604,996	138	19261
34	San Jacinto River		4.4	1,002,066	139	20931
35	San Jacinto River	11200	6.0	2,872,016	140	23813
36	San Jacinto River		6.0	2,117,683	141	14788
37	San Jacinto River	16622	6.0	2,548,103	142	12319
38	San Jacinto River		7.0	2,721,462	143	7618
39	San Jacinto River		6.9	2,469,456	144	25535
40	San Jacinto River		6.9	1,753,735	145	16382
41	San Jacinto River	11197	6.9	2,137,915	146	23863
42	San Jacinto River		5.4	1,913,739	147	19488
43	San Jacinto River		5.7	911,068	148	26325
44	San Jacinto River	11193	8.9	985,179	149	12916
45	San Jacinto River@I-10		10.9	1,478,173	150	15667
46	San Jacinto River		10.9	4,808,094	151	30717
47	San Jacinto River		10.9	3,564,684	152	20999
48	San Jacinto River@HSC		10.9	1,841,458	153	12098
49	Old River		4.9	1,601,679	154	15253
50	Old River		4.9	1,704,900	155	13254
51	Old River		4.9	1,885,544	156	14802
52	Old River		4.9	2,061,574	157	14662
53	Old River@HSC		5.9	1,584,291	158	23309

Surface Water Segments					Underlying Benthic Segments	
Segment ID	Location	Monitoring Station ^a	Average Depth ^b (m)	Average Volume ^b (m ³)	Segment ID	Volume ^c (m ³)
85	Tabbs Bay	13336	2.5	17,437,362	190	718423
86	Barbours Cut	13355	14.9	3,905,292	191	26272
87	Upper Galveston Bay		1.8	21,461,145	192	1180849
88	Upper Galveston Bay		2.1	13,799,665	193	671964
89	Upper Galveston Bay	15908	2.7	39,777,959	194	1503609
90	Bayport Channel	13589/13363	14.8	9,808,054	195	66351
91	Upper Galveston Bay		3.9	26,332,570	196	675902
92	Upper Galveston Bay		2.0	22,597,602	197	1158454
93	Upper Galveston Bay		2.5	44,919,793	198	1850129
94	Upper Galveston Bay		2.4	28,388,566	199	1176705
95	Upper Galveston Bay		2.5	17,198,830	200	701960
96	Upper Galveston Bay		2.5	19,679,820	201	805282
97	Upper Galveston Bay		2.6	38,754,074	202	1529439
98	Upper Galveston Bay		2.1	21,462,678	203	1039174
99	Upper Galveston Bay	16213	2.6	19,607,013	204	760937
100	Upper Galveston Bay	15464	2.4	22,537,142	205	954646
101	Upper Galveston Bay		2.3	22,027,313	206	968431
102	Upper Galveston Bay		2.1	25,064,341	207	1229546
103	Upper Galveston Bay		2.7	41,667,599	208	1551452
104	Upper Galveston Bay		2.5	19,561,265	209	777524
105	Clear Lake		2.9	23,214,846	210	801755

^a Stations sampled for dioxin as part of this project

^b Averages for the March 20-April 21, 2005 simulation period

^c Assuming a layer depth of 0.10 m

Point Sources

Input from point sources is simulated in WASP7 by a series of loading versus time values. It is important to note that mass entered as loads is not directly accompanied with inflow. Thus, flows from point sources were input to the RMA2 model as summarized in Table 3.5. For the WASP model, point sources discharging directly to the main channel were aggregated by segment to determine total loads. Point sources discharging to the major tributaries upstream of the sections simulated in the WASP model were not input separately to avoid duplication given that flows and concentrations for the boundary segments already include point sources discharging directly into the tributaries. Figure 3.15 shows the distribution of point sources discharging to the main channel. Dioxin data from point sources (PS) gathered in this project during Spring 2003 were used to calculate load input. For the point sources that were not sampled for effluent and the SIC was among those identified as potential dioxin dischargers, the 2378-TCDD concentration in effluent was assumed equal to the average concentration for effluent from facilities with the same SIC code. If the SIC was not among the potential dioxin dischargers, the 2378-TCDD concentration was assumed equal to zero. The loads were calculated using 5-year averages of self-reported values, as included in the TCEQ permittee database (as of May 2003). A summary of the point source data for the model is included in Table 3.11. The total load of dioxins from PS discharging directly to the HSC system (not to the tributaries) calculated in this manner was estimated to be 1.72×10^{-7} kg/day.

Stormwater Runoff

Stormwater runoff loads were input to the model at the upstream boundary segments for the time steps at which a rain event occurred (as indicated by the closest HCOEM gage for each

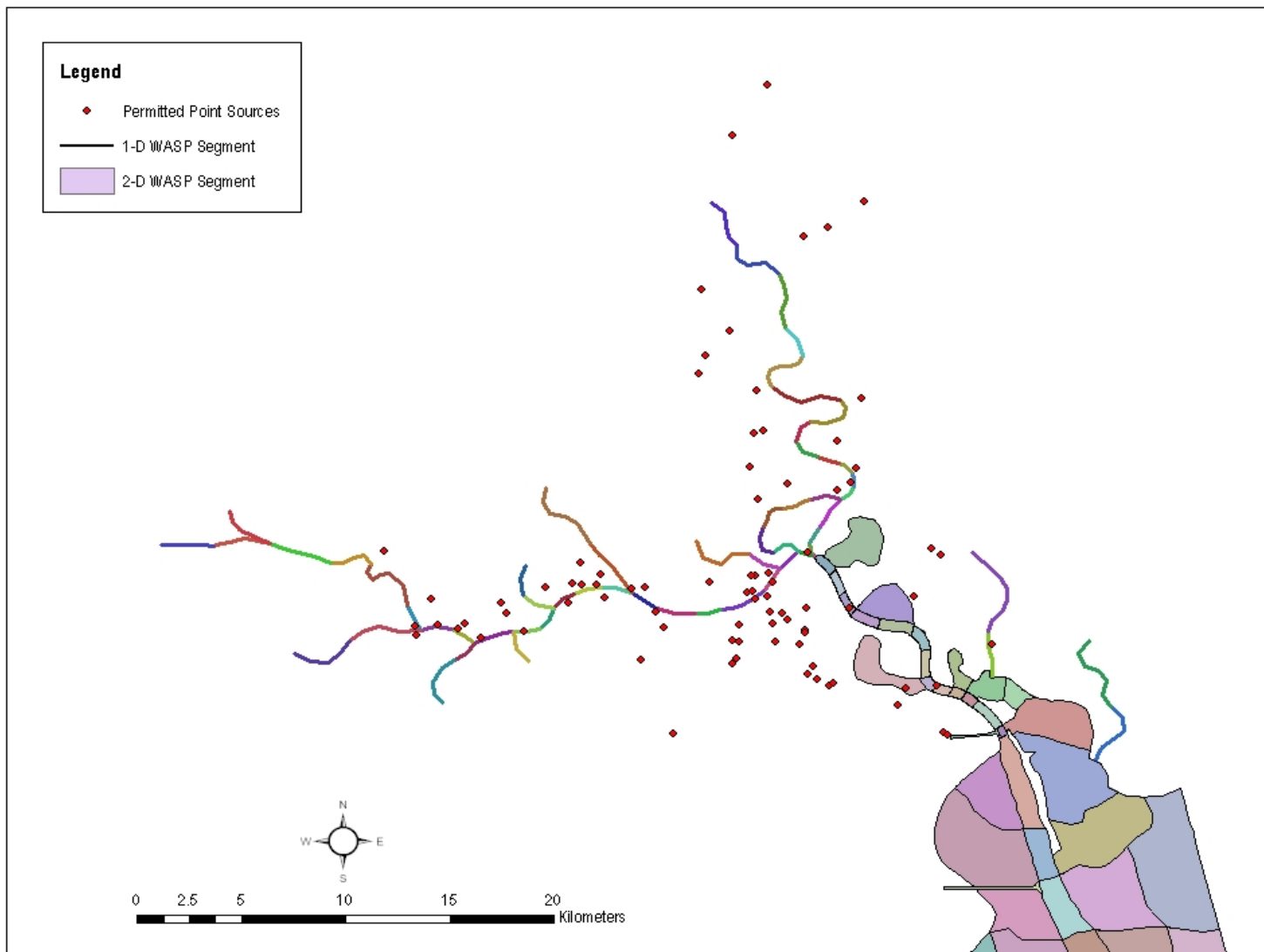


Figure 3.15 Point Sources in the WASP Model

Table 3.11 Point Sources in the WASP Model

WASP Segment	TCEQ Permit #	Self-reported Flow (m ³ /s)	2378-TCDD	
			Concentration (pg/L)	Load (kg/day)
5	11773-001	6.37E-05	0.0882	4.85E-13
6	10495-090	3.5 ^a	0.3267	9.88E-08 ^a
7	02034-000	5.04E-03	0	0
7	10495-010	2.28E-02	0.0669	1.32E-10
9	00542-000	1.72E-02	0	0
10	03133-000	1.92E-03	0	0
11	00456-000	9.48E-04	0	0
11	00535-000	5.71E-02	0.7314	3.61E-09
12	10495-002	5.29E-01	0.0165	7.53E-10
12	00393-000	3.18E-02	0.0448	1.23E-10
14	00353-000	8.60E-03	0.4784	3.56E-10
14	00786-000	4.39E-03	0.5311	2.01E-10
15	10053-005	3.32E-01	0.0312	8.94E-10
16	01740-000	1.29E+00	0.0882	9.86E-09
19	01745-002	1.03E-02	0	0
19	10831-001	3.30E-02	0.0882	2.51E-10
20	00649-001	2.11E-02	0	0
20	00649-002	2.45E-02	0	0
20	00649-006	1.69E-02	0	0
20	00649-007	1.14E-02	0	0
21	00509-003	6.43E-03	0	0
21	00671-000	2.61E-03	0	0
21	03889-000	4.39E-03	0	0
22	00815-000	1.39E-01	0	0
22	03767-000	4.22E-01	0	0
23	10495-077	1.62E-01	0.0242	3.38E-10
23	00662-000	2.84E-03	0	0
23	03792-001	1.52E-04	0	0
23	11727-001	1.97E-02	0.0265	4.51E-11
24	00749-000	1.96E-02	0.0332	5.61E-11
24	00445-000	3.87E-03	0.0448	1.50E-11
24	00492-000	4.29E-02	0.5311	1.97E-09
24	03828-001	6.25E-05	0.4784	2.58E-12
24	03828-002	3.44E-05	0.4784	1.42E-12
25	01160-000	5.49E-01	0.4925	2.33E-08

Dioxin TMDL Project –Work Order# 582-6-70860-02 – Final Report

WASP Segment	TCEQ Permit #	Self-reported Flow (m ³ /s)	2378-TCDD	
			Concentration (pg/L)	Load (kg/day)
26	00002-001	1.37E-01	0	0
26	02067-004	5.77E-03	0.7074	3.53E-10
26	10053-002	1.33E-01	0.0882	1.02E-09
26	10053-003	2.42E-01	0.0717	1.50E-09
28	00305-001	1.94E-01	0.3354	5.61E-09
28	00305-003	1.82E-01	0.3354	5.28E-09
28	00305-005	3.76E-02	0.3354	1.09E-09
28	00402-004	2.92E-01	0.7074	1.79E-08
28	00403-001	4.03E-02	0.7314	2.55E-09
28	00403-007	2.79E-01	0.7314	1.76E-08
28	00458-001	2.29E-01	0.5311	1.05E-08
28	00458-007	5.12E-02	0.5311	2.35E-09
28	00639-000	1.22E-01	0.5311	5.60E-09
28	01173-000	2.28E-03	0	0
28	01429-000	3.60E-02	0.0859	2.67E-10
28	01984-002	2.57E-03	0	0
28	01984-007	8.76E-04	0	0
28	02177-000	1.25E-04	0	0
28	02558-000	4.60E-02	0.5311	2.11E-09
28	03375-002	5.64E-03	0.5311	2.59E-10
28	03937-000	0.00E+00	0.0859	0.00E+00
28	10519-002	1.44E-01	0.0357	4.43E-10
28	12318-001	4.51E-05	0.0882	3.44E-13
28	13203-001	1.26E-05	0.0882	9.56E-14
29	01731-000	5.99E-03	0.0859	4.44E-11
29	12314-001	2.75E-05	0.0882	2.09E-13
30	03129-003	4.58E-03	0	0
31	02160-000	7.93E-04	0.4784	3.28E-11
31	12375-001	3.40E-04	0.0882	2.59E-12
37	02712-000	1.75E-03	0.5311	8.04E-11
37	11388-001	1.68E-02	0.1257	1.82E-10
37	10668-001	1.17E-02	0.0882	8.90E-11
37	10530-001	3.49E-03	0.0882	2.66E-11
37	11329-001	2.33E-02	0.3286	6.61E-10
43	10541-002	2.68E-03	0.0882	2.04E-11
43	03540-000	5.96E-05	0.4784	2.46E-12

WASP Segment	TCEQ Permit #	Self-reported Flow (m ³ /s)	2378-TCDD	
			Concentration (pg/L)	Load (kg/day)
43	03540-000	5.96E-05	0.4784	2.46E-12
43	03540-000	5.96E-05	0.4784	2.46E-12
43	03787-001	3.26E-04	0.4784	1.35E-11
43	03787-002	7.43E-04	0.4784	3.07E-11
43	10541-002	2.68E-03	0.0882	2.04E-11
43	12386-001	1.06E-04	0.0882	8.10E-13
44	10558-001	2.51E-02	0.1787	3.88E-10
44	10105-001	5.90E-02	0.0882	4.49E-10
44	00391-000	1.80E-01	0.5311	8.27E-09
44	12863-001	4.77E-04	0.0882	3.63E-12
44	02845-002	6.31E-03	0	0
44	02927-000	8.61E-02	0.7074	5.26E-09
44	03517-000	1.47E-03	0	0
44	10104-001	6.21E-02	0.0830	4.46E-10
44	03349-000	9.43E-04	0	0.00E+00
44	10395-008	9.35E-02	0.0840	6.79E-10
44	02605-000	1.54E-03	0	0
57	10395-002	1.81E-01	0.0959	1.50E-09
68	00592-003	5.21E-02	0.7314	3.29E-09
68	00592-001	7.97E-01	0.0606	4.17E-09
80	02184-000	1.19E-02	0.5311	5.46E-10
81	00474-000	1.02E-01	0.1252	1.11E-09
81	01280-001	1.75E-03	0	0
81	00534-001	1.36E-01	0.5311	6.23E-09
81	00534-002	3.50E-01	0.5311	1.61E-08
81	00534-004	5.54E-02	0.5311	2.54E-09
81	00534-007	3.18E-02	0.5311	1.46E-09
81	00663-001	5.35E-02	0.1877	8.67E-10
81	01785-001	3.45E-03	0	0
81	02107-001	1.80E-02	0	0
81	02529-001	4.46E-03	0	0
81	10779-001	3.97E-03	0.0882	3.02E-11
81	00440-001	7.66E-03	0.5311	3.51E-10
86	00440-000	7.66E-03	0.5311	3.51E-10
86	10779-001	3.97E-03	0.0882	3.02E-11

^a Average values. One-hr time series were input to the model

upstream segment). The load was calculated by multiplying the flow measured at the USGS gage by the 2378-TCDD concentration measured in runoff. It is noted that the initial simulation period (March 20 to April 21, 2005 corresponded to a dry period and, thus, the stormwater runoff loads are lower than expected for the rest of the year. The long-term simulation (2002 to 2005) will account for both dry and wet periods.

Direct Deposition

Dry and wet direct deposition to the channel was simulated by multiplying the deposition fluxes measured in this study (see Appendix A for a summary of data) times the surface area of each of the WASP segments. Dry deposition was assumed to occur during days with no rain, while wet deposition was input for rainy time steps. Table 3.12 summarizes the average deposition loads input to the model. The average total deposition load was estimated to be 1.3×10^{-7} kg/day.

Boundary and Initial Concentrations

Boundary concentrations for the upstream segments of the major tributaries were assumed equal to the 2378-TCDD concentrations measured during 2005 at the mouths of the tributaries. These concentrations correspond to dry-weather conditions and are assumed to include the effect of point sources discharging to the tributaries upstream of the WASP model domain as previously mentioned. For the surface water segments, initial dioxin concentrations were input on a segment-basis using the water concentrations (dissolved+ suspended) of 2378-TCDD for the stations sampled in this project, while initial suspended sediment concentrations were assumed to be equal to the average TSS concentrations also collected in this project. In addition, for the benthic

Table 3.12 Direct Deposition in the WASP Model

WASP Segment	Surface Area (m ²)	Average Deposition Loads (kg/day)		
		Dry ^a	Wet ^b	Total
1	64,870	3.97E-11	3.98E-13	3.18E-11
2	133,700	8.18E-11	8.20E-13	6.56E-11
3	87,150	5.33E-11	3.95E-13	4.27E-11
4	146,350	8.95E-11	6.64E-13	7.17E-11
5	151,210	9.26E-11	6.86E-13	7.42E-11
6	328,650	2.02E-10	1.50E-12	1.62E-10
7	398,060	2.44E-10	1.81E-12	1.96E-10
8	198,370	1.22E-10	9.03E-13	9.75E-11
9	279,190	1.71E-10	1.27E-12	1.37E-10
10	208,580	1.28E-10	9.50E-13	1.03E-10
11	230,760	1.42E-10	1.05E-12	1.13E-10
12	115,470	7.07E-11	5.24E-13	5.66E-11
13	58,820	3.60E-11	2.67E-13	2.88E-11
14	354,260	2.17E-10	1.61E-12	1.74E-10
15	90,490	5.52E-11	4.09E-13	4.42E-11
16	243,350	1.49E-10	1.10E-12	1.19E-10
17	214,870	1.32E-10	9.77E-13	1.06E-10
18	54,580	3.35E-11	2.48E-13	2.68E-11
19	70,350	4.31E-11	3.20E-13	3.46E-11
20	231,780	1.42E-10	1.05E-12	1.14E-10
21	260,120	1.59E-10	1.18E-12	1.28E-10
22	285,560	1.75E-10	1.30E-12	1.41E-10
23	223,070	1.37E-10	1.01E-12	1.10E-10
24	230,610	1.41E-10	1.05E-12	1.13E-10
25	287,400	1.76E-10	1.30E-12	1.41E-10
26	507,040	3.11E-10	2.30E-12	2.49E-10
27	401,000	2.46E-10	1.82E-12	1.97E-10
28	691,460	4.24E-10	3.14E-12	3.39E-10
29	434,470	2.66E-10	1.97E-12	2.13E-10
30	115,660	7.08E-11	5.24E-13	5.67E-11
31	82,670	5.06E-11	3.75E-13	4.05E-11
32	379,400	2.32E-10	1.72E-12	1.86E-10
33	192,610	1.18E-10	8.75E-13	9.46E-11
34	209,310	1.28E-10	9.51E-13	1.03E-10

WASP Segment	Surface Area (m ²)	Average Deposition Loads (kg/day)		
		Dry ^a	Wet ^b	Total
35	238,130	1.46E-10	1.08E-12	1.17E-10
36	147,880	9.07E-11	6.72E-13	7.27E-11
37	123,190	7.54E-11	5.59E-13	6.04E-11
38	76,180	4.67E-11	3.46E-13	3.74E-11
39	255,350	1.57E-10	1.16E-12	1.25E-10
40	163,820	1.00E-10	7.45E-13	8.05E-11
41	238,630	1.46E-10	1.08E-12	1.17E-10
42	194,880	1.19E-10	8.86E-13	9.57E-11
43	263,250	1.61E-10	1.20E-12	1.29E-10
44	129,160	7.91E-11	5.86E-13	6.34E-11
45	156,670	9.60E-11	7.12E-13	7.70E-11
46	307,170	1.88E-10	1.40E-12	1.51E-10
47	209,990	1.29E-10	9.55E-13	1.03E-10
48	120,980	7.42E-11	5.50E-13	5.94E-11
49	152,530	9.35E-11	6.93E-13	7.49E-11
50	132,540	8.12E-11	6.02E-13	6.51E-11
51	148,020	9.07E-11	6.73E-13	7.27E-11
52	146,620	8.99E-11	6.66E-13	7.20E-11
53	233,090	1.43E-10	1.06E-12	1.15E-10
54	207,790	1.27E-10	9.45E-13	1.02E-10
55	83,840	5.15E-11	3.82E-13	4.13E-11
56	18,420	1.13E-11	8.35E-14	9.03E-12
57	18,420	1.13E-11	8.35E-14	9.03E-12
58	21,140	1.29E-11	9.58E-14	1.04E-11
59	21,140	1.29E-11	9.58E-14	1.04E-11
60	20,000	1.22E-11	9.06E-14	9.81E-12
61	469,790	2.88E-10	2.14E-12	2.31E-10
62	453,340	2.78E-10	2.06E-12	2.23E-10
63	401,100	2.46E-10	1.82E-12	1.97E-10
64	674,850	4.14E-10	3.07E-12	3.32E-10
65	887,930	5.44E-10	4.04E-12	4.36E-10
66	603,770	3.70E-10	2.75E-12	2.97E-10
67	586,580	3.60E-10	2.67E-12	2.88E-10
68	361,360	2.21E-10	1.64E-12	1.77E-10
69	352,730	2.16E-10	1.60E-12	1.73E-10
70	321,960	1.97E-10	1.46E-12	1.58E-10

WASP Segment	Surface Area (m ²)	Average Deposition Loads (kg/day)		
		Dry ^a	Wet ^b	Total
71	343,160	2.10E-10	1.56E-12	1.69E-10
72	737,870	4.52E-10	3.35E-12	3.63E-10
73	201,100	1.23E-10	9.14E-13	9.87E-11
74	4,286,830	2.63E-09	1.95E-11	2.11E-09
75	2,623,650	1.61E-09	1.19E-11	1.29E-09
76	3,849,310	2.36E-09	1.75E-11	1.89E-09
77	6,835,790	4.19E-09	3.11E-11	3.36E-09
78	7,247,100	4.44E-09	3.29E-11	3.56E-09
79	4,581,380	2.81E-09	2.08E-11	2.25E-09
80	3,495,040	2.14E-09	1.59E-11	1.72E-09
81	3,927,060	2.41E-09	1.79E-11	1.93E-09
82	1,242,630	7.62E-10	5.65E-12	6.11E-10
83	1,884,200	1.15E-09	8.56E-12	9.26E-10
84	1,202,170	7.37E-10	5.46E-12	5.91E-10
85	7,184,230	4.40E-09	3.27E-11	3.53E-09
86	262,720	1.61E-10	1.20E-12	1.29E-10
87	11,808,490	7.24E-09	5.37E-11	5.80E-09
88	6,719,640	4.12E-09	3.05E-11	3.30E-09
89	15,036,090	9.22E-09	6.83E-11	7.39E-09
90	663,510	4.07E-10	3.02E-12	3.26E-10
91	6,759,020	4.14E-09	3.07E-11	3.32E-09
92	11,584,540	7.10E-09	5.27E-11	5.69E-09
93	18,501,290	1.13E-08	8.41E-11	9.09E-09
94	11,767,050	7.21E-09	5.35E-11	5.78E-09
95	7,019,600	4.30E-09	3.19E-11	3.45E-09
96	8,052,820	4.94E-09	3.66E-11	3.96E-09
97	15,294,390	9.37E-09	6.95E-11	7.51E-09
98	10,391,740	6.37E-09	4.72E-11	5.11E-09
99	7,609,370	4.66E-09	3.46E-11	3.74E-09
100	9,546,460	5.85E-09	4.34E-11	4.69E-09
101	9,684,310	5.94E-09	4.40E-11	4.76E-09
102	12,295,460	7.54E-09	5.59E-11	6.04E-09
103	15,514,520	9.51E-09	7.05E-11	7.62E-09
104	7,775,240	4.77E-09	3.53E-11	3.82E-09
105	8,017,550	4.91E-09	3.64E-11	3.94E-09

^a Dry deposition flux: 0.62 pg/m²/day; ^b Wet deposition flux: 0.40 pg/m²/day

segments, the average 2378-TCDD concentrations in sediment measured in this project were assumed as initial conditions.

In addition to chemical concentrations, the dissolved fractions must be specified for each segment at the beginning of the simulation. For dioxin, the dissolved fraction was set to 0.25. This fraction is internally recalculated by the model at each time step using partition coefficients and suspended sediment concentrations.

Solid Transport Parameters

Sediment transport is a very important process in modeling dioxins because dioxins sorb strongly to sediment and thus undergo settling, scour, and sedimentation. In addition, sorption affects the transformation rates. The suspended sediment was simulated as a single solid class. The major processes affecting sediment distribution are advection and dispersion between the water column segments, and settling to and scour from the benthic segment.

Water Column Transport

Sediment and particulate dioxin in the water column may settle and deposit to the surficial benthic layer. Settling and scour rates in WASP7 are described by velocities and surface areas. Particulate transport velocities are multiplied by cross-sectional areas to obtain flow rates for solids and the particulate fractions of dioxins.

Settling velocities should be set within the Stoke's range of velocities corresponding to the size distribution of suspended particles (Ambrose et al., 1993):

$$V_s = \frac{8.64g}{18\mu} (\rho_p - \rho_w) \cdot d_p^2 \quad (3.11)$$

where V_s = Stokes velocity for particle with diameter d_p and density ρ_p (m/d)

g = acceleration of gravity = 981 cm/s²

μ = absolute viscosity of water = 0.01(g/cm³-s) at 20 °C

ρ_p = density of the solid (g/cm³)

ρ_w = density of water =1.0 g/cm³

d_p = particle diameter (mm)

Benthic exchange of sediment and particulate chemicals is driven by the net scour and deposition velocities. WASP calculates benthic exchange as:

$$W_{BS} = A_{ij}(w_R S_i - w_D S_j) \quad (3.12)$$

where: W_{BS} = net sediment flux rate (g/d)

S = sediment concentration (g/m³)

w_D = deposition velocity (m/d). The deposition velocity can be calculated as the product of the Stoke's settling velocity and the probability of deposition: $w_D = V_s \alpha_D$ (α_D is probability of deposition upon contact with the bed).

w_R = scour velocity (m/d)

A_{ij} = benthic surface area (m²)

i = benthic segment

j = water segment

Grain size analyses of suspended particles were not completed in this project, so it was assumed that the majority of the particles correspond to the size range for silt (0.0039-0.0625 mm). Thus, settling velocities should be within the range 0.716 and 183.9 m/day (8.29x10⁻⁶ to 0.002 m/s). Initial settling velocities were assumed equal to 0.001 m/s for the main channel segments and 0.002 m/s for the side bays. Settling within the side bays was assumed to be higher as they are less affected by disturbances created from ship traffic.

There are no sediment studies in the HSC that allow determination of scour rates. These rates were initially assumed to be 2 orders of magnitude lower than the settling rates (i.e. 1×10^{-5} m/s). It is noted that there are no special process descriptions for solids transport in WASP7. Scour rates, for example, are not programmed as a function of water column shear stress. Consequently, the TOXI sediment model is considered descriptive and must be calibrated to site data (Ambrose et al., 1993). Scour rates were used as a calibration parameter.

Water Column-Sediment Bed Exchange

A dispersion coefficient of 5×10^{-9} m²/s and a mixing length of 0.5 m were applied to predict vertical dispersive exchange between sediments and the water column throughout each bayou. The dispersion coefficient was estimated from literature values (Roychoudhury, 2001).

Parameters and Constants

In this model, the fraction organic carbon (f_{oc}) of the suspended sediments was the only parameter input to the model. Particulate organic carbon data collected in the Fall 2004 as part of this project was used for the model. The f_{oc} for the benthic layers was assumed equal to the average of the fractions measured in sediments collected between 2002 and 2004.

The only constant input to the model corresponds to the logarithm of the organic-carbon partitioning coefficient (K_{oc}), which was estimated to be 7.11 (University of Houston, 2004). Transformation processes (biodegradation, photolysis, and volatilization) were not included in the initial simulation period, but will be modeled as a lumped first-order decay rate in the long-term run.

3.4.3 Salinity Model

Prior to running the dioxin model, a salinity models was run to calibrate the longitudinal

dispersive mixing and exchange coefficients. The WASP dispersion formulation is based on the cross-sectional area between adjacent reaches and a characteristic mixing length, taken to be the distance between midpoints of the adjacent reaches. The model was calibrated to the salinity data collected during flow measurement activities in April 2005. The salinity model was run using the TOXI module without benthic segments. It is noted that WASP is a depth-averaged model, however, the salinity concentrations measured in 2005 correspond to a single depth and do not represent the whole depth of each segment. Thus, the goal was to match patterns and ranges rather than absolute values. Salinity series collected by TCOON at Eagle Point were input at the downstream boundaries to simulate the salt exchange with Galveston Bay. Boundary concentrations for freshwater inflows were assumed equal to 0.2 ‰. Initial concentrations for the various WASP segments were calculated as the average salinity concentrations measured in 2005. Figure 3.16 illustrates the locations at which salinity was calibrated. Calibrated dispersion coefficients for surface waters ranged from 10 to 500 m²/s. Figure 3.17 shows time-series of observed and modeled salinity concentrations and Table 3.13 summarizes two statistical error measures calculated for salinity runs. It can be seen that the model simulates the salinity patterns observed at most locations with the exception of Vince Bayou. Field data at Brays Bayou shows a sudden increase in salinity that could not be reproduced by the model; that peak could have been the result of the passing of a large ship that moved a significant amount of saltwater into the bayou or could be the result of a measurement error. Regarding the San Jacinto River location, the model was able to reproduce the peaks but not the low concentrations measured in the field.

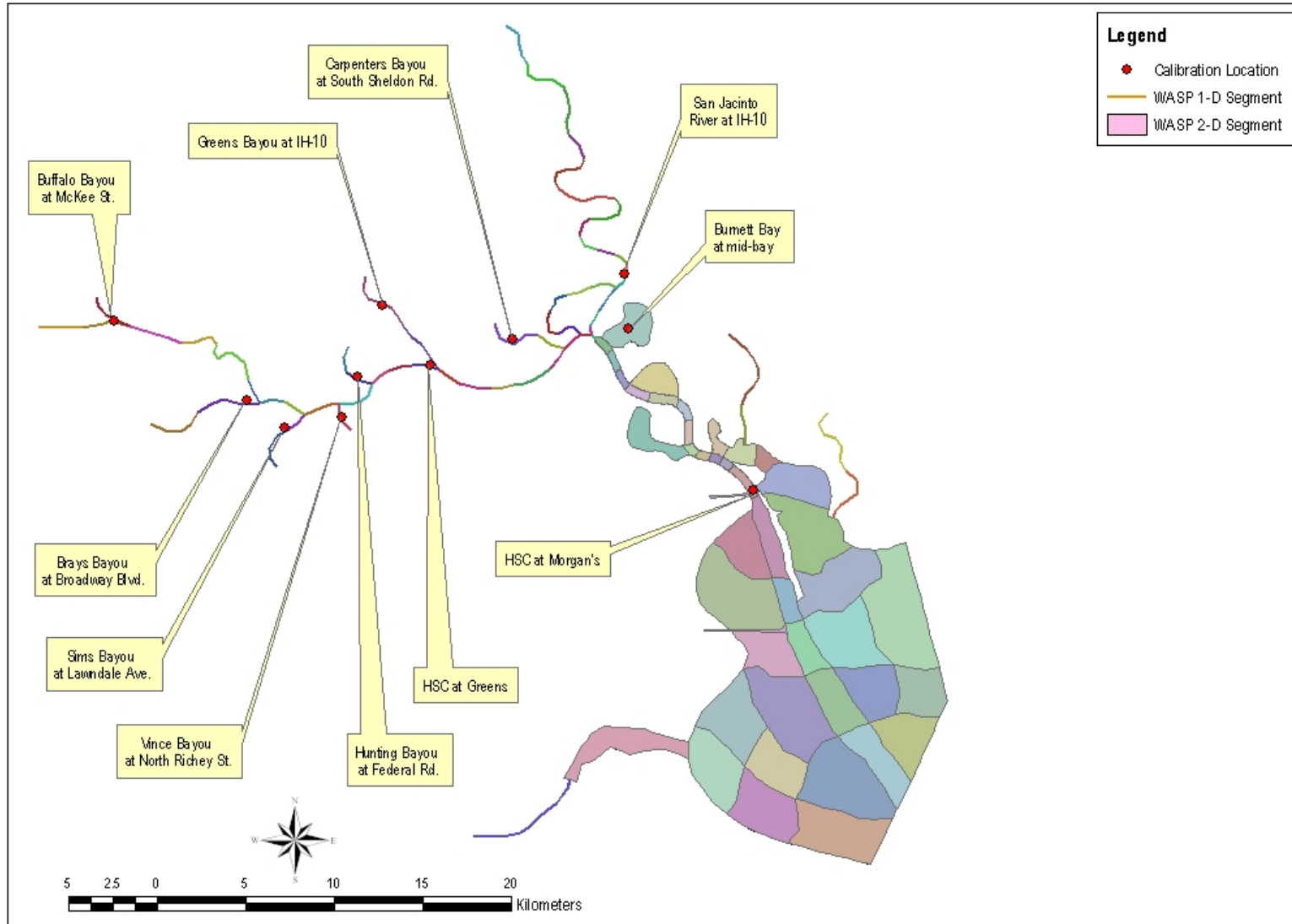


Figure 3.16 Salinity Calibration Locations

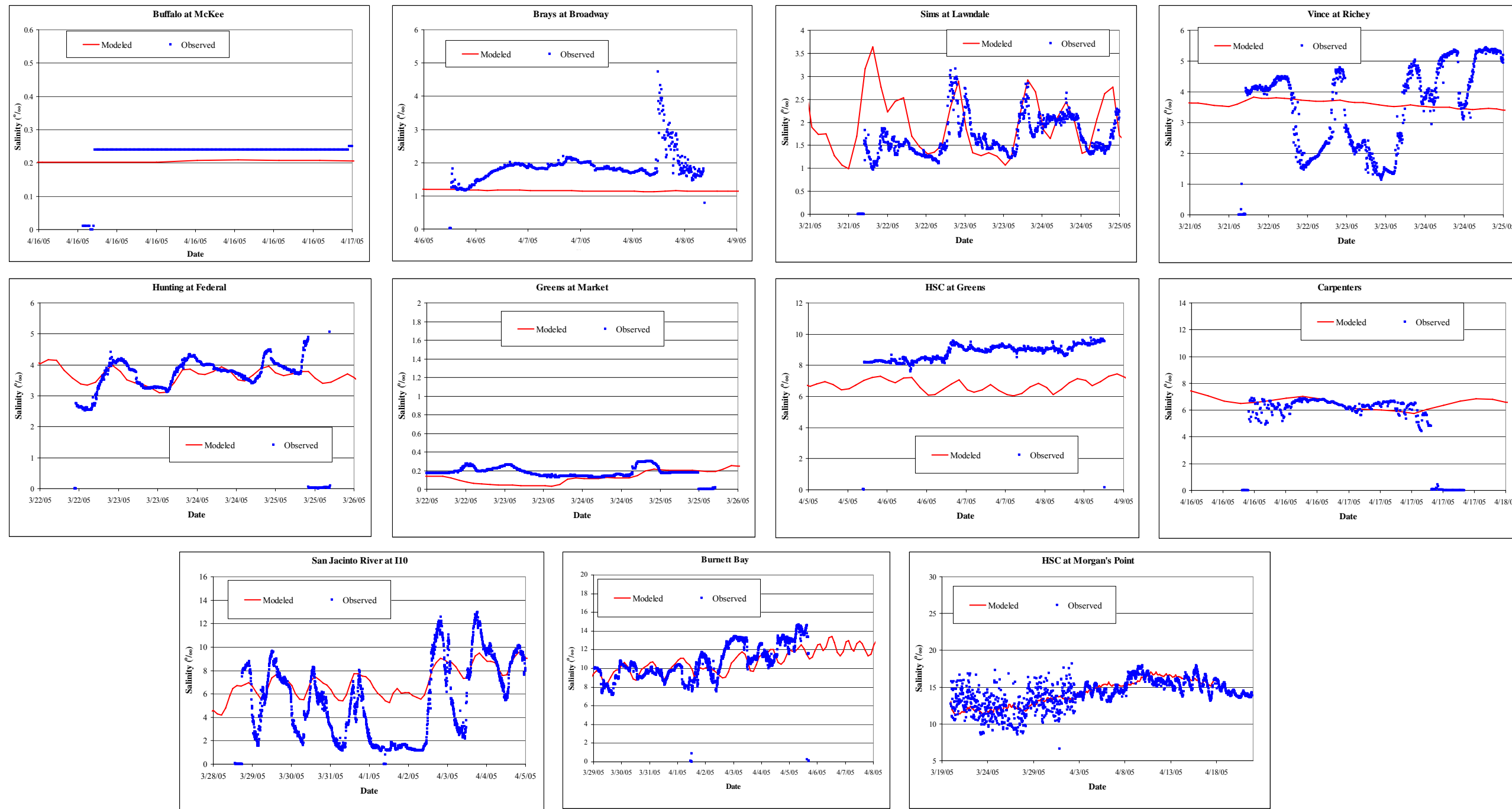


Figure 3.17 Modeled and Measured Salinity Concentrations

Table 3.13 Model Summary Statistics for Salinity

Observation Point	RMSE(‰)^a	Average Abs. Error^b
Buffalo Bayou	0.01	19%
Brays Bayou	0.11	36%
Sims Bayou	0.07	34%
Vince Bayou	0.10	44%
Hunting Bayou	0.03	8%
Greens Bayou	0.01	40%
HSC@Greens	0.19	25%
Carpenters Bayou	0.12	14%
San Jacinto River	0.15	102%
Burnett Bay	0.07	10%
HSC@Morgan's	0.05	10%

^a Calculated using equation 3.7

$$^b \text{ Abserror} = \frac{1}{n} \sum_{i=1}^n \frac{\text{abs}(P_i - O_i)}{O_i}$$

3.4.4 Dioxin Model Calibration

The 2378-TCDD model was run using the loads described in section 3.4.2 and the dispersion coefficients calibrated in the salinity model. The goal of the dioxin model calibration was to match the average concentrations for the simulation period to the average concentrations measured in the channel as part of this project. The calibration parameters were those related to the exchange of contaminants between the benthic and the surface water layers (i.e. scour/settling velocities and pore water diffusion). Figure 3.18 shows longitudinal profiles of modeled and observed average concentrations along the main channel and San Jacinto River. The model was able to reproduce the peaks observed in segments 1001 and 1006. However, the model predicted a much wider peak in the main channel, which may indicate that the dispersion in the section of the

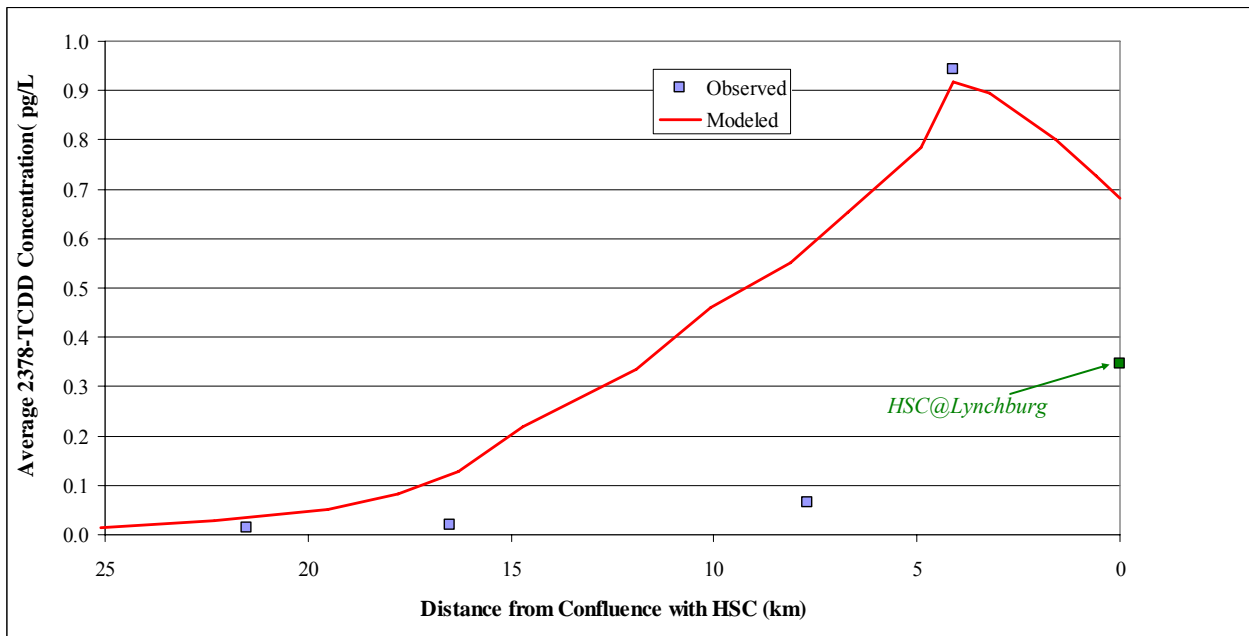
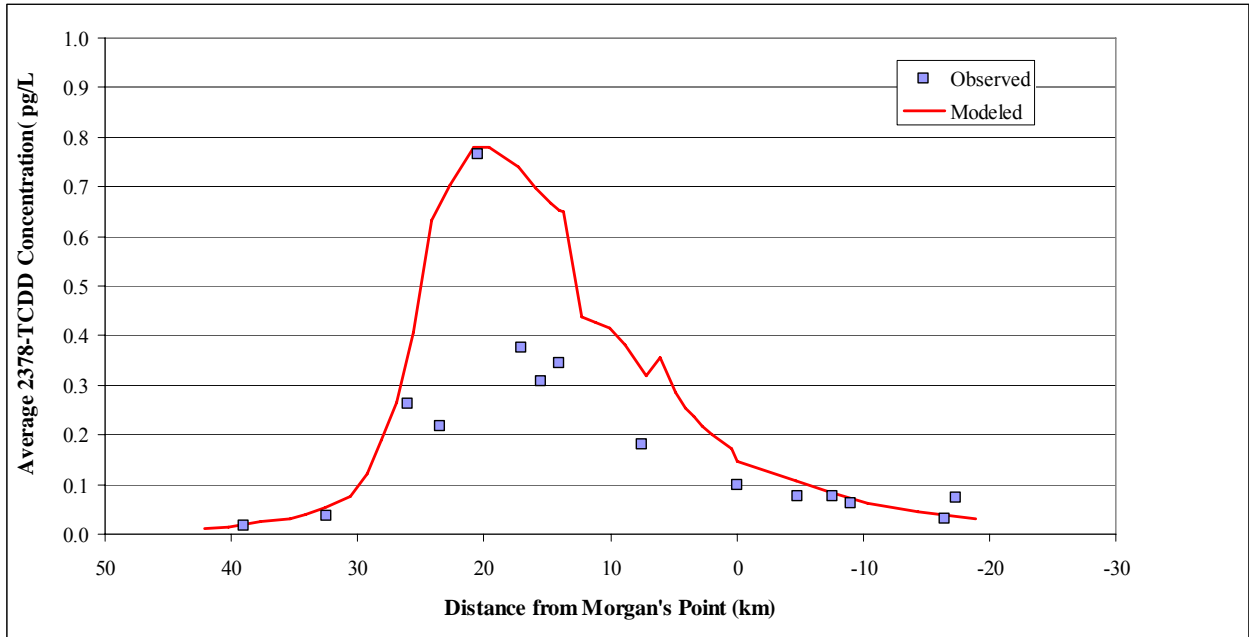


Figure 3.18 Longitudinal Profiles of Average Dioxin Concentrations

channel in the vicinity of the San Jacinto River mouth is much higher than for the rest of the channel. For the San Jacinto River, the modeled concentrations at the mouth are much higher than those measured at Lynchburg Ferry, which again may suggest the presence of processes that cause large dispersion of contaminants in that section of the river.

To measure model performance, scatterplots of modeled versus observed data were prepared and compared to 1:1 lines for all the observation locations (Figure 3.19). When one-to-one comparisons are made, the model performance is relatively good but with concentrations generally over predicting the measured values. Finally, the statistics described in equations 3.4 through 3.7 were computed to quantify model performance and compare the goodness-of-fit for the main channel and San Jacinto River. The summary statistics are presented in Table 3.14 and confirm a reasonable model performance with regard to average concentrations.

Table 3.14 Model Summary Statistics for 2378-TCDD

Statistic	Main Channel	San Jacinto River
r^a	0.541	0.589
MEF^b	-0.197	0.604
d^c	0.804	0.900
$RMSE$ (pg/L)	0.060	0.125

^a A value close to 1 indicates a good match

^b A value near 1 indicates a close match, a value near zero indicates that the model predicts individual observations no better than the average of observations, a negative value indicates that the observation average would be a better predictor than the model results (Stow *et al.*, 2003)

^c Higher values indicate higher agreement between the model and observations

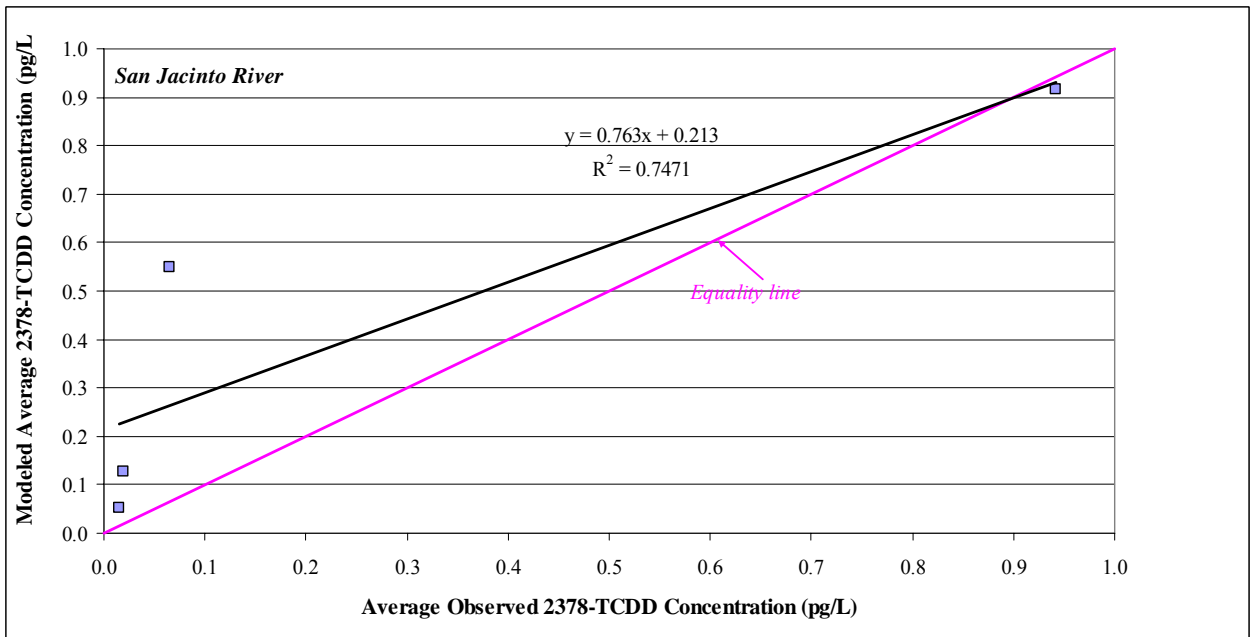
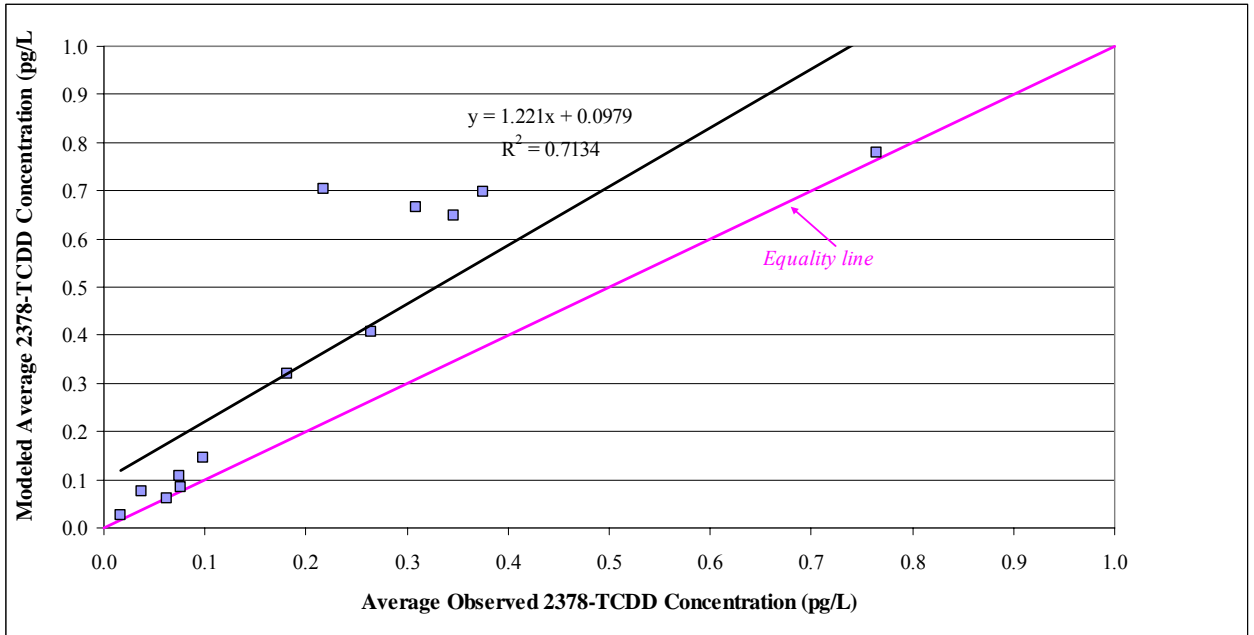


Figure 3.19 Observed versus Modeled Average Dioxin Concentrations

3.4.5 Sensitivity Analysis

Sensitivity analyses were conducted to examine the effect of changing the settling/scour rates, source loadings, and dispersion coefficient on the overall concentration profile. Parameters were varied individually and the results compared to the base case (calibrated model) as shown in Figures 3.20 and 3.21 for the main channel and San Jacinto River, respectively. Overall concentrations of 2378-TCDD were most sensitive to changes in the scour velocity, with model concentrations increasing with increasing scour rates. Dispersion rates also showed some impact on the average concentration profiles, mainly for the main channel, with wider peaks for lower dispersion coefficients.

3.4.6 Preliminary Load Scenarios

Once the dioxin model was calibrated, different load scenarios were run to evaluate the effect of the various sources contributing to dioxin concentrations in the HSC. It can be seen from Figure 3.22 that removing point sources, stormwater runoff, and direct deposition has very little impact on the concentration profile. Removing the benthic layer has the greatest effect on model results. Dioxin concentrations in the benthic layer underlying segment 44 (hot spot found during 2005 sampling) showed a significant effect on concentrations in segments 1006 and 1005, in addition to 1001.

It is also noted that when all the sources are removed, the Texas WQS (0.0933 pg/L) is met for most of the segments, with the exception of segment 1006. Possible explanations include (i) the simulation period is not long enough to “flush” the mass of contaminant included in the initial concentrations, or (ii) segment 1006 may act as a “reservoir” for concentrations and there

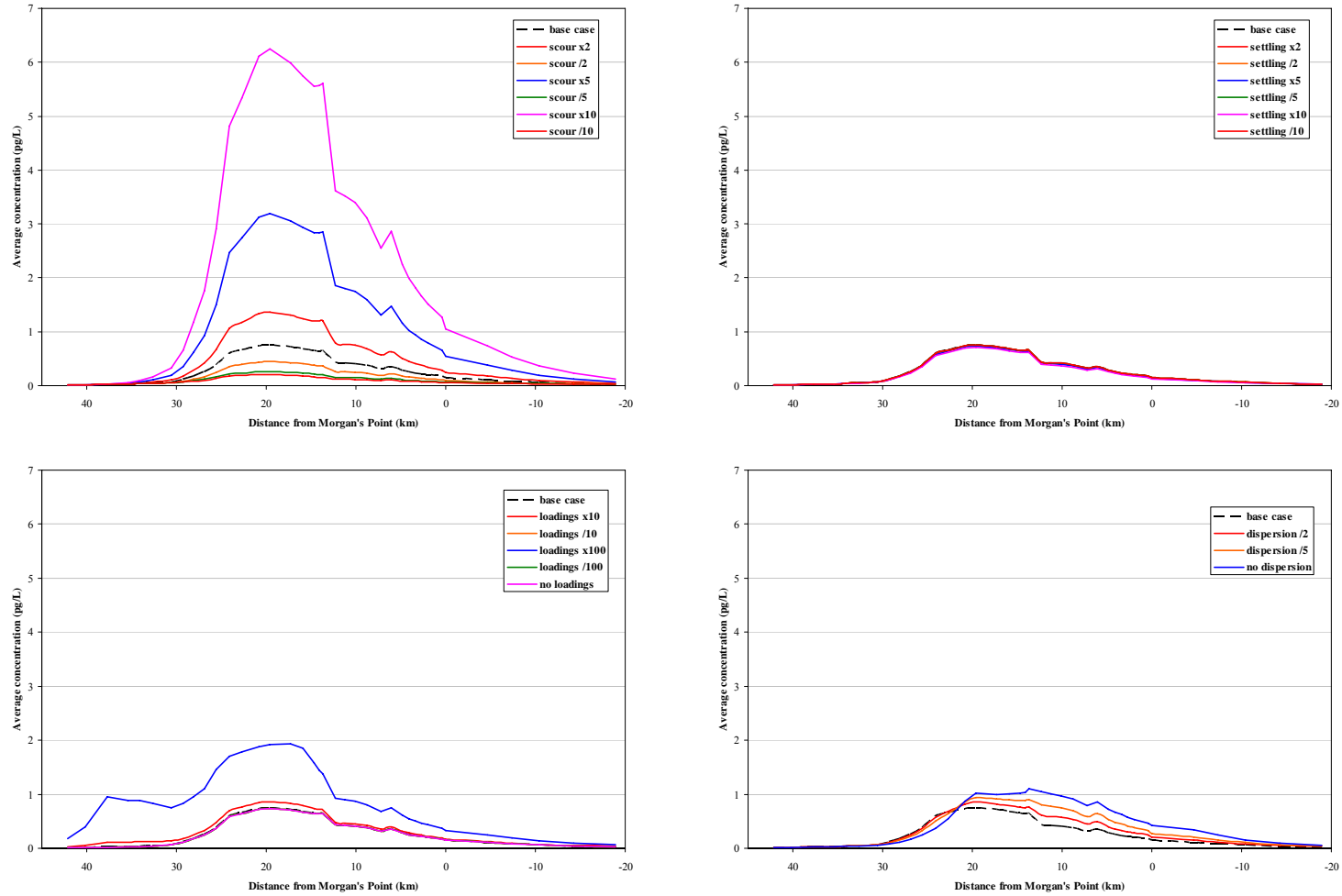


Figure 3.20 Sensitivity Analysis Results - Main Channel

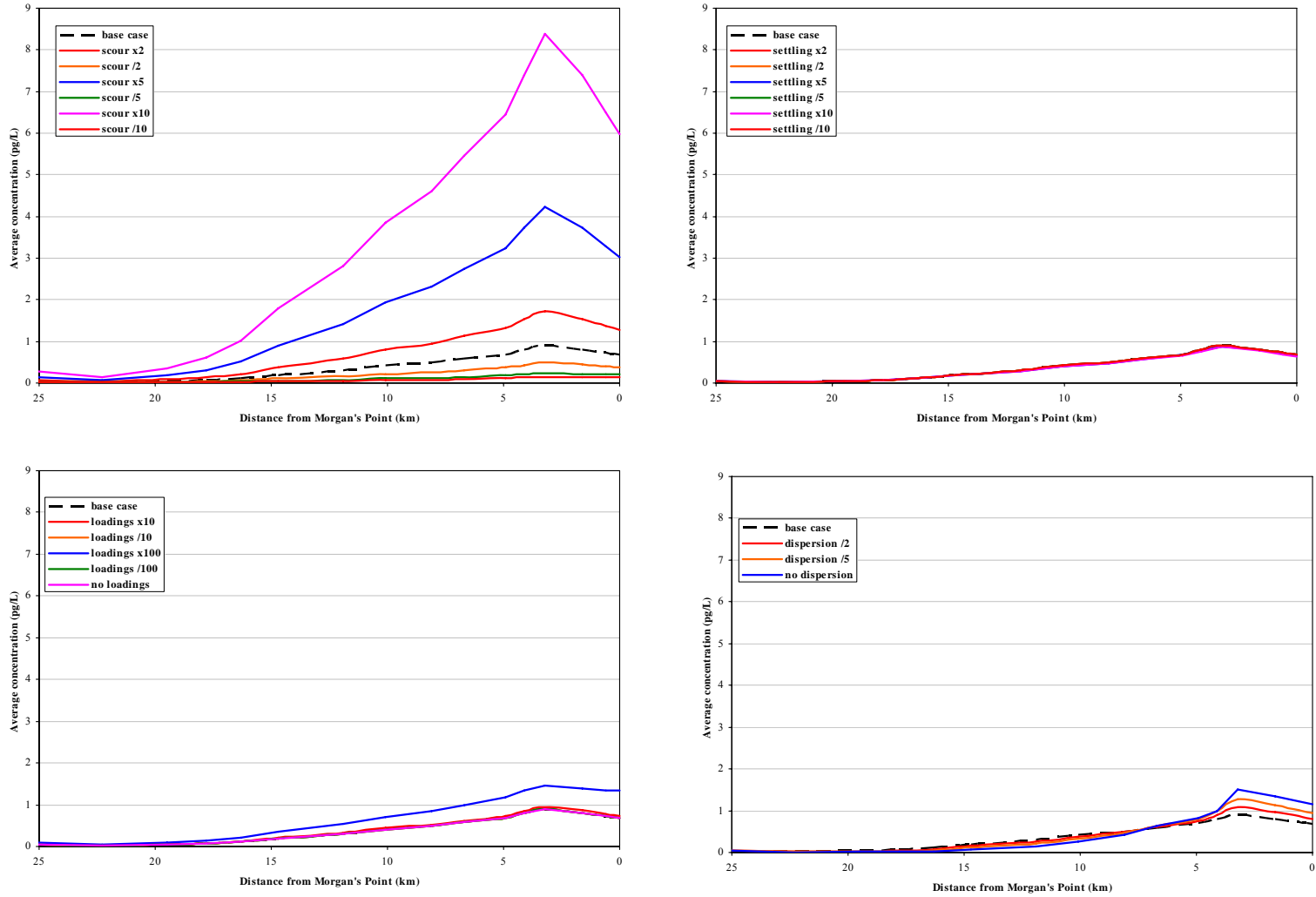


Figure 3.21 Sensitivity Analysis Results – San Jacinto River

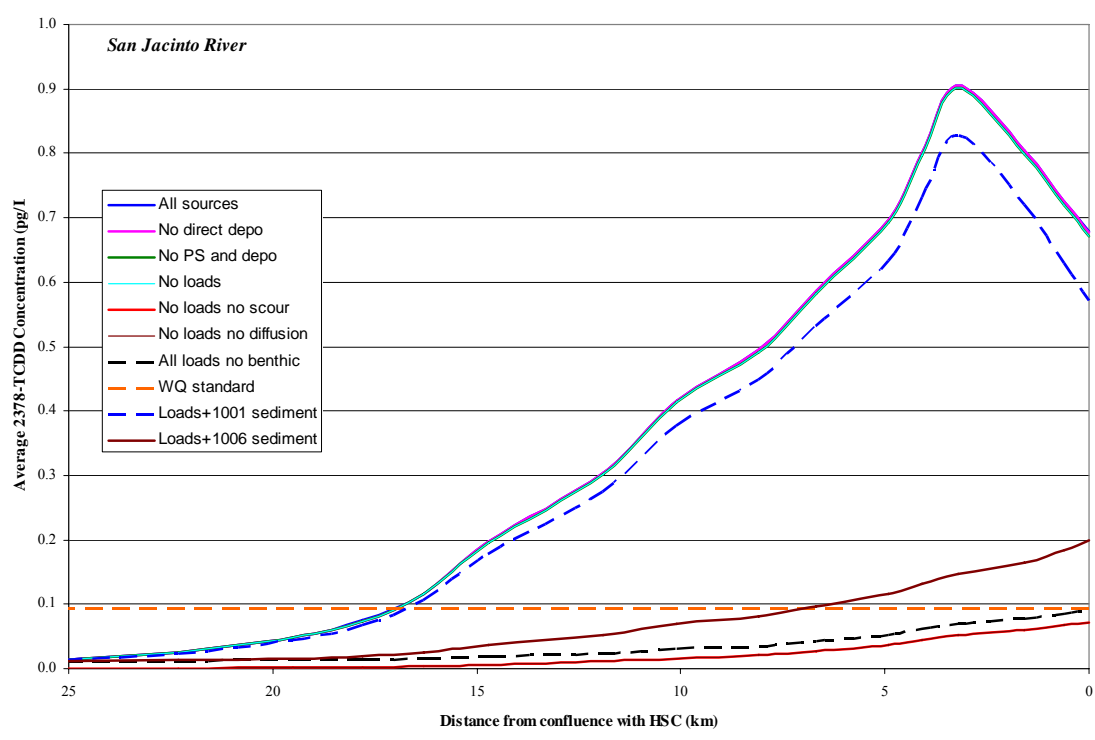
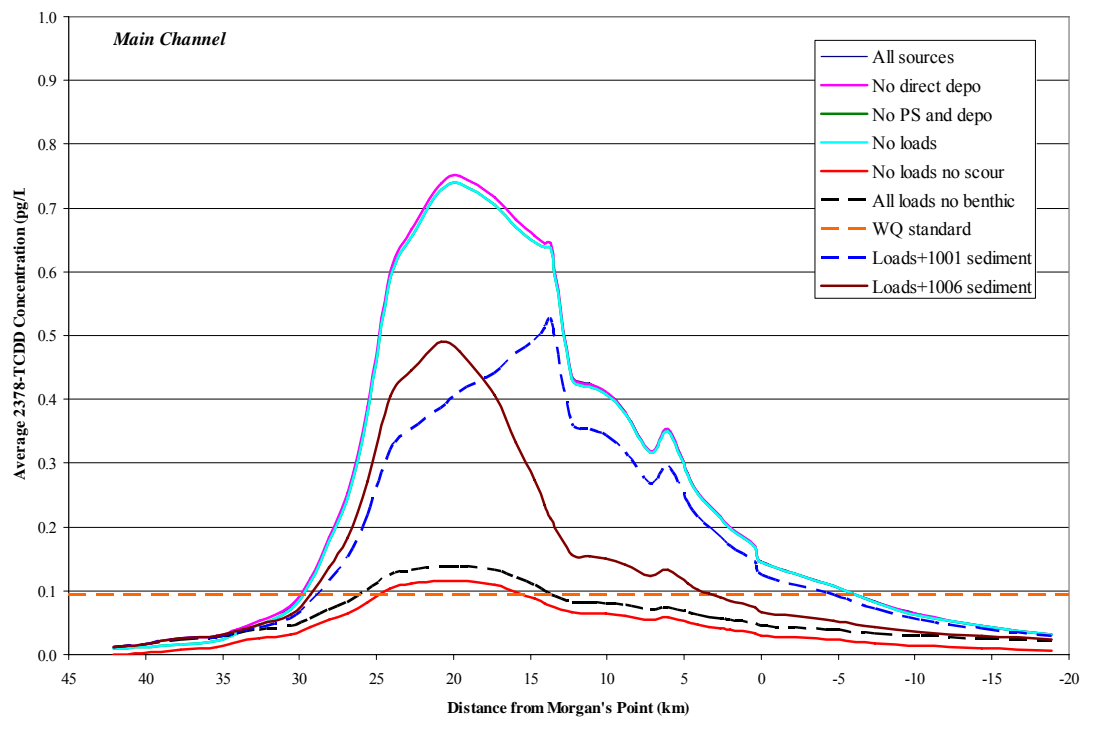


Figure 3.22 Summary of Load Scenarios

might be an amount of contaminant that never leaves that portion of the HSC system.

3.4.7 Next Steps in WASP Model Development

A number of issues with the WASP model for salinity and dioxins are still being addressed. Once these issues have been resolved, a long-term run (2002 to 2004) will be completed and load allocations completed. The parameters that define scour and settling in WASP are still being refined.

CHAPTER 4

LOAD CALCULATION SPREADSHEET MODEL

This chapter presents a mass-balance spreadsheet model developed for this project. The dioxin load spreadsheet can be used as a screening tool to evaluate different load scenarios and to provide insight into the relative magnitude of the different sources of dioxins to the HSC. The spreadsheet can also be used as a means to summarize long data sets obtained from the dioxin model described in the previous chapter. The spreadsheet provides estimates of sources of 2378-TCDD and total TEQ to the HSC by segment and compares them to estimated in-stream loads.

4.1 SOURCE LOADS BY SEGMENT

The primary purpose of the source load assessment is to develop estimates of point and non-point source loadings that contribute to the observed dioxin concentrations within the impaired water segments. Three main sources are considered in this preliminary assessment: (i) point sources; (ii) wet weather (runoff) loadings, and (iii) direct wet/dry deposition to the HSC surface area.

4.1.1 Point Source Loads

A database with all the permitted dischargers to the HSC system was obtained from the TCEQ. The database contains permitted and self-reported flows. Thus, loads were estimated using both permitted flows and the 5-year average of the self-reported flows. Dioxin concentrations from point sources gathered in this project during Spring 2003 were used. For the point sources that were not sampled for effluent, one of the following three approaches was used

to estimate a dioxin concentration:

1. If the PS was sampled for sludge, the dioxin concentration in effluent was extrapolated from a regression between dioxin in sludge and dioxin in effluent for the point sources sampled for both (Figure 4.1).
2. If the PS was not sampled for sludge or for effluent and the SIC was among those identified as potential dioxin dischargers, the dioxin concentration in effluent was assumed equal to the average dioxin for effluent from facilities with the same SIC code. If no facilities with the SIC code of the PS were sampled, the dioxin concentration was assumed as the average dioxin concentration of all the sampled industrial outfalls.
3. If the PS was not sampled and the SIC code was not among those identified as potential sources of dioxins, the concentration was assumed zero.

A database with calculated loads by stream is included in Appendix E. Table 4.1 and 4.2 present a summary of calculated loads by segment for 2378-TCDD and TEQ, respectively. Estimated loads using permitted flows were 97,890 and 434,960 ng/day for 2378-TCDD and TEQ, respectively. Using average self-reported flows yielded daily loads of 46,079 ng for 2378-TCDD and 214,611 ng for TEQ.

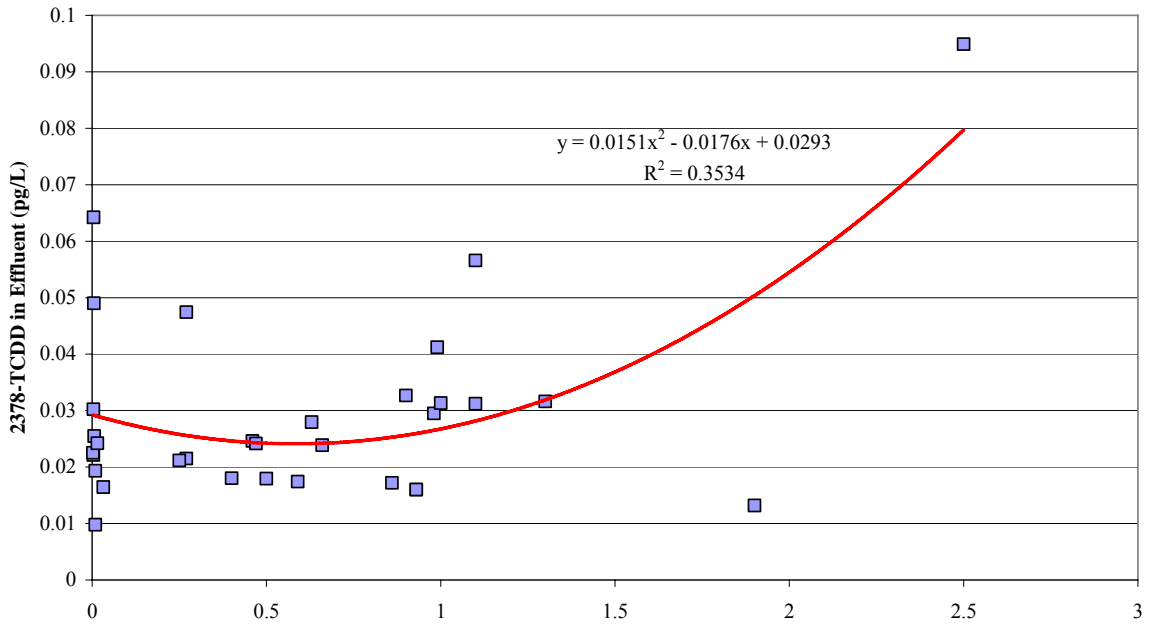
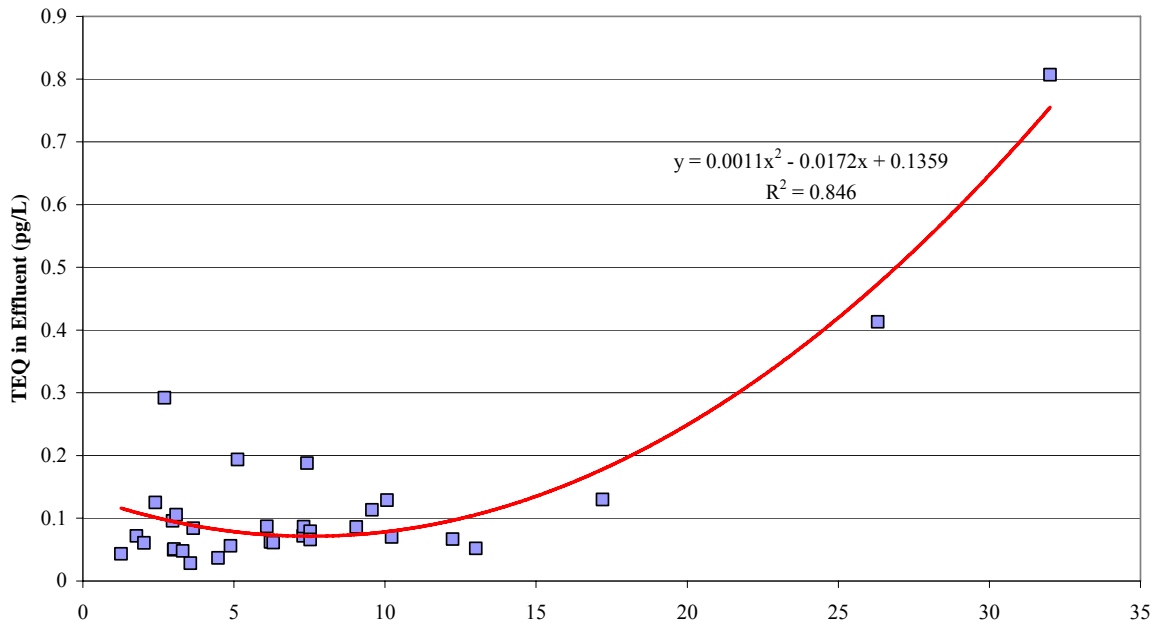


Figure 4.1 Relationship between Measured Dioxin Levels in Sludge and Effluent
(a) TEQ (b) 2378-TCDD

Table 4.1 Estimated 2378-TCDD Loads from Point Sources

SEGMENT	Permitted (as of 2002)		Self-reported (as of 2002)	
	FLOW (m ³ /s)	LOAD (ng/day)	FLOW (m ³ /s)	LOAD (ng/day)
1014	4.6	11,091	1.8	4,407
1017	2.2	4,862	0.8	1,830
1007	19.3	43,941	9.2	20,205
1016	3.1	7,434	1.0	2,505
1006	5.6	19,275	3.2	9,878
1001	0.9	4,071	0.6	2,844
1005	1.8	4,876	1.2	3,119
2426	0.3	593	0.2	407
2427	0.4	1,696	0.2	833
2436	0.0	50	0.0	50
TOTAL	38.3	97,890	18.2	46,079

Non-detects assumed as 1/2 MDL

Table 4.2 Estimated TEQ Loads from Point Sources

SEGMENT	Permitted (as of 2002)		Self-reported (as of 2002)	
	FLOW (m ³ /s)	LOAD (ng/day)	FLOW (m ³ /s)	LOAD (ng/day)
1014	4.6	31,540	1.8	12,255
1017	2.2	12,863	0.8	4,629
1007	19.3	181,948	9.2	85,784
1016	3.1	30,135	1.0	10,811
1006	5.6	97,418	3.2	50,534
1001	0.9	32,637	0.6	22,841
1005	1.8	28,507	1.2	17,525
2426	0.3	2,600	0.2	1,777
2427	0.4	16,701	0.2	7,873
2436	0.0	610	0.0	582
TOTAL	38.3	434,960	18.2	214,611

Non-detects assumed as 1/2 MDL

4.1.2 Runoff Loads

Runoff flows were determined via the SCS runoff curve number method (Natural Resource Conservation Service, 1986) using average daily precipitation for the year 2002, the HGAC 2002 land cover data for the HSC watershed, and the watershed delineation completed by the Harris County Flood Control District. Wet weather loadings were then computed using the dioxin concentrations in runoff measured in 2003 and 2005 as part of this project. The available runoff dioxin data were assigned to the different subwatersheds based on proximity between the sampled stations and the specific watersheds. The resulting daily loads by subwatershed are summarized in Table 4.3. The estimated 2378-TCDD loads ranged from 326 to 63,424 ng/day, while the TEQ loads ranged from 3,299 to 641,840 ng/day.

4.1.3 Direct Deposition Loads

Deposition loads were estimated using the dry/wet deposition fluxes measured in this project multiplied by the area of the different water quality segments. Only direct deposition to the channel was included since deposition to the watershed is ultimately carried to the channel via runoff and, thus, was included in the wet weather load calculation. Table 4.4 presents a summary of deposition loads by segment. Deposition loads varied from 5,073 to 21,265 ng/day for 2378-TCDD and from 44,941 to 188,375 ng/day for TEQ.

Table 4.3 Estimated Dioxin Runoff Loads by Subwatershed

Watershed	Precipitation (in/day)	Area m ²	Runoff Flow		Runoff Concentration (pg/L)		Load (ng/day)	
			L/day	m ³ /s	2378-TCDD	TEQ	2378-TCDD	TEQ
ADDICKS RESERVOIR	0.133	3.59E+08	6.7E+08	7.73	0.019	0.124	12687	82802
BARKER RESERVOIR	0.121	3.33E+08	7.1E+08	8.16	0.019	0.124	13395	87423
BRAYS BAYOU	0.126	3.33E+08	1.6E+08	1.91	0.032	0.315	5276	51850
BUFFALO BAYOU	0.117	2.64E+08	1.9E+08	2.19	0.019	0.124	3588	23415
CARPENTERS BAYOU	0.172	8.07E+07	2.6E+08	3.01	0.018	0.182	4673	47295
GREENS BAYOU	0.139	5.47E+08	1.3E+09	14.77	0.024	0.165	30633	210599
HUNTING BAYOU	0.164	8.03E+07	1.2E+08	1.42	0.016	0.311	1962	38142
SAN JACINTO & GALVESTON BAY	0.138	5.01E+07	8.7E+07	1.00	0.018	0.182	1557	15760
SAN JACINTO RIVER	0.158	1.23E+09	3.5E+09	40.90	0.018	0.182	63424	641840
SIMS BAYOU	0.144	2.42E+08	2.4E+08	2.78	0.004	0.028	961	6603
SPRING GULLY & GOOSE CREEK	0.175	8.49E+07	9.6E+07	1.11	0.018	0.271	1722	25880
VINCE BAYOU	0.158	3.96E+07	1.8E+07	0.21	0.018	0.182	326	3299
WHITE OAK BAYOU	0.135	2.88E+08	2.4E+08	2.81	0.023	0.235	5456	56990

Non-detects assumed as 1/2 MDL

Table 4.4 Dioxin Loads from Direct Deposition

Segment	Description	Area (m ²)	2378-TCDD Load (ng/day)			TEQ Load (ng/day)		
			Wet	Dry	Total	Wet	Dry	Total
1001 upper	San Jacinto River	4,552,714	1,821	2,823	4,644	71,478	9,561	81,038
1001 lower	San Jacinto River	1,517,571	607	941	1,548	23,826	3,187	27,013
1005	Houston Ship Channel	13,057,642	5,223	8,096	13,319	205,005	27,421	232,426
1006	Houston Ship Channel	6,136,058	2,454	3,804	6,259	96,336	12,886	109,222
1007	Houston Ship Channel	4,476,536	1,791	2,775	4,566	70,282	9,401	79,682
1014+1017	Buffalo Bayou	285,000	114	177	291	4,475	599	5,073
1016	Greens Bayou	570,000	228	353	581	8,949	1,197	10,146
2426	Tabbs Bay	10,189,730	4,076	6,318	10,394	159,979	21,398	181,377
2427	San Jacinto Bay	5,233,915	2,094	3,245	5,339	82,172	10,991	93,164
2428	Black Duck Bay	3,115,207	1,246	1,931	3,178	48,909	6,542	55,451
2429	Scott Bay	3,783,511	1,513	2,346	3,859	59,401	7,945	67,346
2436	Barbours Cut	262,720	105	163	268	4,125	552	4,676
2438	Bayport Channel	663,509	265	411	677	10,417	1,393	11,810
Old River	Old San Jacinto	505,857	202	314	516	7,942	1,062	9,004
2430	Burnett Bay	5,416,711	2,167	3,358	5,525	85,042	11,375	96,417

Wet Deposition Fluxes: 2378-TCDD 0.4 pg/m²/day; TEQ 15.7 pg/m²/day

Dry Deposition Fluxes: 2378-TCDD 0.62 pg/m²/day; TEQ 2.1 pg/m²/day

Non-detects assumed as 1/2 MDL

4.2 IN-STREAM LOADS

In-stream loads were calculated using average water concentrations for the different water quality segments and the net flow out of each segment. The net flow was estimated as the average of the modeled flows at the downstream end of each water quality segment. This was done to ensure that the same time period was used for all the segments given that the flow was not measured simultaneously at all the locations monitored in March-April 2005. As expected, in all cases, the net flow was positive indicating discharge from the upstream end of the segment to the downstream end of the segment. In-stream loads were calculated on a segment by segment basis and not in a cumulative manner (i.e., the loads from upstream segments were subtracted from the loads leaving a given segment). So, for example, the load in segment 1007 is calculated as the average flow leaving the segment (WASP segment 22) times the average concentration at station 15979 minus the load leaving segments 1014 and 1017. Table 4.5 summarizes the in-stream loads by segment. It is noted that segments 1001 lower, 1006, and 1005 lower account for most of the loads in the system with a total of 9,679,346 ng/day and 13,780,965 ng/day for 2378-TCDD and TEQ, respectively. Interesting enough is the fact that segment 1005-upper seems to be acting as a sink for dioxins as indicated by the negative loads for both 2378-TCDD and TEQ.

These in-stream loads were then compared to the sum of source loads calculated in Section 4.1 to complete a mass balance. Tables 4.6 and 4.7 summarize this comparison. It can be seen in Tables 4.6 and 4.7 that for most of the main channel segments more than 90% of the in-stream load cannot be attributed to the dioxin sources assessed in Section 4.1. Possible additional sources include dioxin fluxes from the bottom sediment to the water column, unidentified current sources (e.g. source in 1001 at I-10 bridge), groundwater sources, and dredge spoil leachate.

Table 4.5 In-stream Loads of Dioxin by Segment

Segment	Concentration data from station	Net Flow ^a (m ³ /s)	Average Water Concentration (pg/L) ^b		Loads out of segments (ng/day) ^c		In-stream Segment Loads (ng/day) ^d	
			2378-TCDD	TEQ	2378-TCDD	TEQ	2378-TCDD	TEQ
1014+1017	11347+11382	10.3	0.009	0.076	7,867	67,942	7,867	67,942
1007	11280	24.7	0.264	0.4067	563,482	869,378	555,615	801,437
1016	11274	5.4	0.059	0.2574	27,736	120,191	27,736	120,191
1006	15979	30.8	0.756	1.0825	2,014,088	2,882,785	1,430,737	1,961,158
1001 upper	16622	90.3	0.019	0.0784	145,107	611,632	145,107	611,632
1001 lower	11193	90.1	0.942	1.3446	7,330,699	10,468,201	7,185,593	9,856,569
Old River	^e	0.7	0.019	0.0784	1,170	4,828	1,170	4,828
1005 upper	11261	121.7	0.3462	0.535	3,638,958	5,623,462	-4,977,372	-6,194,265
2430	13344	0.05	0.158	0.2718	640	1,104	640	1,104
2429	13342	0.2	0.188	0.307	2,985	4,884	2,985	4,884
2428	13340	0.07	0.035	0.1058	207	619	207	619
2427	16499	0.21	0.342	0.5049	6,234	9,211	6,234	9,211
2426	13337	5.1	0.170	0.3198	75,048	141,013	75,048	141,013
2436	13355	0.01	0.374	0.5957	465	741	465	741
1005 lower	11252	124.8	0.099	0.1821	1,063,016	1,963,238	1,063,016 ^f	1,963,238 ^f
2438	13589	3.2	0.017	0.0743	4,807	20,525	4,807	20,525

^a Average flow from simulation period (March 20 to April 21, 2005). Model data used to have comparable time periods for all segments

^b Average dioxin concentration in water measured in this project

^c Concentration at the end of segment times net outflow

^d Load out of a segment minus loads from upstream segments

^e Concentration assumed equal to that measured at location 16622 in San Jacinto River since no stations in the Old River were sampled for dioxin

^f Net load exported to Upper Galveston Bay

Table 4.6 Mass Balance Calculations for 2378-TCDD

Segment	In-stream load ^a	Source Loads (ng/day)			
		Point Sources	Stormwater Runoff	Direct deposition	Unaccounted ^b
1014+1017	7,867	6,237	35,127	291	-33,788
1007	555,615	20,205	34,607	4,566	496,237
1016	27,736	2,505	30,633	581	-5,982
1006	1,430,737	9,878	4,673	6,259	1,409,927
1001 upper	145,107	2,844	47,568	4,644	90,050
1001 lower	7,185,593		15,856	1,548	7,168,189
1005 upper	-4,977,372		1,557		
2430	640		379	5,525	-5,264
Old River	1,170			516	654
2429	2,985		344	3,859	-1,219
2428	207		207	3,178	-3,177
2427	6,234	833	310	5,339	-248
2426	75,048	407	517	10,394	63,730
2436	465	50		268	147
1005 lower	1,063,016	3,119	1,557	13,319	1,045,021
2438	4,807			677	4,130

^a Average concentration measured in 2002-2004 times net flow out of segment

^b Difference between in-stream load and the sum of loads from Non-detects assumed equal to 1/2MDL for load calculations

Table 4.7 Mass Balance Calculations for TEQ

Segment	In-stream load ^a	Source Loads (ng/day)			
		Point Sources	Stormwater Runoff	Direct deposition	Unaccounted ^b
1014+1017	7,867	16,884	250,630	5,073	-264,720
1007	555,615	85,784	350,524	79,682	39,625
1016	27,736	2,505	210,599	10,146	-195,513
1006	1,430,737	9,878	257,894	109,222	1,053,743
1001 upper	145,107	2,844	481,380	81,038	-420,156
1001 lower	7,185,593		160,460	27,013	6,998,120
1005 upper	-4,977,372		15,760		
2430	640		5,694	96,417	-101,471
Old River	1,170			9,004	-7,834
2429	2,985		5,176	67,346	-69,538
2428	207		3,106	55,451	-58,349
2427	6,234	833	4,658	93,164	-92,422
2426	75,048	407	7,764	181,377	-114,501
2436	465	50		4,676	-4,261
1005 lower	1,063,016	3,119	15,760	232,426	811,711
2438	4,807			11,810	-7,004

^a Average concentration measured in 2002-2004 times net flow out of segment

^b Difference between in-stream load and the sum of loads from Non-detects assumed equal to 1/2MDL for load calculations

4.3 LOADS FROM SEDIMENT

Fugacity calculations (see Final Report WO No. 582-0-80121-07) suggested flux of dioxins from the bottom sediment to the water column. Quantification of such a load is complex and can be completed using fate and transport models that account for partitioning of dioxins from the different phases. Since the WASP model for the HSC is still under development, an initial load calculation was completed using the partitioning data from a side bay that has no point sources (segment 2428-Black Duck Bay). Sediment and water data collected at stations 13340 and 13341 yielded median log K_{oc} values of 7.36 and 7.20 L/kg for 2378-TCDD and TEQ, respectively. Using these bottom sediment-dissolved partitioning coefficients and average dioxin concentrations in sediment at various locations, it is possible to estimate an “expected” dissolved concentration due to flux from the sediment to the water column. Once the dissolved concentration for each segment is estimated, the suspended concentration is calculated using the average dissolved-suspended partitioning coefficients computed using the entire database for water concentrations collected in this project. As discussed in the Final Report for WO7, the Langmuir isotherm is the best representation of suspended-dissolved partitioning for the HSC. The Langmuir isotherm is defined by a coefficient ($\log K_p$) and an exponent ($1/n$). Calculated $\log K_p$ values are 5.16 and 4.84 for 2378-TCDD and TEQ, respectively, while $1/n$ values are 1 for 2378-TCDD and 0.787 for TEQ. Table 4.8 presents a summary of expected water concentrations due to fluxes of dioxins from the underlying sediment to the water column. The concentrations were multiplied by the average flow simulated at the downstream boundary of each water quality segment to estimate loads. As can be seen in Table 4.8, 2378-TCDD loads from sediment varied from 386 to 9,699,821 ng/day, while TEQ loads varied from 1,830 to 11,244,582 ng/day. A

Table 4.8 Estimated Dioxin Loads from Bottom Sediment (with average from same station as water column)

Segment	Average Sediment Concentration (ng/kg-oc) ^a		Estimated Dissolved Concentration (pg/L) ^b		Estimated Suspended Concentration (pg/L) ^c		Estimated Water Concentration (pg/L)		Average Flow (m ³ /s)	Estimated Load (ng/day)	
	2378-TCDD	TEQ	2378-TCDD	TEQ	2378-TCDD	TEQ	2378-TCDD	TEQ		2378-TCDD	TEQ
1001 lower	13342	19807	0.262	0.568	0.984	0.876	1.246	1.444	90.1	9,699,821	11244,582
1005	244	503	0.010	0.031	0.038	0.021	0.049	0.052	124.8	523,960	561,051
1016	101	296	0.004	0.017	0.016	0.010	0.020	0.028	5.4	9,221	12,945
1007	8814	11899	0.083	0.345	0.312	0.465	0.395	0.809	24.7	845,421	1,730,386
1014	18	175	0.001	0.011	0.003	0.006	0.004	0.017	6.3	2,011	9,226
1017	5	97	0.000	0.006	0.001	0.003	0.001	0.009	4.4	386	3,353
1006	4295	6136	0.209	0.434	0.786	0.623	0.995	1.057	30.8	2,648,802	2,816,166
2430	1058	1641	0.099	0.207	0.374	0.243	0.473	0.451	0.05	1,921	1,830

^a Average flow from simulation period (March 20 to April 21, 2005). Model data used to have comparable time periods for all segments

^b Using the log Koc values from segment 2428

^c Using Langmuir Isotherm data for suspended-dissolved partitioning derived using water data collected in this project

comparison between Table 4.8 with Tables 4.6 and 4.7 indicates that resuspension loads for both 2378-TCDD and TEQ using this approach exceed the unaccounted for loads in Table 4.7 for most segments. Thus, contributions from sediments need to be estimated using other methods such as the WASP model under development.

4.4 PRELIMINARY LOAD REDUCTION SCENARIOS

Preliminary load reduction scenarios for 2378-TCDD were run using the dioxin load spreadsheet. A first step was to calculate the overall reduction needed to meet the standard for the various water quality segments in the HSC as summarized in Table 4.9.

Table 4.9 Dioxin Load Spreadsheet – Overall Reductions

Segment	Net Flow ^a (m ³ /s)	Allowable Load ^b (ng/day)	In-stream Load (ng/day)	% Overall Reduction
1014+1017	10.3	8,341	7,867	0%
1007	24.7	19,944	555,615	96%
1016	5.4	4,357	27,736	84%
1006	30.8	24,847	1,430,737	98%
1001 upper	90.3	72,787	145,107	50%
1001 lower	90.1	72,637	7,185,593	99%
2430	0.05	38	640	94%
Old River	0.7	575	1,170	51%
2429	0.2	148	2,985	95%
2428	0.07	55	207	74%
2427	0.21	170	6,234	97%
2426	5.1	4,114	75,048	95%
2436	0.01	12	465	98%
1005 lower	124.8	100,588	1,063,016	91%
2438	3.2	2,577	4,807	46%

^a Average flow from simulation period (March 20 to April 21, 2005). Model data used to have comparable time periods for all segments

^b Net outflow times the Texas WQS (0.0933 pg/L)

Overall in-stream load reductions needed to meet the allowable load vary between 46 and 99%. The headwater segments (1014 and 1017) showed an in-stream load lower than that allowable and, thus, according to this calculation do not require a reduction.

The spreadsheet was designed such that it allows for calculation of the total load for each segment resulting from different load allocation scenarios. Tables 4.10 and 4.11 present two examples. In this case, the load reductions are applied by source category uniformly across the HSC system and as can be seen, many of the segments do not meet the standards with these scenarios. The spreadsheet is being updated to allow for reduction scenarios on a segment by segment basis.

4.10 Dioxin Load Spreadsheet – Load Reduction Scenario 1

WWTP Reduction	70%
Stormwater Runoff Reduction	70%
Direct Depo Reduction	70%
Sediment Load Reduction	90%

Segment	Net Flow ^a (m ³ /s)	Allowable Load (ng/day)	Reduced Loads				Meet Allowable Load?
			Point Sources		Non-point Sources		
			WWTPs	Stormwater runoff (MS4s)	Direct deposition	Sediment?	
1014+1017	10.3	8,341	1,871	10,538	87	0	No
1007	24.7	19,944	6,061	10,382	1,370	49,624	No
1016	5.4	4,357	751	9,190	174	0	No
1006	30.8	24,847	2,963	1,402	1,878	140,993	No
1001 upper	90.3	72,787	853	14,270	1,393	9,005	Yes
1001 lower	90.1	72,637	0	4,757	464	716,819	No
2430	0.05	38	0	114	1,658	0	No
Old River	0.7	575	0	0	155	65	Yes
2429	0.2	148	0	103	1,158	0	No
2428	0.07	55	0	62	953	0	No
2427	0.21	170	250	93	1,602	0	No
2426	5.1	4,114	122	155	3,118	6,373	No
2436	0.01	12	15	0	80	15	No
1005 lower	124.8	100,588	936	467	3,996	104,502	No
2438	3.2	2,577	0	0	203	413	Yes

4.11 Dioxin Load Spreadsheet – Load Reduction Scenario 2

WWTP Reduction	0%
Stormwater Runoff Reduction	0%
Direct Depo Reduction	0%
Sediment Load Reduction	95%

Segment	Net Flow ^a (m ³ /s)	Allowable Load (ng/day)	Reduced Loads				Meet Allowable Load?
			Point Sources		Non-point Sources		
			WWTPs	Stormwater Runoff (MS4s)	Direct deposition	Sediment?	
1014+1017	10.3	8,341	6,237	35,127	291	0	No
1007	24.7	19,944	20,205	34,607	4,566	24,812	No
1016	5.4	4,357	2,505	30,633	581	0	No
1006	30.8	24,847	9,878	4,673	6,259	70,496	No
1001 upper	90.3	72,787	2,844	47,568	4,644	4,503	Yes
1001 lower	90.1	72,637	0	15,856	1,548	358,409	No
2430	0.05	38	0	379	5,525	0	No
Old River	0.7	575	0	0	516	33	Yes
2429	0.2	148	0	344	3,859	0	No
2428	0.07	55	0	207	3,178	0	No
2427	0.21	170	833	310	5,339	0	No
2426	5.1	4,114	407	517	10,394	3,187	No
2436	0.01	12	50	0	268	7	No
1005 lower	124.8	100,588	3,119	1,557	13,319	52,251	Yes
2438	3.2	2,577	0	0	677	206	Yes

CHAPTER 5

STAKEHOLDER/PUBLIC EDUCATION AND INVOLVEMENT

5.1 SUMMARY OF SUPPORT ACTIVITIES

The project team supported the stakeholder process facilitated by the Houston Galveston Area Council (HGAC) and the Environmental Institute of Houston at UH Clear Lake. The following support tasks were undertaken:

- Development of informational materials summarizing the technical aspects of the project for electronic and paper distribution at stakeholder meetings. These materials included documents, maps, and the QAPP for this project;
- Preparation of web based project informational briefs;
- Participation in two stakeholder meetings (01/12/2006 and 06/16/2006);
- Preparation of responses to questions and information requests from stakeholders and providing rationale for whether or not certain requests by stakeholders for refinement in technical analysis can or cannot be achieved.
- Preparation of data to be submitted to H-GAC for development of informational map and brochure on the project.

5.2 TECHNICAL PRESENTATIONS AT STAKEHOLDER MEETINGS

Copies of the technical presentations given at the stakeholder meetings are included in Appendix E. The QAPP and other related documents can be found on the web at <http://www.hgac.cog.tx/intro/introtmdl.html>.

CHAPTER 6

SUMMARY AND CONCLUSIONS

This report summarizes the activities conducted by the dioxin project team during the period September 28, 2005 to August 31, 2006. These activities are part of Phase III of the dioxin TMDL project.

As part of Work Order 582-6-70860-02, one long-term location air deposition/ambient air experiment was conducted, and 2 locations were sampled for stormwater runoff. In addition, all the analytical results for samples collected between 2002 and 2005 were compiled and analyzed as presented in Chapter 2.

The majority of the activities conducted under this work order were focused on the development of a time-varying model of dioxins in the HSC. The model approach consisted of an RMA2 hydrodynamic model for the channel and Upper Galveston Bay, linked to a WASP dioxin model. A short-term run (March 20 to April 21, 2005) was completed and the results summarized in Chapter 3. A long-term run (June 2002 to May 2005) is underway and the results will be used to calculate long-term dioxin averages to be used in the load allocation scenarios.

Preliminary results of the WASP dioxin model indicate that the sediment load in the San Jacinto River at I-10 affects the dioxin levels in segments 1006 and 1005. Results also suggest that the processes affecting the concentrations in the main channel in the vicinity of the San Jacinto River mouth cause a greater spread of dioxin concentrations than that simulated in the model. Short-term results also indicate that segment 1006 may act as a “reservoir” for dioxin mass and that contaminants have a long residence time in the segment.

Finally, preliminary load calculations using both the dioxin load spreadsheet and WASP model results support the significant contributions from bottom sediment to dioxins in the water column.

REFERENCES

- Ambrose, R.B., T.A. Wool, and J.L. Martin. 1993. The Water Quality Analysis Simulation Program, WASP5. Environmental Research Laboratory, US Environmental Protection Agency, Athens, Georgia.
- Legates, D. and G. McCabe Jr (1999). Evaluating the Use of “Goodness-of-fit” Measures in Hydrologic and Hydroclimatic Model Validation. *Water Resources Research*, 35(1): 233-241.
- Roychoudhury, A.N. 2001. Dispersion in unconsolidated aquatic sediments. *Estuarine, Coastal and Shelf Science*. 53:745-757.
- Stow, C., C. Roessler, M. Borsuk, J. Bowen, and K. Reckhow (2003). Comparison of Estuarine Water Quality Model for Total Maximum Daily Load Development in Neuse River Estuary. *Journal of Water Resources Planning and Management*, 129(4): 307-314.
- University of Houston (2005a). Final Report for the Total Maximum Daily Loads for Fecal Pathogens in Buffalo Bayou and Whiteoak Bayou – Work Order No. 582-0-80121-06. Prepared for the Texas Commission on Environmental Quality. January, 2005.
- University of Houston (2005b). Final Report for the Total Maximum Daily Loads for Dioxins in the Houston Ship Channel – Work Order No. 582-0-80121-07. Prepared for the Texas Commission on Environmental Quality. November, 2005.
- U.S. Army, Engineer Research and Development Center-ERDC (2005). User’s Guide to RMA2 WES Version 4.5. Revised April 22, 2005.
- U.S. Environmental Protection Agency (2000a). “Dioxin: Scientific Highlights from Draft Reassessment.” *Information Sheet 2*, National Center for Environmental Assessment,

Office of Research and Development, Washington, DC.

U.S. Environmental Protection Agency (2000b). “Exposure and Human Health Reassessment of 2,3,7,8-Tetrachlorodibenzo-p-Dioxin (TCDD) and Related Compounds. Part I: Estimating Exposure to Dioxin-Like Compounds. Volume: Sources of Dioxin-Like Compounds in the United States.” *EPA600/P-00/001Ab*.

Wool, T.A., R.B. Ambrose, J.L. Martin, and E.A. Comer. 2004. The water quality analysis simulation program (WASP) version 6.0: Draft User’s Manual. Distributed by USEPA Region 4, Atlanta, GA.

APPENDIX A

**SUMMARY OF DIOXIN DATA
COLLECTED IN THIS PROJECT
(Electronic)**

APPENDIX B

CROSS-SECTIONS FROM BEAMS USED TO SET UP THE 1-D PORTION OF THE MAIN CHANNEL

APPENDIX C

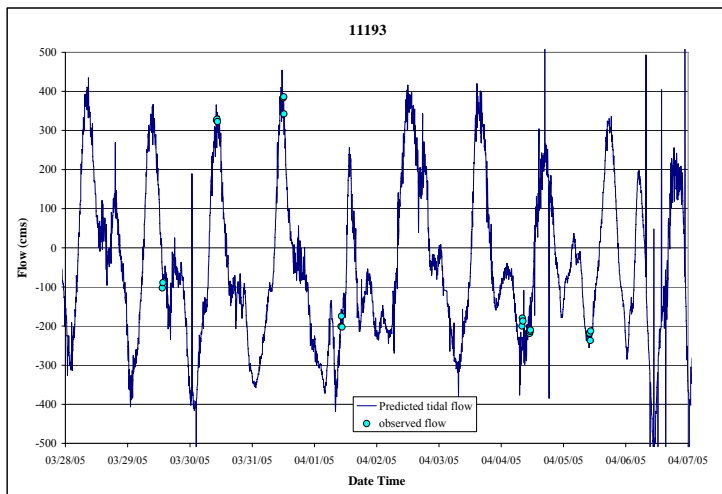
TIME SERIES FOR BOUNDARY CONDITIONS

Appendix C1 – Tide and Inflow Database (Electronic)

Appendix C2 – Rating Curve used to Estimate Hourly Discharges from the Lake Houston to the San Jacinto River

Appendix C3 – Flow Regression for the San Jacinto River

All the measured flows were used for the regression rather than the averages for the various events. It was considered that the freshwater inflow from Lake Houston was significant when compared to the measured flows at I-10. Thus, the freshwater flows were subtracted from the measured flows (assuming a 6-hour lag) and a regression between the resulting flows and the change in tide height was completed. To obtain predicted flows, the freshwater inflows were added to the flows obtained using the regression equation.



Site	Date	Time	Measured Q	Predicted Q
11193	03/29/05	13:11	-184.38	8.76
11193	03/29/05	13:24	-171.19	-65.72
11193	03/30/05	10:06	268.50	364.22
11193	03/30/05	10:16	271.64	332.62
11193	03/30/05	10:27	265.37	321.34
11193	03/31/05	11:48	326.25	357.21
11193	03/31/05	11:58	325.99	332.38
11193	03/31/05	12:05	282.02	382.04
11193	04/01/05	10:06	-232.58	-181.91
11193	04/01/05	10:15	-206.42	-206.73
11193	04/01/05	10:27	-234.21	-188.68
11193	04/04/05	7:50	-244.55	-270.00
11193	04/04/05	8:00	-229.19	-260.97
11193	04/04/05	8:12	-236.72	-242.91
11193	04/04/05	10:47	-273.19	-180.42
11193	04/04/05	10:57	-271.37	-148.82
11193	04/04/05	11:06	-267.47	-212.02
11193	04/05/05	9:51	-237.62	-230.44
11193	04/05/05	10:08	-256.22	-232.70
11193	04/05/05	10:18	-232.01	-232.70

SUMMARY OUTPUT

Regression Statistics

Multiple R	0.989
R Square	0.978
Adjusted R	0.977
Standard Err	39.19
Observation	20

ANOVA

	df	SS	MS	F	Significance F
Regression	1	1244977.792	1244978	810.7377618	2.01493E-16
Residual	18	27640.99726	1535.61		
Total	19	1272618.789			

	Coefficient	Standard Error	t Stat	P-value	Lower 95%	Upper 95%	Lower 95.0%	Upper 95.0%
Intercept	12.89	8.890232746	1.44966	0.164353865	-5.78987252	31.56549926	-5.78987252	31.56549926
96	-2257	79.25570332	-28.473	2.01493E-16	-2423.193926	-2090.173818	-2423.193926	-2090.173818

APPENDIX D

MODEL INPUT AND OUTPUT FILES

(Electronic)

Appendix D-1 RMA2 Model Input Files (Electronic)

Appendix D-2 WASP Model Input and Output Files (Electronic)

APPENDIX E

POINT SOURCE DATABASE

(Electronic)

APPENDIX F

SLIDES PRESENTED AT STAKEHOLDER MEETINGS